APPLICATION OF RHODIUM-CATALYZED ALKYNE HYDROTHIOLATION TO THE SYNTHESES OF K777 AND ANALOGUES: POTENTIAL THERAPEUTICS FOR THE TREATMENT OF CHAGAS' DISEASE

by

ERICA ROSE KIEMELE

B.Sc. (Hon), The University of Calgary, 2009

A THESIS SUBMITTED IN PARTIAL FULFILLMENT OF
THE REQUIRMENTS FOR THE DEGREE OF

MASTER OF SCIENCE

in

THE FACULTY OF GRADUATE STUDIES

(Chemistry)

THE UNIVERSITY OF BRITISH COLUMBIA

(Vancouver)

July 2012

Abstract

Chagas' disease is a neglected global disease that affects millions of people in Latin America and has started to spread to different areas around the world. This disease is the leading cause of heart failure in Latin America and has many other symptoms including digestive track problems and myocardial damage. The causative organism of this disease is T. *Cruzi*, which is spread though an insect vector as well as human methods such as blood transfusions, organ donation and food contamination.

Current drug therapies are not sufficient; they suffer from lengthy dosage duration and have many dangerous side effects. In the last two decades the organism's cysteine protease, cruzain has become a desired target for inhibition. Many cysteine protease inhibitors have been studied in the last two decades with one potential therapeutic - K777, an irreversible cysteine protease inhibitor, having the most promise. K777 contains a potent vinyl sulfone warhead, which acts as a Michael-acceptor to the cysteine residue in the catalytic triad of cruzain. K777 is currently entering phase 1 clinical trials.

The potent warheard vinyl sulfone in K777 is of interest to the laboratory of Dr. Jennifer Love due to our methodology for synthesizing vinyl sulfides. We proposed that we could synthesize K777 and a variety of analogues using our rhodium-catalyzed alkyne hydrothiolation method as the first application of this method in total synthesis. Here we present the total synthesis of K777 and analogues highlighting the wide substrate scope of our methodology.

Table of Contents

List of Tables

List of Figures

List of Schemes

List of Symbols and Abbreviations

α	alpha
Ac	acetyl
AIDS	acquired immunodeficiency syndrome
ala	alanine
ALT	alanine aminotransferase
Ar	aromatic
arg	arginine
Boc	*tert*-butoxy carbonyl
Bn	benzyl
Bu	butyl
°C	degrees Celcius
CDC	Center for disease control and prevention
CYP3A	Cytochrome P450, family 3, subfamily A
Cys	cysteine
Cbz	carboxy benzyl
D	deuterium
d	doublet
dd	doublet of doublets
ddd	doublet of doublet of doublets
DCC	N-N`-dicyclohexylcarbodiiamide
DCE	1,2-dichloroethane
DCM	dichloromethane
DIC	diisopropylcarbodiiamide
DIPEA	`diisopropylamine
DMAP	4-dimethylaminopyridine
DMF	dimethylformamide
DMSO	dimethylsulfoxide
DNA	deoxyribonucleic acid
DND*i*	Drugs for Neglected Diseases Initiative

d.r	diastereomeric ratio
E	Entgegen
ee	enantiomeric excess
EDC	1-ethyl-3-(3-dimethylaminopropyl)carbodiimide
Et	ethyl
ESI	electrospray ionization
FDA	US Food and Drug Administration
FTIR	fourier transform infrared spectroscopy
h	hours
HBTU	O-benzotriazole-N,N,N`,N`-tetramethyl-uronium-hexafluorophosphate
His	histidine
HIV	Human immunodeficiency virus infection
HOBT	hydoxybenzotriazole
HPLC	high performance liquid chromatography
HRMS	high resolution mass spectrometry
HWE	Horner-Wadsworth-Emmons
Hz	hertz
IR	infrared
i-Pr	isopropyl
J	coupling constant
µL	microliter
m	multiplet
M	molar (mol/L)
m-CPBA	*meta*-Chloroperoxybenzoic acid
Me	methyl
mg	miligram
MHz	mega hertz
Min	minute
mL	milliliter
mol	mole
mmol	millimole

MS	mass spectrometry
MTPA	α-methoxy-α-trifluoromethylphenylacetic acid
m/z	mass to charge ratio
NGD	neglected global disease
NIAID	National Institute of Allergy and Infectious Diseases
NIH	National Institutes for Health
NMR	nuclear magnetic resonance
NOAEL	no observable adverse effect level
Ph	phenyl
P. *falciparum*	Plasmodium *falciparum*
PG	protecting group
Ppm	parts per million
Pr	propyl
Phe	phenylalanine
PMFK	peptide fluoromethylketones
q	quartet
rt	room temperature
s	singlet
SAR	structural activity relationship
SFC	supercritical fluid chromatography
SRI	Stanford Research Institute
t	triplet
TBAF	tetrabutylammonium fluoride
T. *brucei*	Trypanosoma *brucei*
T. *cruzi*	Trypanosoma *cruzi*
TFA	trifluoro acetic acid
THF	tetrahydrofuran
TLC	Thin layer chromatography
TMS	trimethylsilane
Ts	tosyl
Tp	hydrotrispyrazolylborate

UBC	The University of British Columbia
UV	ultraviolet
Z	zussamen
Z (Cbz)	carboxy benzyl

Acknowledgments

I am so thankful to be blessed with so many supportive people in my life who over many years have given me guidance, care and love. I would not be where I am today with out their positivity.

First and foremost, I would like to thank my adviser Dr. Jennifer Love. Jen – I thank you for your encouragement and most of all your patience with me as I made very difficult decisions during graduate school. I know that it is not easy to have an unconventional graduate student such as myself, and I am truly appreciative that you allowed me to pursue my dreams and juggle so many things.

I would like to thank all the past and present group members of the Love group: Paul Bichler, Carla Rigling, Alex Dauth, Tongen Wang, Shiva Shoai, Kanghee Park, Alex Sun, Lauren Keyes, Charmian Yeo, Nicole LaBerge, Matt Wathier, Alireza Azhardi, Tareneh Hajiashrafi, Philip Provencher, Nick Cowper, Anita Restivo, Amy Kim, Kaylyn Leung, Margaret Hwu, Chris Tehennepe and Tin Nguyen for their support, laughs and adoption of the word "bear". I would like to particularly thank Carla grizzly bear Rigling who is the best friend and lab mate anyone could ask for; I'd like to thank Alex Dauth Vader for keeping our faith strong. I would also like to thank our past volunteer undergrad/close friend/study buddy/interview buddy Amy bear Kim who is awesome!

I'd like to thank my close friends I made in graduate school Kim Osten for our love of the same books/chapter's hot dates/McDonald's ice cream and "Jack" Jaklyn Chau who I could always count on to talk to at all hours of the day/night. I would like to thank everyone over at the First Nations House of Learning, my home away from home. I also thank the support I received as an undergrad from my amazing group, in particular Danica "Fluffiest" Rankic and supervisor Dr. Brian Keay who is like a second father to me. I am thankful for my excellent high school chemistry education from Colin Crichton who was the funniest/coolest person I ever met. Colin - you saved me from business school, you inspired me to become a chemist. I'm sure somewhere up there you are happy with my pursuit and still happy with my new endeavors.

Finally I would like to thank my wonderful family. I thank my parents Lolita and Gordon who always let me make my own decisions, follow any pursuit and were a 100% behind me in my career changes. I thank my brother Paul who is always my go to Treky I mean techy. I thank

my Godparents Brian and Sharon and their children Tony, Kristy and especially Jellofur/skenny Jenny. Last but not least I thank my loving fiancé Trevor Martin who knows me better than anyone, you make me a better person.

Dedication

For: Trevor Martin

and

Colin Crichton, may you rest in the chemistry heavens

1 Introduction

1.1 Neglected Global Diseases

At the Millennium Summit in 2000, the United Nations established a set of eight goals for positive global development, collectively known as the Millennium Development Goals.[1,2] Specific objectives of these goals include ending poverty, achieving universal education and establishing gender equality.[2] The sixth goal of the Millennium Development Goals is to combat HIV/AIDS, malaria, and other diseases.[1] However, what is not clearly stated in the Millennium Development Goals is a commitment to eradicate the many tropical diseases endemic to impoverished regions of the Americas, Africa and Asia. Collectively these diseases are referred to by the World Health Organization as neglected global diseases.[3] Unfortunately, as this group of illnesses remain largely localized to undeveloped and developing nations, they are often overlooked by the developed world, even though they affect hundreds of millions of people annually and together have just as much impact as the "big 3" (malaria, tuberculosis and AIDS).[4] To date, there are 13 neglected global diseases.[3] Generally, these diseases are classified into three categories based on the source organism for infection: infections caused by protozoa, such as Chagas' disease and Human African trypanosomiasis; bacterial infections, such as leprosy and trachoma and finally helminth infections (parasitic worms), such as schistosomiasis.[1]

Poverty, poor living conditions and lack of proper health infrastructure are common components to areas affected by these diseases. Poverty prevents healthy living environments and access to education, both of which can result in the spread of neglected global diseases. Neglected global diseases prevent citizens from reaching their potential, which further promotes their poverty. In the end, many of the Millennium Development Goals are intricately intertwined.[1] Unfortunately, since many of those who suffer from these diseases are impoverished; there is little economic gain in developing drugs for these diseases. Thus, research into drug development for treatment of these neglected global diseases has been limited.[5,6] In response to these challenges, several non-profit initiatives have emerged. One organization is the Drugs for Neglected Diseases Initiative

(DND*i*) located in Geneva, which started in 2003.[6,7] DNDi does not conduct its own research but acts as project manager that facilitates collaboration for clinical trials, media and drug development.[6,7] In the past few years various treatments have been produced. One example is a collaboration with Sanofi where they developed a fixed dose combination of artesunate and amodiaquine (Figure 1.1, **1** and **2**, respectively) for the treatment of malaria in Africa.[8]

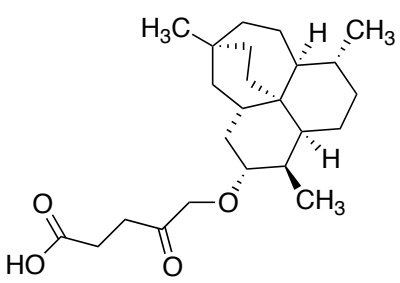

artesunate

1

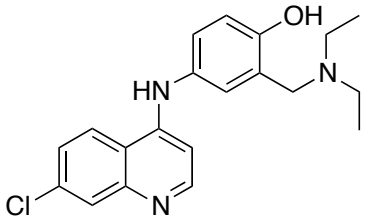

amodiaquine

2

Figure 1.1: Drugs developed in collaboration with Drugs for Neglected Diseases Initiative (DND*i*)

Another initiative is the Neglected Global Diseases Initiative (NGDI) at the University of British Columbia (UBC).[9] NGDI was created as a network of various research developments throughout the university that are involved in various aspects of neglected global diseases.[9] What is particularly advantageous is that this multidisciplinary network offers new perspectives and collaborations within the university. Current programs being explored are drug synthesis, vaccines, therapeutics, diagnostics and micronutrients.[9] Dr. Jennifer Love is a member of UBC NGDI.

1.2 Chagas' Disease

Chagas' disease (American trypanosomiasis) is one of the leading causes of heart failure in Latin America. Chagas' disease is caused by the protozoa Trypanosoma *cruzi* (T. *cruzi*) and is mainly spread by an insect host vector.[10,11] The insect vectors belong to the triatomine group, a subfamily of the family Reduviidae.[12] There are over 100 species of triatomine that can act as vectors.[13] T. *cruzi* is transmitted from organism to organism when the feces of an infected insect contaminate a mucosal surface, broken skin (e.g., an insect bite) or the lining of the eyes.[11] Both humans and animals can be infected. It is also important to note that T. *cruzi* can be obtained from non-vector based sources such as blood transfusions, organ transplants and food contamination, as well as through the process of child birth.[14-17] This results in human-to-human spread and potential human/animal spread from contamination with body fluids.

The World Health Organization estimates that there are roughly 10 million people currently infected with Chagas' disease and many more at risk, particularly those living in areas endemic to these diseases.[18] Furthermore, these regions are plagued by poor health infrastructure, which frequently leads to transmission of these diseases through non-vector based sources (as described above). Additionally, poor housing quality results in a higher frequency of insect infestations, which, in turn, leads to increased contact with disease carrying organisms.[11] However, due to ever increasing immigration and population mobility, Chagas' disease is starting to appear in various developed countries such at the United States, Japan and Australia.[19,20] In a study done by Schmunis and co-workers they estimated that there are 325,671 immigrants in the USA (2% of 16 689 172 South American immigrants) and 5,553 in Canada (3.5% of 156 960 of South American immigrants) currently infected.[19] Unfortunately, there is currently no vaccine available for preventative treatment of Chagas' disease. Nevertheless, there are several protocols for minimizing the spread of the disease.[18] These protocols include vector control, home improvements, personal preventive measures, good hygiene practices and screening for blood for donations and transplantations.[18]

T. *cruzi* enters the infected host in the trypomastigote stage. The site of inoculation is sometimes marked as a Chagoma (an inflamed site).[10] Once in the bloodstream of the host organism, the trypomastigotes enter the cytoplasm of host cells

where they become amastigotes, divide intracellularly, rupture and cause host cell damage (Figure 1.2).[21,22] The sites of tissue damage are mainly cardiac muscle and digestive tract.

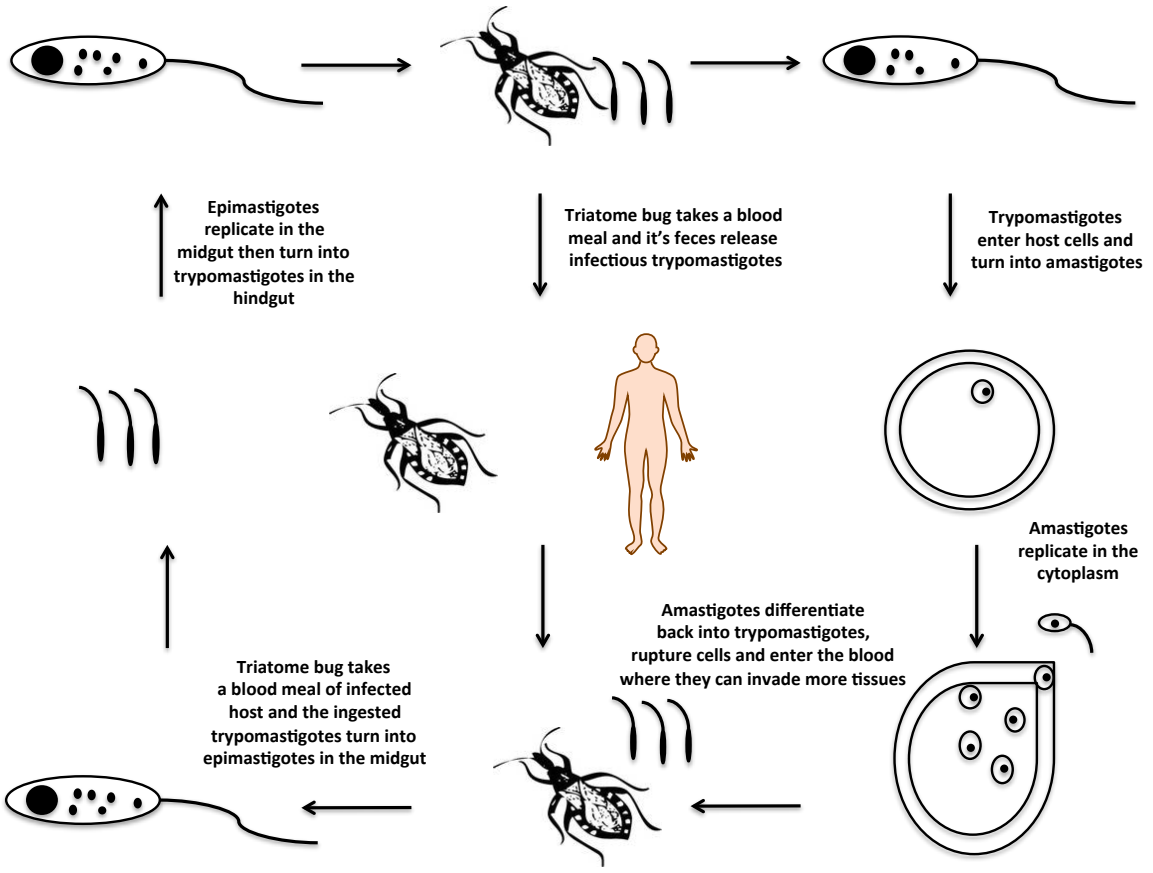

Figure 1.2: Life cycle of T. *cruzi*

The acute stage (initial short term stage) of illness, which typically lasts 2 months, is characterized by symptoms including: edema (accumulation of fluid) of the face and lower extremities, fever, generalized inflammation, skin lesions, swelling of eyelids (if this is the site of entry) and enlarged lymph glands.[10,11,13,23] During the acute stage, the parasite is present in the bloodstream of the host organism. Therefore, simple blood tests can be used as a means of identifying the presence of the disease.[18] Once out of the acute stage of illness, infected individuals enter the intermediate stage, which can last from months to an entire lifetime. At this stage, a definitive diagnosis can be made from positive serological tests for specific antibodies, absence of symptoms and absence of

electrocardiographic abnormalities signifying a dormant stage of the disease.[10,13] About 30% of those in the intermediate stage will progress to the chronic (long term) stage.[11] The main symptoms of the chronic stage are congestive heart failure, arrhythmias and thromboembolic events (blood clots); less common are digestive system syndromes such as dilation of the intestines (megacolon) and esophageal paralysis (megaesophagus).[10,11, 13,23]

1.3 Current Drug Therapeutics for the Treatment of Chagas' Disease

There are two drugs, both nitro heterocycles, currently being used for the treatment of Chagas' disease: benznidazole (**3**) and nifurtimox (**4**) (figure 1.3).[24-26] Neither of these drugs are approved in the United States or Canada but are available from the Centers for Disease Control and Prevention (CDC) for investigational protocols.[24, 25] These drugs target DNA structure and work predominantly only in the acute stage. However, there are several problems with the use of these drugs, including lengthy drug dosage regiments (benznidazole 5 mg/kg for 60 days, nifurtimox 10 mg/kg for 60 – 120 days), severe toxic side effects and increasing drug resistance. In addition, this treatment is not suitable for pregnant women and specific formulations for children are still needed.[24, 25]

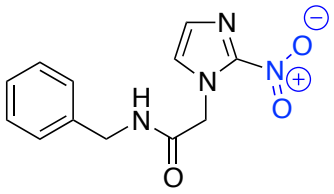

benznidazole

3

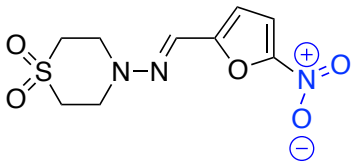

nifurtimox

4

Figure 1.3: Current therapeutics for the treatment of Chagas' disease

Side effects of benznidazole include bone marrow suppression, inflammation, rashes and peripheral neuropathy.[13, 25, 27] Nifurtimox affects the central nervous system and can cause irritability, insomnia, anorexia, disorientation and depression.[25, 27] Both benznidazole and nifurtimox are absorbed by the gastrointestinal tracts.[27] They are

metabolized in the liver and both are eliminated in the renal system. Benznidazole can also be excreted in feces.[27] The harmful side effects associated with both benznidazole and nifurtimox (thought to be caused by reactive nitro radicals such as nitro anion radical $RNO^{\bullet}_{2}^{-}$ and/or hydronitroxide free radical $RNHO^{\bullet}$.[25] These highly reactive intermediates react with DNA, lipids and proteins.[25] Both drugs are thought to be mutagenic and carcinogenic.[28-30] Thus, with the many downsides of the use of these drugs, and lack of drugs that work well in the chronic stages, new therapeutics are greatly needed.

1.4 Peptidomimetics as Key Therapeutics in Drug Design

Inhibition of the life cycle of pathogenic organisms and the inhibition of the machinery of viruses have been the targets of many therapeutics. Ideally, inhibition would occur at an enzyme that is vital to the organism or virus. Inhibitors can bind to the catalytic site of the enzyme preventing association of the substrate or they can allosterically inhibit the enzyme by binding to a non-catalytic site, promoting a conformational change in the enzyme.

One possibly strategy involves the use of peptidomimetics. These molecules resemble the natural substrate of an enzyme and can act as competitive inhibitors of a given enzyme's catalytic site.[31] The development of peptidomimetic inhibitors begins with structure-activity relationship studies (SAR) to identify key chemical moieties that are important biologically. Peptidomimetics are particularly advantageous as they are designed to be very specific. Non-specific treatments from other therapeutics can cause many side effects. An example of a peptidomimetic is the HIV protease inhibitor indinavir (crixivan) (**5**) developed by Merck. This particular drug has been available since the mid 90's.[32,33] Another example is odanactib (**6**), a cathepsin K (cysteine protease) inhibitor, which is currently in phase three clinical trials for the treatment of post-menopausal osteoporosis.[34-36]

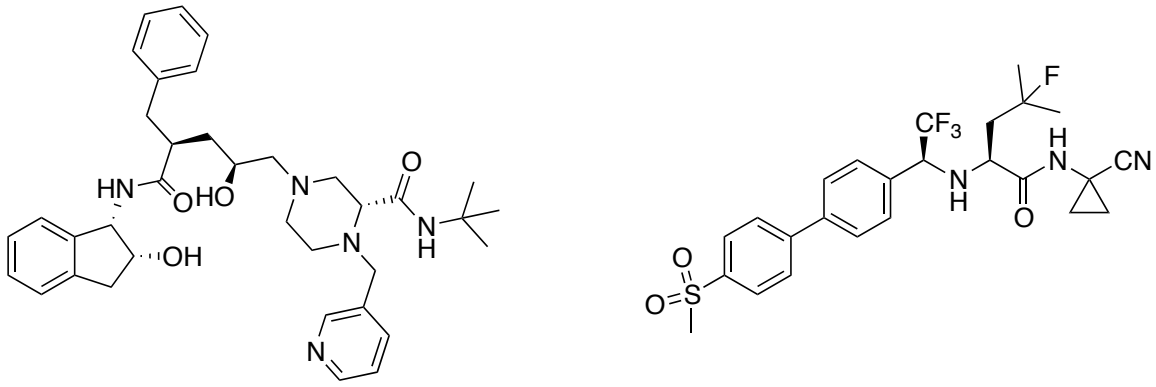

indinivir

5

odonacatib

6

Figure 1.4: Examples of peptidomimetics

Several targets of interest have been examined over the last two decades as potential sites of chemotherapy for Chagas' disease. To date, two of the largest areas explored have been the inhibition of sterol synthesis and the inhibition of cruzain - a cysteine protease essential to the lifecycle of the protozoa *T. cruzi*. Anti-fungal agents such as posaconazole (**7**) and ravuconazole (**8a**) inhibit C14 Lanosterol demethylase, an enzyme critical for ergosterol synthesis and successful growth of the pathogen.[6, 37-39] Posaconazole is currently entering phase two clinical trials.[6] However, despite not having FDA approval, posaconazole has been already used successfully in the treatment of Chagas' disease. In this particular case, posaconazole was used to treat a patient who had systemic lupus erythematosus and chronic Chagas' disease. Treatment of lupus involves using immune-suppressing drugs that would be threatening for a person who had chronic Chagas' disease. The patient was administered posaconazole (800 mg/ day for 90 days) and is currently free of parasitic infection.[6,40] Unfortunately, posaconazole is very costly and difficult to synthesize.[6] The prodrug E12-24 (**8b**) of ravuconazole is currently entering phase two clinical trials under the guidance of DND*i*.[6,38,39,41]

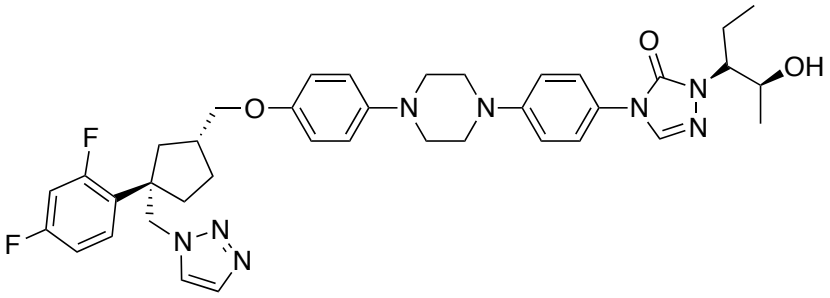

posaconazole

7

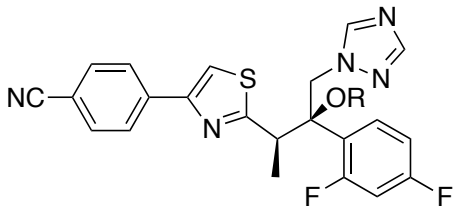

ravuconazole **8a** R = H

E-1224 **8b** R= $CH_2OPO_3H_2$

Figure 1.5 Inhibitors of ergosterol biosynthesis

Many therapeutic interventions employ protease inhibitors to induce cell cycle arrest. Proteases are enzymes that catalyze the cleavage of peptide bonds. When they break down interior protein peptide bonds they are referred to as proteinases or endoproteases. When they cleave peptides at the amino or carboxy terminus they are called exopeptidases. Proteases can be classified based on their catalytic site. Serine proteases use the hydroxyl moiety of serine in their catalytic site (catalytic triad), whereas cysteine proteases use the thiol moiety of cysteine in their catalytic site. Aspartyl proteases use two aspartyl groups, whereas metalloproteases use a metal ion in their active site.[42] The classifications of proteases are important, as they hint to the function of the protease. Proteases are essential for degradation and activation of various proteins in an organism. Specifically in parasitic protozoa they can be used for the metabolism of host molecules for energy, immune evasion (breaking down host immune molecules) and breakdown of important cytoskeletal proteins in host molecules to name a few. Since they

are crucial to the life cycle of protozoa, inhibitors of specific proteases can be very useful.[42]

Cysteine proteases in general have been therapeutic targets for numerous diseases including malaria, schistosomiasis and African sleeping sickness.[36,43-45] Cruzain is the key cysteine protease in T *cruzi* and is thus thought to play an important role in the life cycle of T. *cruzi*. It is thought to play a role in cell differentiation, replication and processing/breakdown of host molecules in lysosome like – vesicles called reservosomes [42,46] Cruzain is a glycoprotein and is homologous in structure to cysteine proteases such as papain (found in papayas, commonly used in meat tenderizers as it is non-selective) and the cathepsins (mammalian cysteine protease inhibitors).[47] The gene sequence of cruzain is very similar to the gene sequence of the cysteine protease in Trypanosoma *brucei*, the causative organism of African sleeping sickness (59% similar) and that of cathepsin L (42% similar).[21] The protease is expressed in all parasitic stages but more often in the amastigote stages.[21] The catalytic triad is composed of cysteine 25, histidine 159 and aspargine 175 residues.[22]

Many of the original inhibitors for cruzain were developed for other cysteine proteases, such as the previously mentioned proteases papain and the cathepsins.[48-50] Cathepsins are mammalian cysteine proteases that perform protein degradation intracellularly and are found predominantly only in the lysosome.[51] Exocytosis (secretion to extracellular environment) of cathepsins was found to be irregular and an indication of a diseased state. The presence of these proteases in an atypical area is thought to cause harmful degradation in that location.[52] Inhibition of cathepsin S has been chosen as a target for inflammation, cathepsin K for Osteoporosis and capthepsins B and L for oncology targets.[51]

There are many different types of inhibitors for cysteine proteases. Generally, these inhibitors can be divided into reversible inhibitors and irreversible inhibitors.[53, 54] Reversible inhibitors include peptidyl aldehydes, nitriles and α-ketocarbonyl compounds.[55-57] These inhibitors form short-lived intermediates and are thus, reversible. Irreversible inhibitors include peptide halomethyl ketones, diazomethyl ketones and vinyl sulfones.[48, 53, 58] Irreversible inhibitors form stable products with the enzyme and are thus irreversible (Schemes 1.1-1.3). Scheme 1.1 shows two possible mechanisms for

peptide halo methyl ketones. The first mechanism **A,** involves the attack of a cysteine residue in the catalytic site to the electrophilic carbonyl, forming a tetrahedral intermediate. The nucleophilic sulfur of the thioether moiety then undergoes a substitution reaction to cleave the leaving group X forming a three-membered ring episulfonium ion. When the tetrahedral intermediate collapses the three-membered ring opens forming an *alpha*-ketothioether. The resulting *alpha*-ketothioether is stable and the thioether residue cannot be cleaved from a substitution reaction with weak nucleophilic leaving groups such as fluoride (Scheme 1.1). The second mechanism **B** involves a direct displacement of the leaving group X with the nucleophilic cysteine residue to give the same product (Scheme 1.1). Diazo methyl ketone inhibitors also form *alpha*-ketothioethers (Scheme 1.2). The first step of this mechanism also involves forming a tetrahedral intermediate with cysteine, followed by protonation by a nearby protonated histidine residue. A very good leaving group (positively charged dinitrogen) is now present that undergoes a substitution reaction with the thioether moiety to release nitrogen gas, forming an episolfonium ion. The three-membered ring of the episulfonium ion is then opened upon collapse of the tetrahedral intermediate to give an *alpha*-ketothioether. Since nitrogen gas is a poor nucleophile the reverse reaction will not take place, rendering this pathway irreversible (Scheme 1.2). Finally vinyl sulfone inhibitors act as potent Michael-acceptors. In the catalytic site, nucleophilic cysteine does a 1,2-addition to the vinyl sulfone. One of the oxygen on the vinyl sulfone initially accepts a proton from a nearby protonated histidine residue. Upon tautomerization the Michael-addition product is formed and is further stabilized by a near by histidine residue (Scheme 1.3).

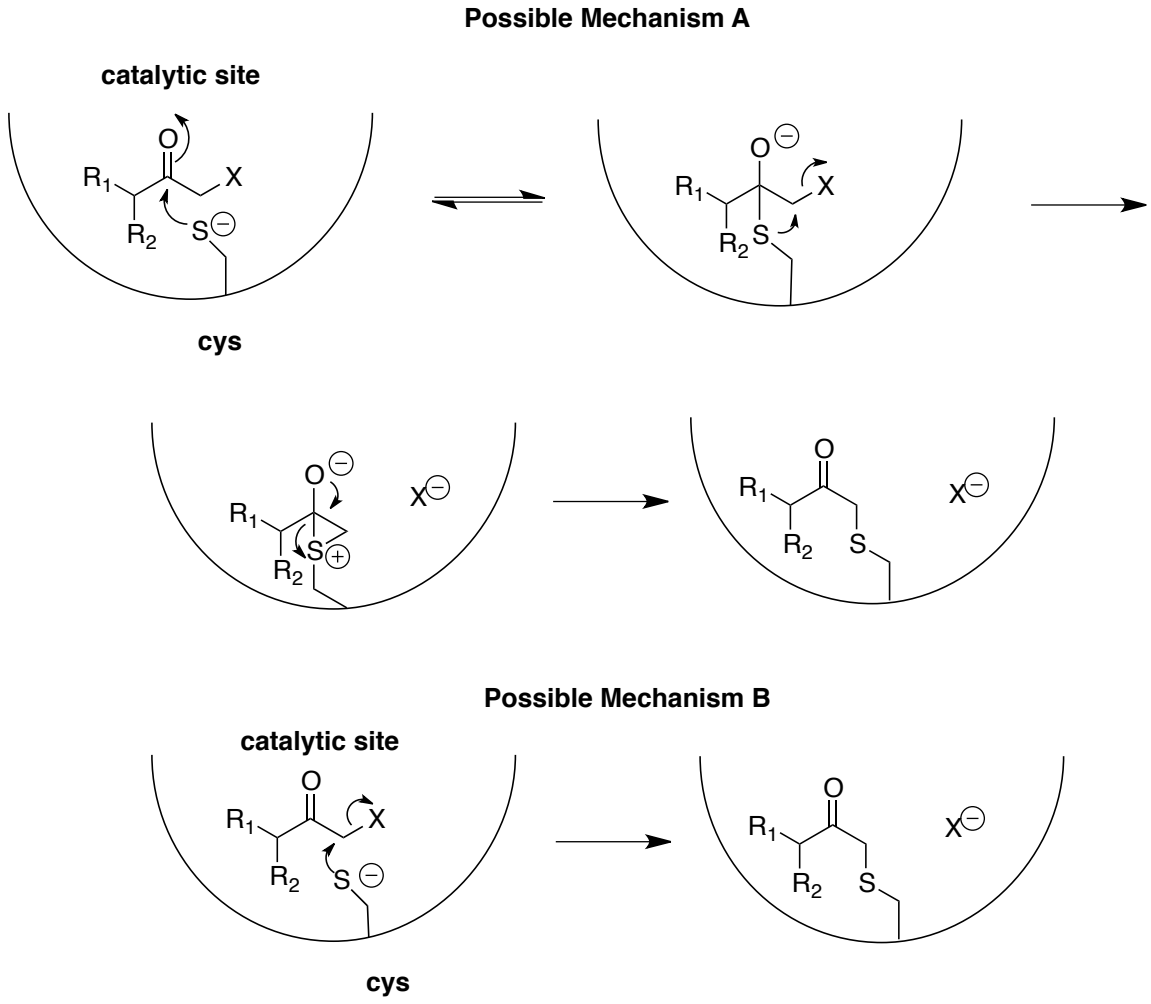

Scheme 1.1: Peptide halo methyl ketone inhibitors

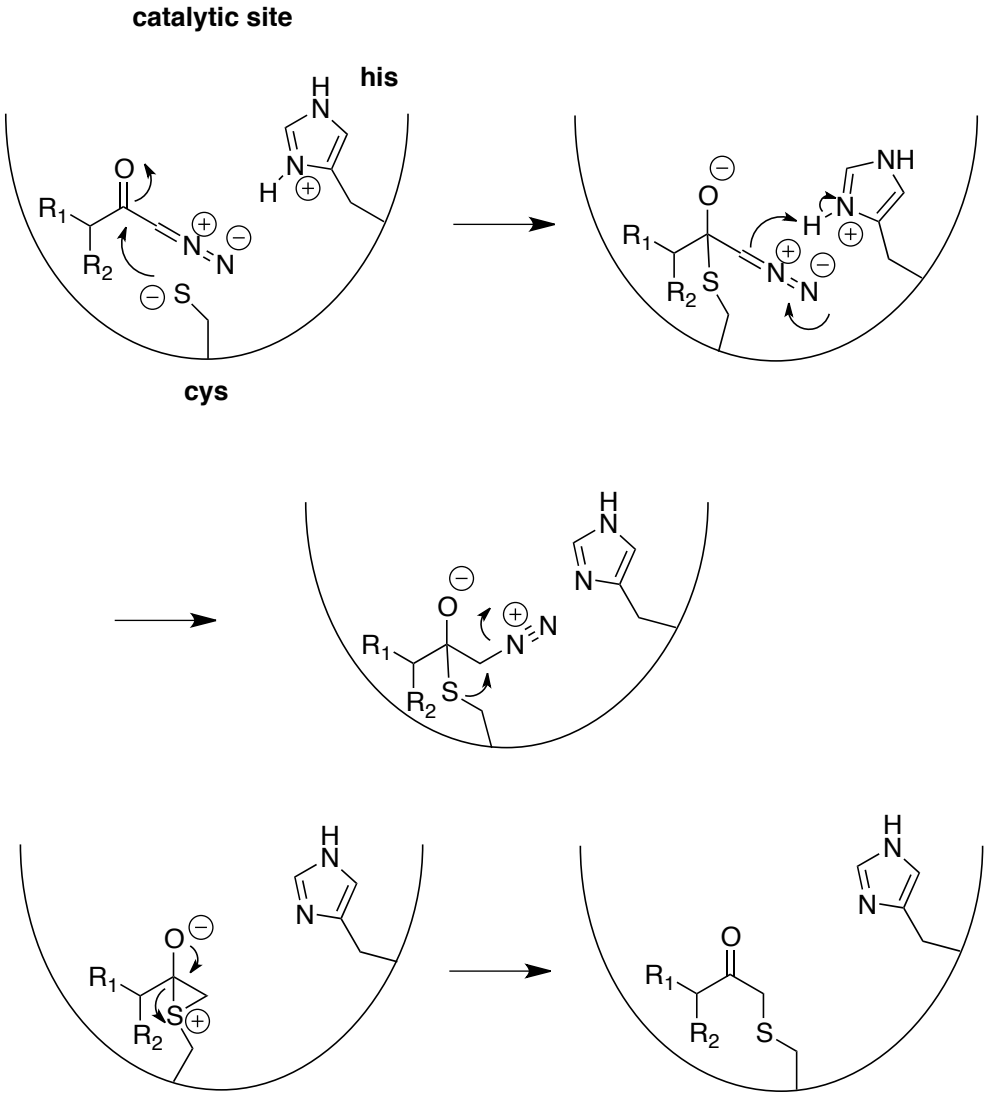

Scheme 1.2: Diazomethyl ketone inhibitors

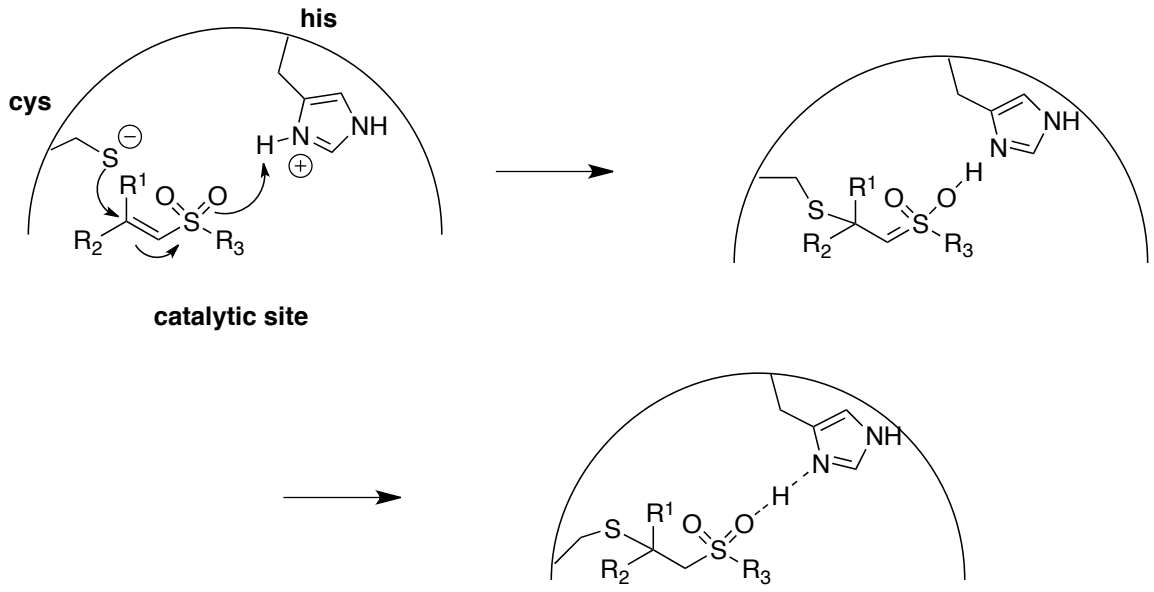

Scheme 1.3: Vinyl sulfone inhibitors

Initial investigations focused on the use of peptide fluoromethyl ketones (PFMK's) as they showed promise in early studies. The fluoro-peptide fragment (PFMK Z-Phe-AlaCH_2F) **9** was first synthesized by Rasnick and was found to inhibit Human cathepsin B.[48] A similar peptide fragment (**10**, PMFK Z-Ala-PheCH_2F) was subsequently shown in the early 90's to cause lysis of T. *cruzi* epimastigote cells. This result demonstrated the importance of a cysteine protease in the life cycle of T. *cruzi.*[59] Related compounds such as Z-Phe-AlaCH_2F **10** and Z-Phe-ArgCH_2F **11** also showed abilities to arrest intracellular replication and intercellular transmission of T. *cruzi* in mouse macrophages.[60] Research in the area progressed until it was found that the PMFKs were metabolized to fluoroacetate - a highly toxic metabolite.[61]

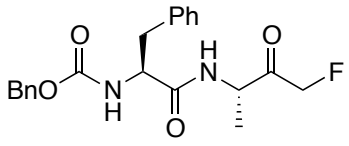

Z - Phe-AlaCH_2F

9

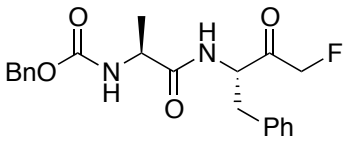

Z - Ala-PheCH_2F

10

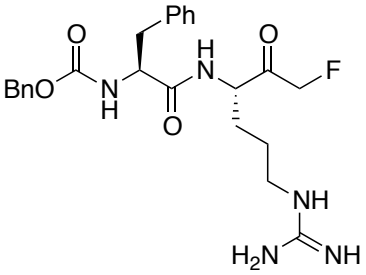

Z - Phe-ArgCH_2F

11

Figure 1.6: Peptide fluoro methyl ketones (PMFK)

During the same time, a different approach to peptidomimetic-based therapies was being explored by Palmer and co-workers. This approach is based on the potential for Michael acceptors to act as inhibitors (Scheme 1.3, page 13).[49,50] To this end, Palmer and co-workers designed potent inhibitors to be tested on cathepsins B, L, S and O2, calpains and cruzain, with a vinyl sulfone as the Michael acceptor.[53] Vinyl sulfones were anticipated to be more inert than vinyl ketones or esters. Therefore, these inhibitors would be unreactive to various proteases, including serine proteases and aspartyl protease and free thiols, such as glutathione.[53] Of additional importance is that the vinyl sulfone would be able to hydrogen bond in the active site thus increasing the binding affinity of these vinyl sulfone inhibitors of various cysteine proteases. The following figure outlines the peptide design and mechanism. P_1, P_2, etc. represent residues on the amino side of the peptide to be cleaved. P_1', P_2', etc. represent residues on the carboxy side of the peptide bond to be cleaved. S_1, S_2 etc. represent the enzyme binding site for residues on the amino side of the peptide to be cleaved, whereas S_1', S_2' represent the enzyme binding site for residues on the carboxy side.

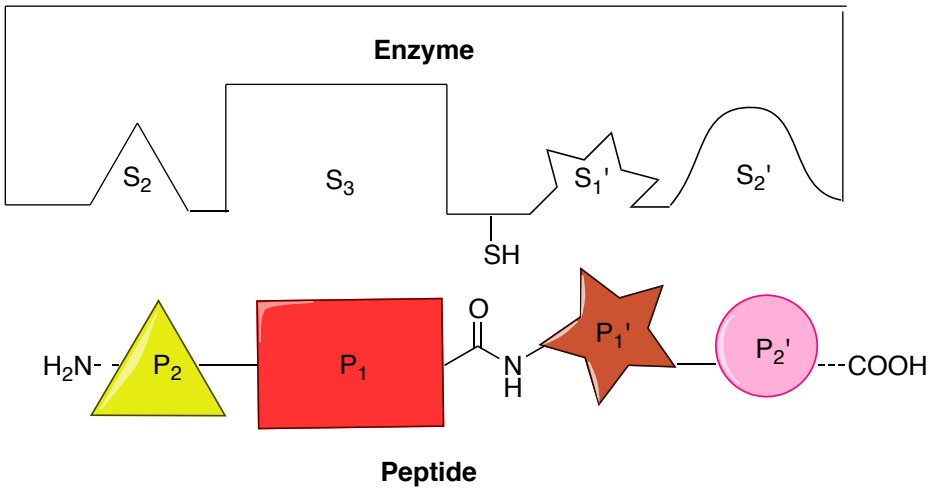

Figure 1.7: Catalytic binding site

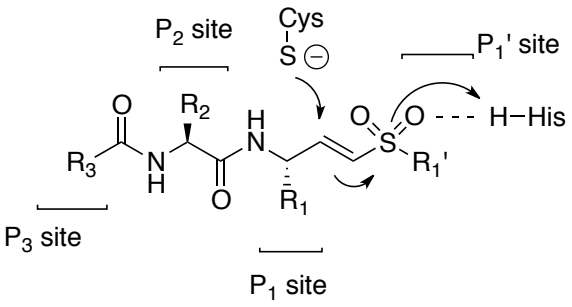

Figure 1.8: Basic vinyl sulfone inhibitor structure

To this day, numerous variations of vinyl sulfone inhibitors have been synthesized and screened for activity with cathepsins, cruzain and many other cysteine proteases. The various peptide sites (P_1, P_2, etc.) have been manipulated based on inhibition studies and crystal structures of inhibitors co-crystallized with proteases.[51,62-67] The S_1' site binds aromatics with tethers between the aryl group and sulfone sufficiently well. If the P_1' site contains only a phenyl ring, this does not make optimal interactions (π stacking). [64,65] The S_2 pocket is outlined with hydrophobic residues, which explains the majority of hydrophobic residues at the P_2 site of an inhibitor. However there is a glutamate at the bottom of the hydrophobic pocket, which can interact with positively charged side chains when appropriate (arginine) and turn away when hydrophobic side chains occupy the P_2 site.[65,67,68] The P_3 site has been manipulated for bioavailability (ability for oral

intake).[69,70] Finally, the P_1 site has been manipulated to have residues that are robust and unable to be cleaved.[65,69]

K11002 (**12**) was one of the first scaffolds to show potency against cruzain. [53] However the morpholine subunit decreased bioavailability.[69,70] K777 (**13**) is another potent inhibitor of cruzain that contains an *N*-methylpiperazine group which increased bioavailability. [67,69,70] The *N*-methylpiperazine group is more soluble in intestinal fluids than the morpholine urea moiety.[70] K777 has also been used in many other cysteine protease studies. For example, several studies have established K777 to be an inhibitor of the cysteine protease of Trypanosome *brucei* - the organism responsible for Human African Sleeping sickness. In addition, K777 has also recently been indicated as a potential inhibitor for the cysteine proteases of Tritrichomonas *foestus* a sexually transmitted organism that causes birth problems in cattle and genital inflammation.[43,71]

Given the promising results obtained by Palmer and others, several other vinyl-sulfone containing peptidomemitic therapeutics have been developed. These include, APC 3328 (**14**): a potent inhibitor of cathepsin K (a protease that is related to osteoclast maladies).[63] K11017 (**15**) has been shown to be an inhibitor of cathepsin B1 an important protease for the organism Schistosoma *monsoni*, the causative organism of schistosomiasis (parasitic worm disease).[45] It is worth noting that K11017 (**16**) has also been used as an inhibitor of the cysteine proteases of the falcipains, which are key proteases in Plasmodium *falciparum* the causative organism of malaria.[36,44,45] Finally another potent inhibitor of cruzain is WRR-483 (**16**).[72]

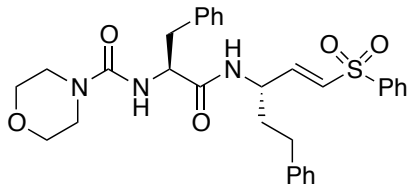

K11002

(**12**)

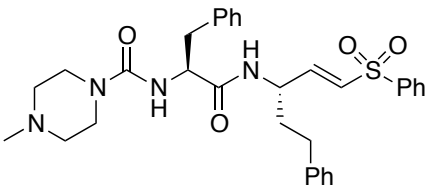

K777

(**13**)

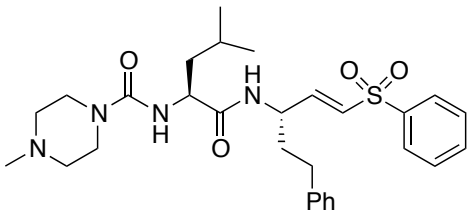

APC 3328

(**14**)

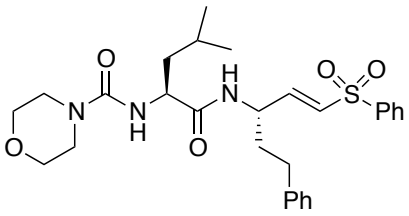

K11017

(**15**)

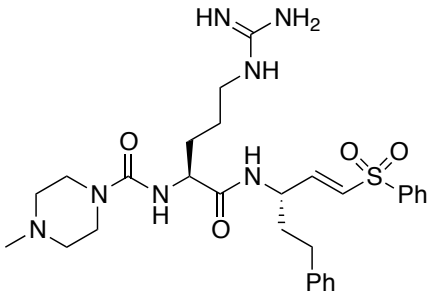

WRR-483

(**16**)

Figure 1.9: Examples of cysteine protease inhibitors containing vinyl sulfone moieties

1.5 K777- A Cysteine Protease Inhibitor of Cruzain

Of the many inhibitors listed previously, K777 is the leading cysteine protease inhibitor based therapeutic for treatment of Chagas' disease.[6,37,73,74] There have been several proof of principle clinical studies done on K777 as an inhibitor of cruzain. Firstly, K777 has been shown to cure mice from an acute stage of a lethal T. *cruzi* infection.[69] K777 has also demonstrated its ability to clear parasitemia in chronically infected mice without toxic side effects.[69] In addition, K777 was also used to decrease myocardial damage in infected dogs.[75] However, there are many concerns that arise with cases where

the host is in an immunocompromised state. Patients who have immune deficiencies such as HIV are at greater risk with therapeutics that have harmful side effects. Clinical studies have shown K777 to be effective in rescuing immunodeficient mice infected with T. *cruzi*, which demonstrates its versatility.[76] Multiple strains of T. *cruzi* have been inhibited by K777, which is critical in combating potential drug resistance.[74, 76] With many of these good results and initial absence of toxicity K777 was FDA approved to enter pre-clinical trials.[6, 74]

Based on the oral dosages of mouse and dog studies, it has been proposed that an oral dosage of ~ 10 mg/kg for 14-30 days may be the administration framework for K777.[74] The time frame is half the time frame required for administration of benznidazole and nifurtimox. Decreased length of time is not only more convenient but lowers the risk of side effects due to prolonged treatments. This proposed dosage is also within the guidelines set out by the WHO for a new drug for Chagas' disease.[74] K777 has now undergone primate, rodent and dog testing.[74] Based on the results obtained from rodent-based tests, the tolerated maximum dosage was found to be 150 mg/kg/day and the NOAEL (no adverse effect level) was 50 mg/kg/day. This study was completed by SRI International (Stanford Research Institute) in conjunction with the National Institute of Allergy and Infectious Diseases (NIAID).[74]

However, despite all of the promising results obtained thus far, in 2005 the progress of K777 towards clinical implementation was stalled due to signs of hepatotoxicity (liver toxicity). At high dosages (200 mg/kg in monkeys and 100 mg/kg in dogs) elevated concentrations of alanine aminotransferase (ALT) were found.[74] Elevation in ALT can be related to hepatotoxicity.[74] However, the proposed dosage for monkeys/dogs (50 mg/kg) is much lower than the dosage required to observe elevated levels of ALT.[74] In rodent studies done by the NIAID they found that elevated ALT levels were observed with dosages above 150 mg/kg. But at even higher levels (300 mg/kg), liver damage was reversible with therapy.[74]

The metabolic break down of K777 has also been studied. Jacobsen conducted an *in vitro* study with liver monooxygenases. Using HPLC/UV and HPLC/MS detection, 3 metabolites were found.[70] These metabolites were *N*-des methyl K777 (**17),** *N*-oxide K777 (**18**) and β-hydroxy hPhe K777 (**19**). CYP3A enzymes were proposed to catalyze

this process. CYP3A enzymes are members of the cytochrome P_{450} super family of important enzymes used for the metabolism of xenobiotics (chemicals not normally found in the body). It has been previously mentioned that K777 (~19%) has increased bioavailability in comparison to K11002 (2%).[70] However, the bioavailability of K777 is still relatively low. The low bioavailability could be a consequence of K777 being a substrate for CYP3A enzymes. These enzymes are not only found in the liver but are also common in intestinal mucosa. It has been proposed that low bioavailability of drugs can be attributed to first-pass metabolism of these compounds in the intestines.[70,77-79] Jacobsen also demonstrated that K777 could also inhibit CYP3A enzymes. This could have a substantial effect on co-administered drugs that are normally metabolized by CYP3A enzymes.[70]

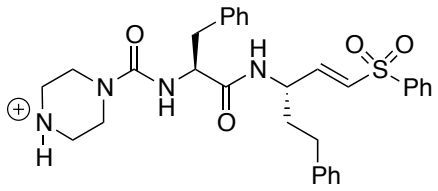

***N*-desmethyl K777**

17

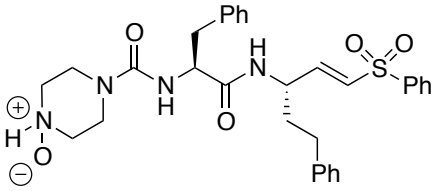

***N*-oxide K777**

18

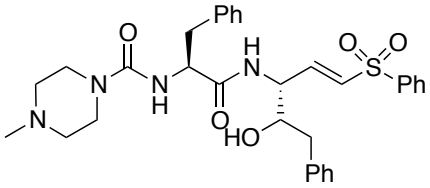

***B*-hydroxy homoPhe K777**

19

Figure 1.10: Proposed metabolites of K777

1.6 Synthesis of K777

The first synthesis of K11002 was reported by Palmer in 1995.[53] Subsequent syntheses of various analogues of K11002, including K777, have followed a similar strategy.[51] Indeed, in each synthesis the critical vinyl sulfone moiety was obtained through standard olefination chemistry. Further retrosynthetic analysis reveals that the rest of the compound can be obtained from a series of peptide couplings. On this basis,

K11002 and related structures can be easily obtained from the union of these fragments. A simple retrosynthetic approach to this general class of compounds is depicted in scheme 1.1. The dipeptide is formed from standard peptide coupling protocol from two residues, a functionalized amino acid and vinyl sulfone with a free amino group. The functionalized amino acid is made from coupling conditions involving phosgene and a group R_3 (morpholine, *N*-methylpiperizine etc.). The vinyl sulfone is normally achieved from olefination reactions of an aldehyde. The aldehyde is achieved from selective reduction of an amino acid or reduction to the alcohol, followed by oxidation to the aldehyde.

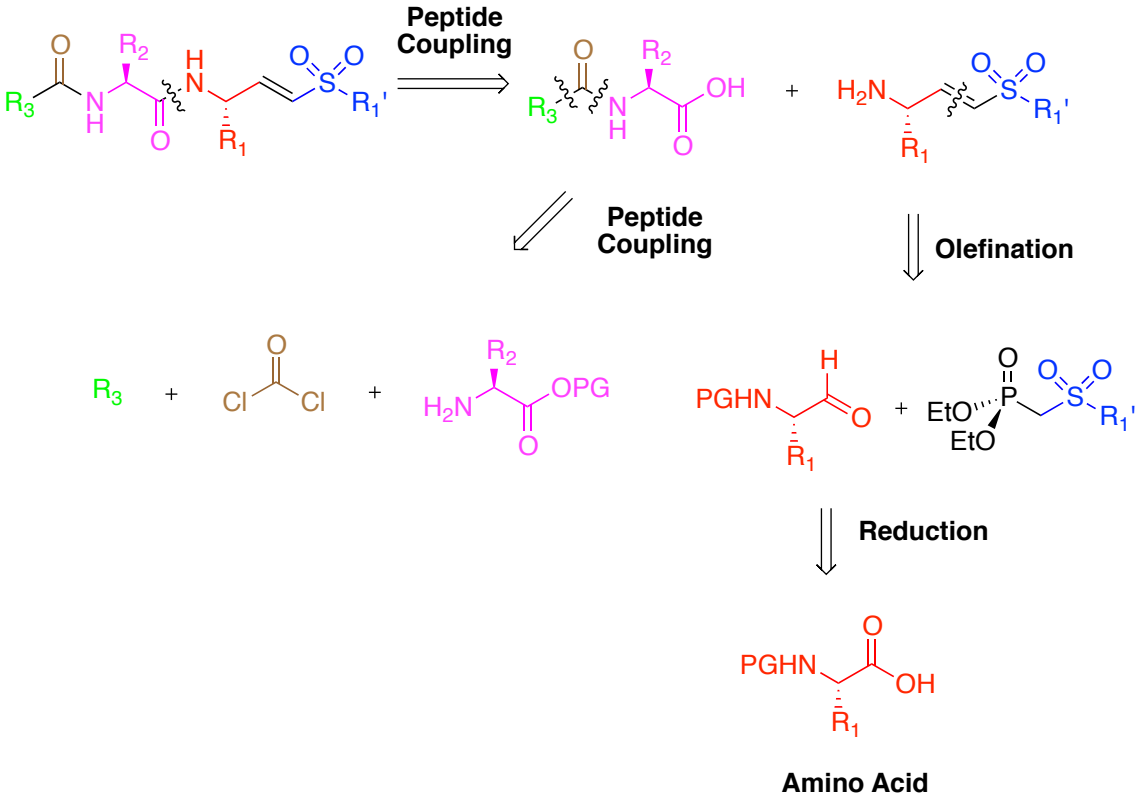

Scheme 1.4: General synthetic strategy of peptidyl vinyl sulfone analogues

The synthesis of K777 commences with the unnatural and expensive amino acid homophenylalanine (**20**) ($24,194/mol TCI America). The protected amino acid (**21**) can be purchased ($32,681/mol Sigma Aldrich). The protected acid was converted to the corresponding Weinreb amine (**22**) in 98% unpurified yield. Weinreb amide **22** is further reduced to aldehyde **23** in 100% yield (unpurified).[80] Aldehyde **23** undergoes a Horner-

Wadsworth-Emmons (HWE) olefination to yield the desired vinyl sulfone (**24**), reportedly in 100% yield (unpurified)[81] The HWE reagent (**25**) is made from the oxidation of diethyl phenylthiomethylphosphonate **26** with peracetic acid in 100% yield. Subsequent removal of the *tert*-butyloxycarbonyl protecting group was accomplished using *p*-TsOH to give the corresponding salt in 76% yield from **23**.[51]

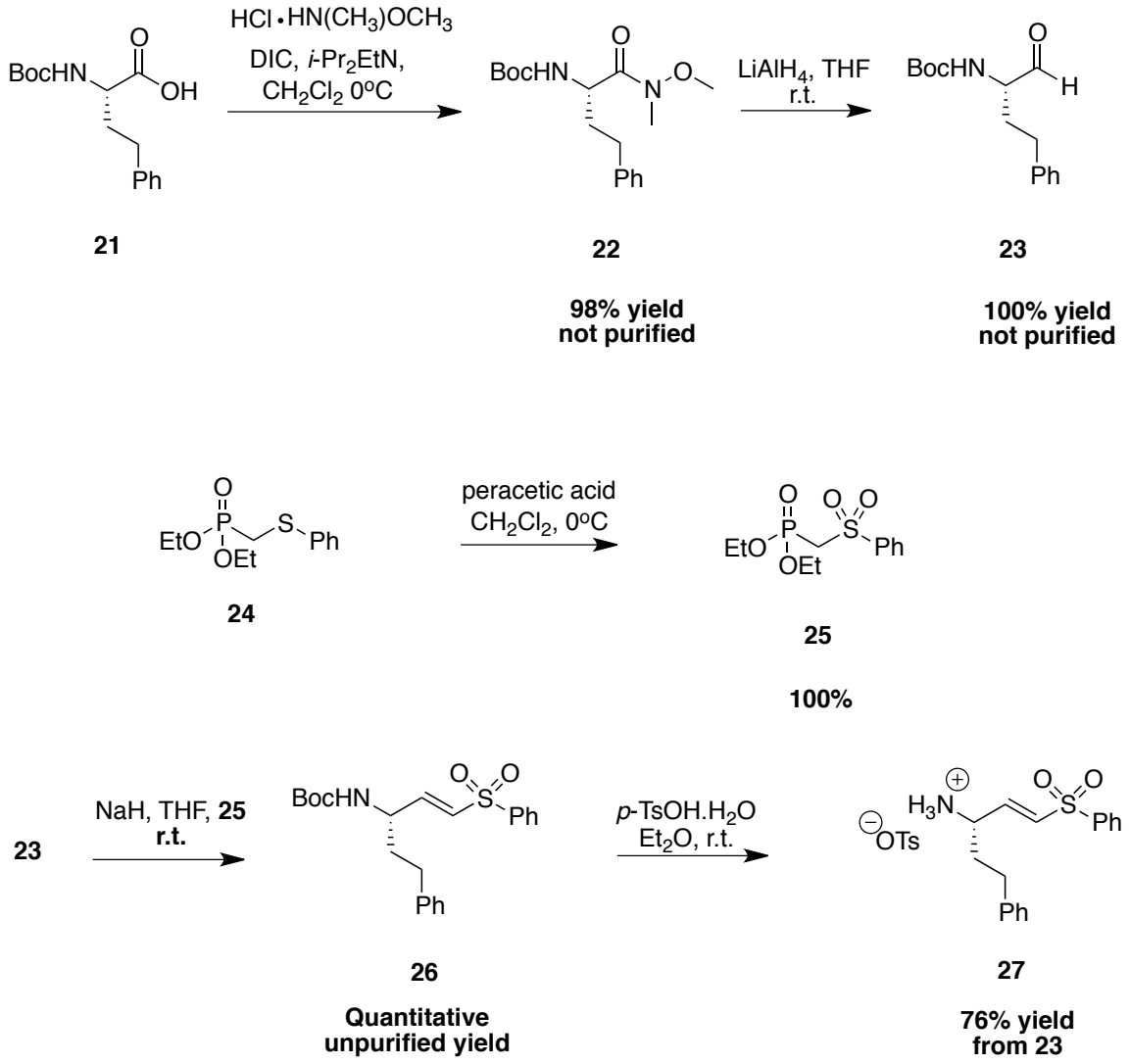

Scheme 1.5: Palmer's synthesis of the compound 27

The remaining synthesis of K777 begins with the (*S*)-benzyl-2-amino-3-phenylpropionate hydrochloride (HCl.PheOBzl) **28**. Benzyl ester **28** was reacted with phosgene to yield the corresponding isocyanate **29** in 85% yield. Isocyanate **29** was

subsequently combined with *N*-methylpiperazine to give **30** (no yield reported). The benzyl group was removed by hydrogenation to give **31** in 93% yield. Peptide **31** was then subjected to coupling conditions using 4-methyl morpholine to suppress racemization and isobutylchloroformate with salt **27** to yield the tosylate salt of K777 (**32**) in 62% yield. The tosylate salt of K777 (**32**) was then converted to the HCl salt of K777 (**33**) in 94% yield. The overall yield of the eight-step synthesis was 34%.[51]

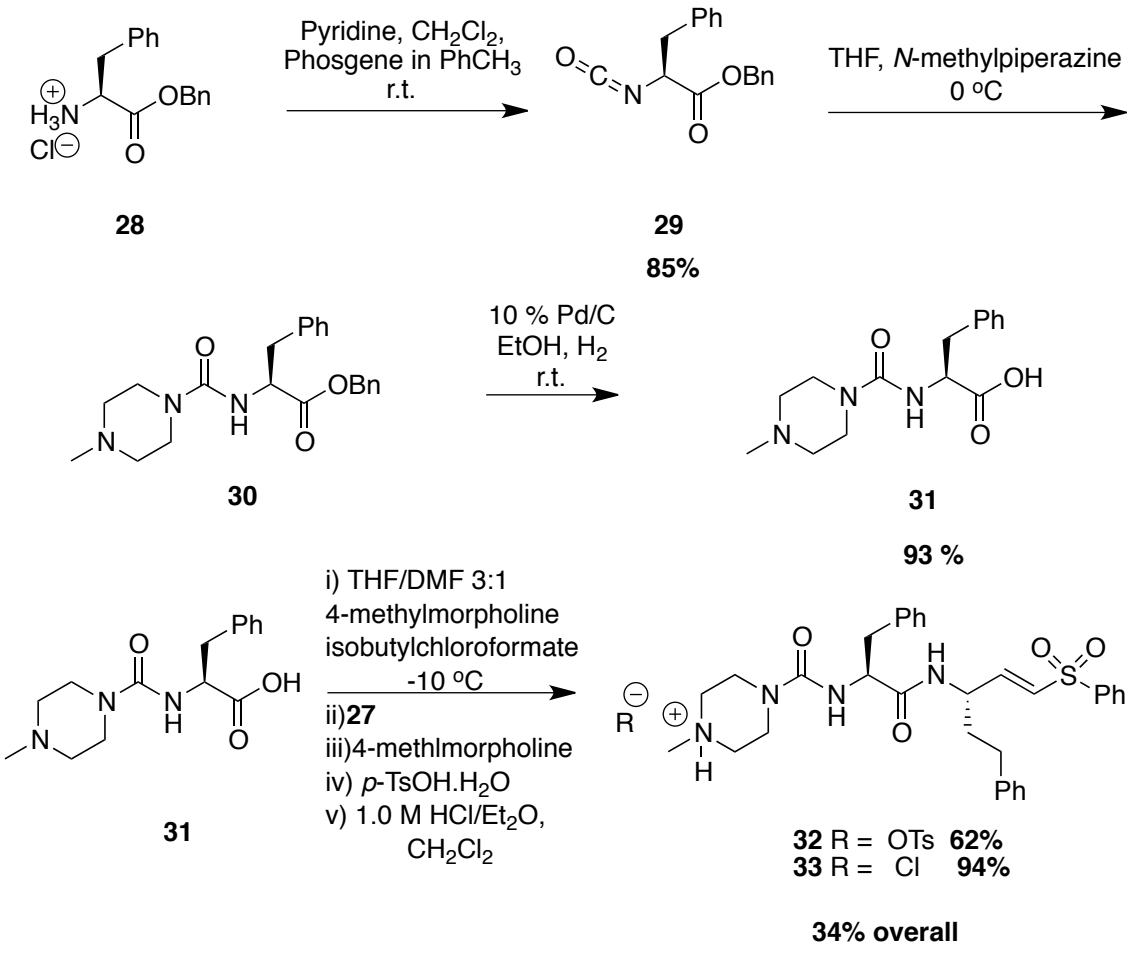

Scheme 1.6: Palmer's synthesis of the left peptide moiety

Notwithstanding the short number of steps to reach K777, there are several limitations in this synthesis: the cost of the starting material, the requirement to make the HWE reagents/atom efficiency of HWE and the use of toxic phosgene. Other analogue syntheses are similar differing only in the types of amino acid residues used and peptide coupling conditions. Unfortunately, many of these published routes require the use of

HOBT (hydroxybenzotriazole) a racemization suppressor with a variety of coupling agents.[44,64,72] HOBT is dangerous to handle and deliver, as it is an explosive.

1.7 Catalytic Alkyne Hydrothiolation as a Proposed Means to the Synthesis of K777 and Analogues.

K777 is of special interest to our research group as its potent "warhead" moiety, a vinyl sulfone, can be readily synthesized by means of rhodium-catalyzed-alkyne hydrothiolation, a methodology being developed in our research laboratory. On this basis, we proposed to synthesize K777 and analogues as a proof of principle of our methodology in synthesis.

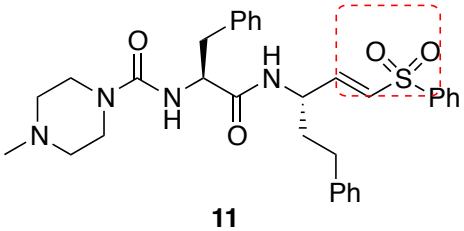

11

Figure 1.11: K777 "Warhead"

Vinyl sulfides and vinyl sulfones are not only desirable synthetic targets but can also be used as key intermediates in a variety of syntheses.[82] For example, they can be used as enolate equivalents, masked carbonyls, cross-coupling partners in Kumada coupling and Michael acceptors among many other reactions.[83-86] Vinyl sulfides can be synthesized in a variety of different ways such as nucleophilic substitution of vinyl halides and Wittig reactions.[87-92] However *E* and *Z* selectivity can be an issue in synthesis.[93]

Alkyne hydrothiolation is a method for synthesizing various vinyl sulfide isomers.[93] Alkyne hydrothiolation involves adding an S-H bond across the π bond of an alkyne. The reaction can yield three isomers, an *E*-linear isomer, a *Z*- linear isomer and a branched isomer.[93] The reaction can be conducted through nucleophilic attack reactions, transition-metal-mediated-catalysis and free radical addition.[90,94-98] For many years, most

protocols produced *Z*-linear isomer and the branched isomer. There were few protocols that favor the *E*-linear isomer selectively.

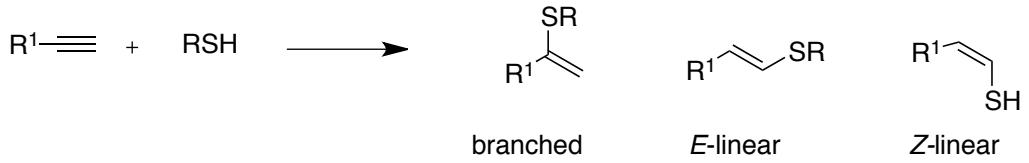

Scheme 1.7: Isomers of alkyne hydrothiolation

Transition metal-catalyzed hydrothiolation as a method for producing vinyl sulfides has many advantages. These reactions can be regio- and stereoselective and are 100 % atom economical. The desired vinyl sulfide for the synthesis of K777 is an *E*-linear vinyl sulfide. In 1992 Ogawa and coworkers reported the first transition-metal-catalyzed production of *E*-linear vinyl sulfide.[94,97] Wilkinson's catalyst ($ClRh(PPh_3)_3$) (**34**) was found to work well for aryl thiols but did not work for aliphatic thiols.[94,97]

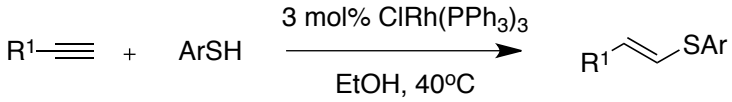

Scheme 1.8: Ogawa's conditions of Wilkinson's catalyzed alkyne hydrothiolation

The Love group demonstrated that a different rhodium catalyst, $Tp^*Rh(PPh_3)_2$ (**35**), produces mainly the branched isomer.[99,100] In the course of that work, we discovered that Wilkinson's catalyst does indeed catalyze alkyne hydrothiolation with aliphatic thiols thiols upon optimization of solvent conditions.[93,101] The Love group demonstrated that Wilkinson's catalyst gives predominantly the *E*-linear isomer with modest amounts of the branched product. [93,101]

Scheme 1.9: Major products of metal-catalyzed alkyne hydrothiolation

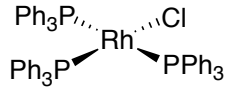

Wilkinson's Catalyst

34

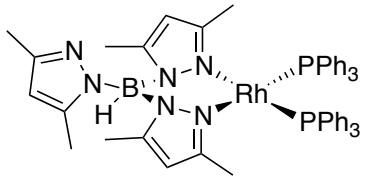

$Tp^*Rh(PPh_3)_2$

35

Figure 1.12: Catalysts used in alkyne hydrothiolation

The mechanism of both of the aforementioned catalyzed reactions is currently under investigation in the Love group. The following figure is the current proposed mechanism of rhodium-catalyzed alkyne hydrothiolation using Wilkinson's catalyst. The mechanism begins with oxidative insertion of the S-H bond into the Rhodium pre-catalyst. Alkyne coordination follows and then 1,2-insertion into the Rh-H bond. Finally, reductive elimination provides the vinyl sulfide and another oxidative addition of an S-H bond regenerates the catalyst.[93,98]

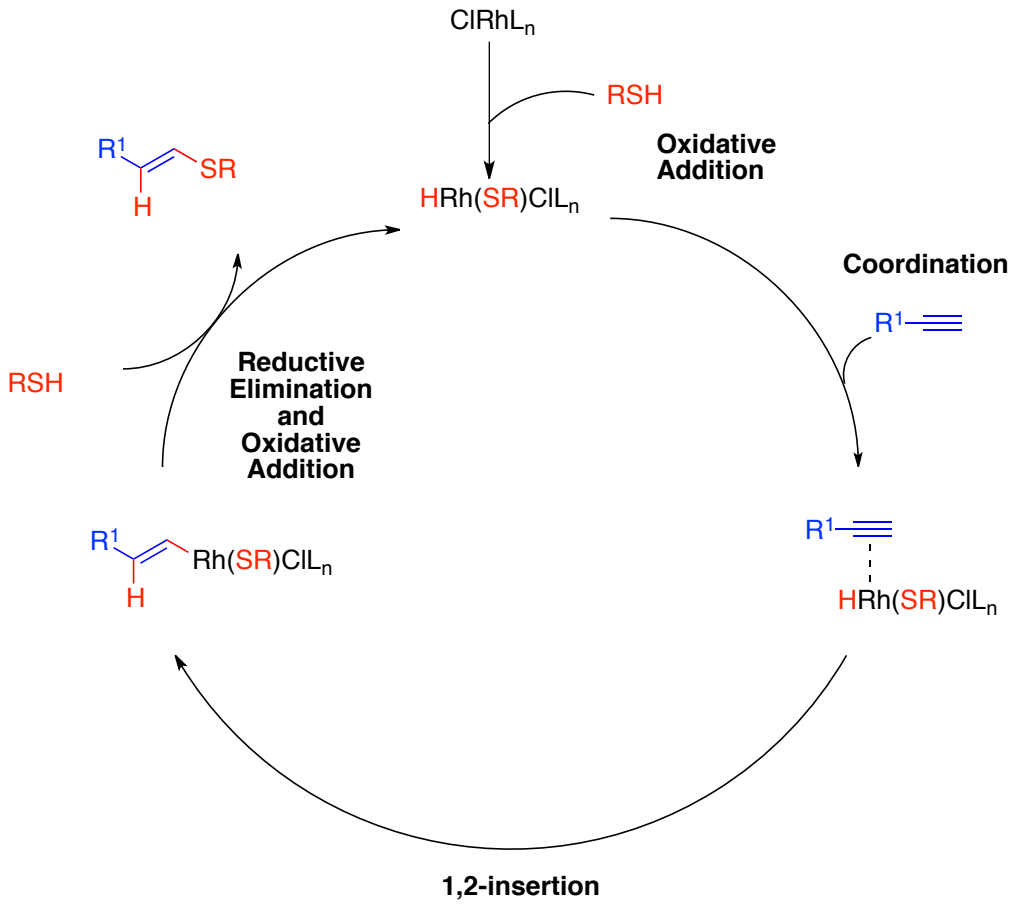

Scheme 1.10: Proposed catalytic cycle of rhodium-catalyzed alkyne hydrothiolation using Wilkinson's catalyst

Building on the substrate scope studies conducted by Paul Bichler and Dr. Shiva Shoai, we propose to use our methodology for rhodium-catalyzed alkyne hydrothiolation for the synthesis of K777. Importantly, the ability to use a variety of thiols will provide a quick efficient route to many analogues of K777. We envision we could make analogues of K777 from the coupling of two fragments **31** and **37** (Scheme 1.8). Fragment **37** could be made from an oxidation of a vinyl sulfide. The vinyl sulfide would be made from rhodium-catalyzed alkyne hydrothiolation using Wilkinson's catalyst to form predominantly the *E*-linear isomer. The alkyne **38** could be made from a variety of different approaches. These approaches will be discussed in more detail in Introduction 2.1 p. 29-32

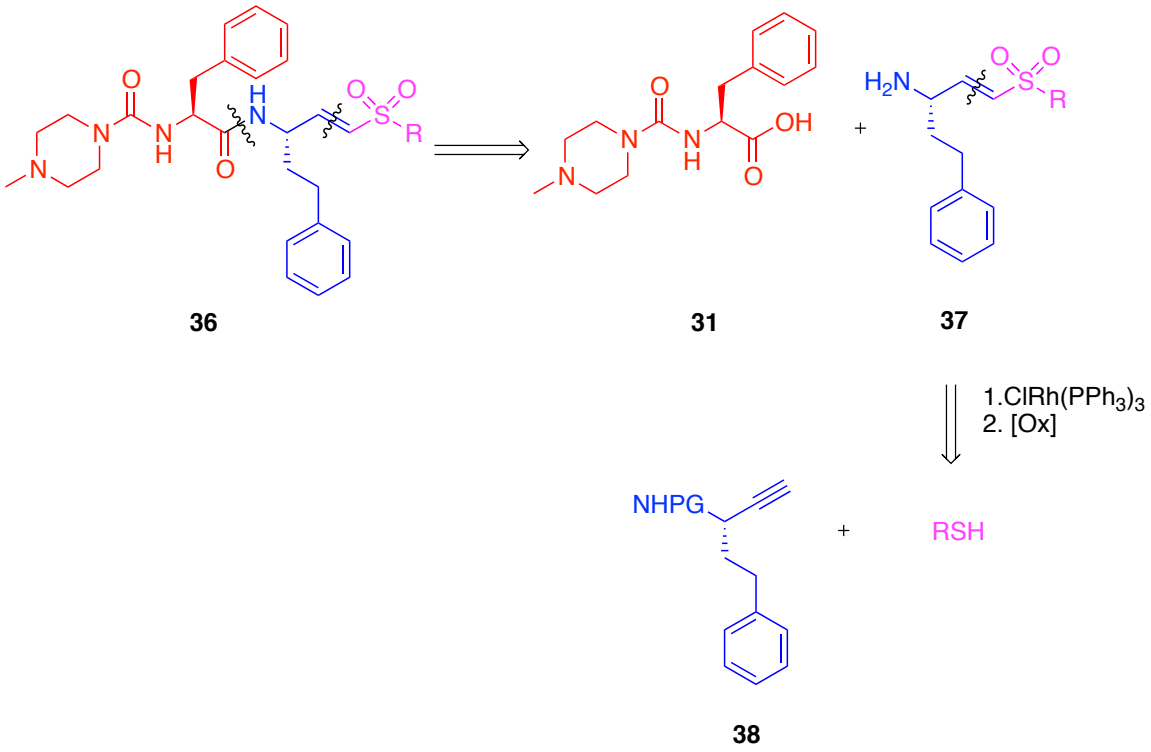

Scheme 1.11: Proposed retrosynthetic analysis

2 Total Syntheses of K777 and Analogues

2.1 Introduction

Rhodium-catalyzed-alkyne-hydrothiolation offers a direct, efficient and atom economic route to a variety of vinyl sulfides. We envisioned that we could apply this methodology to the synthesis of K777. This methodology could also be useful to generate K777 analogues, by modifying the P_1' site (Figure 1.8, p.15) In particular, we proposed to make analogues that differed in the para position of the aryl thiol, as this would likely affect the reactivity of the vinyl sulfone. Key disconnections of dipeptide **36** cleave the molecule into two peptide moieties, **31** and **37**. Fragment **31** can be readily prepared by a peptide coupling previously reported in the literature.[51,72] Moiety **37** would be readily accessible from the oxidation of a vinyl sulfide, a product of metal-catalyzed-alkyne hydrothiolation (Scheme 2.1). Here in this chapter, we present the synthesis of K777 and five analogues.

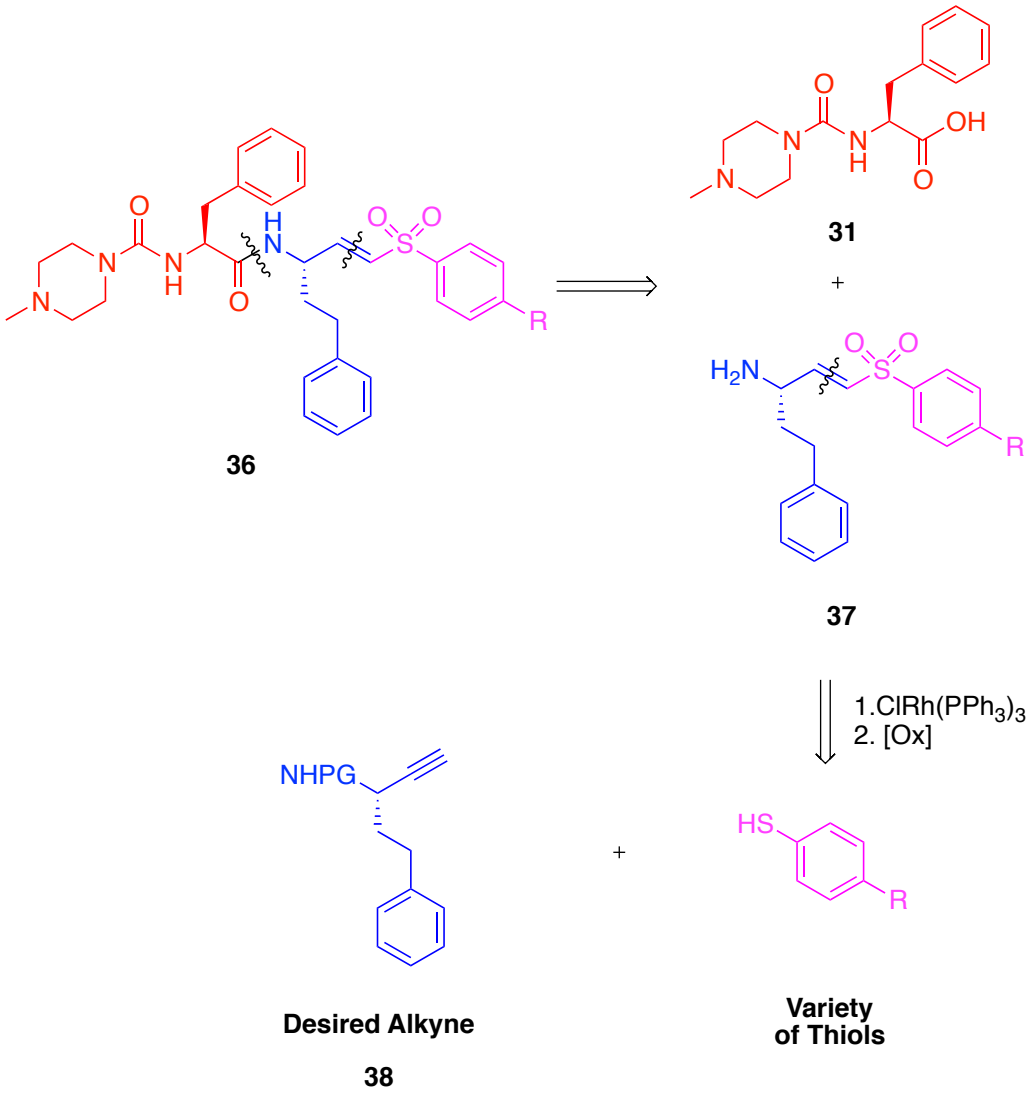

Scheme 2.1: Proposed retrosynthetic analysis

Our initial strategy for the synthesis of K777 involved the use of Palmer's method for the synthesis of **37**, which is derived from alkyne **38**. There are several methods for synthesizing the desired alkyne **38**. Attempts to use the Corey-Fuchs reaction or the Ohira-Bestmann reagent in a modified Seyferth-Gilbert homologation reaction were unsuccessful (Schemes 2.2-2.3).[102-104] It should be noted that neither method is atom economical and both involve the use of an extremely expensive starting material, homophenylalanine **20** ($24,194/mol TCI America) or the protected *tert*-butoxycarbonyl derivative of homophenylalanine **21** ($32,682/mol Sigma-Aldrich) (See introduction Scheme 1.2).

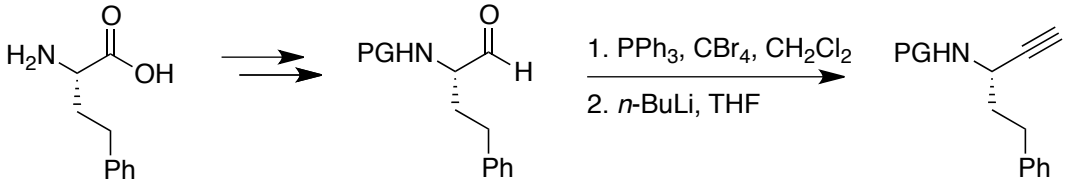

Scheme 2.2: General Corey-Fuchs reaction

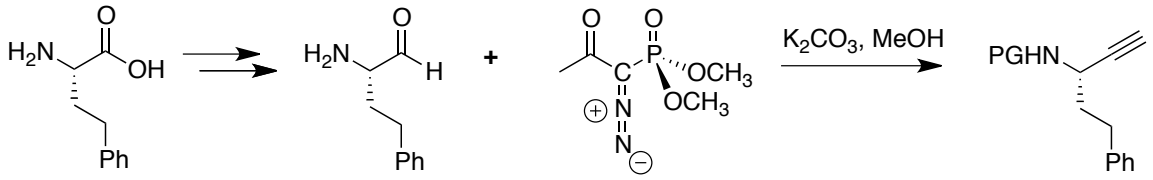

Scheme 2.3: General reaction using the Ohira-Bestmann reagent

We therefore devised a retrosynthetic strategy that would start from a much less expensive starting material, hydrocinnamaldehyde (**39**). An asymmetric synthesis using an Ellman's auxiliary (**40**) would be employed to produce a chiral imine **41** (Scheme 2.4). An addition reaction to the chiral imine **41** would produce the desired protected alkyne **42** with diastereoselective control via a six-membered transition state (Scheme 2.5). Ellman's *N*-*tert*-butanesulfinyl aldimines (sulfinamides) are sources of chiral ammonia equivalents. They are configurationally stable, produce good diastereoselectivity for nucleophilic additions and can be readily cleaved with acid.[105-107] Ellman's sulfinamides can also be recycled, thereby reducing the cost when used in synthesis. When Ellman's auxiliary is cleaved with HCl, a sulfinyl chloride is produced which can be treated with aqueous ammonia to produce the sulfinamide in high enantiomeric excess (*ee*).[108] Scheme 2.6 highlights the envisioned synthetic approach from hydrocinnamaldehyde (**39**) and (*S*)-(-)-2-methyl-2-propanesulfinamide (**40b**). Imine **41** produced can then be treated with an alkynyl Grignard to give a diastereoselective addition product, alkyne **42**.

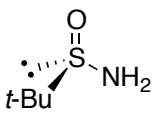

(*R*)-(-)-2-methyl-2-propanesulfinamide

40a

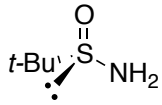

(*S*)-(-)-2-methyl-2-propanesulfinamide

40b

Figure 2.1: Ellman's sulfinamides

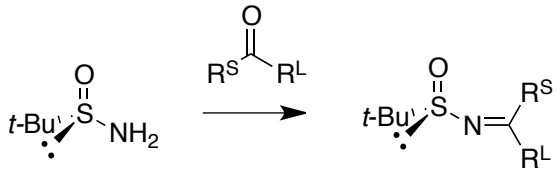

Scheme 2.4: Synthesis of *tert*-butanesulfinyl imines

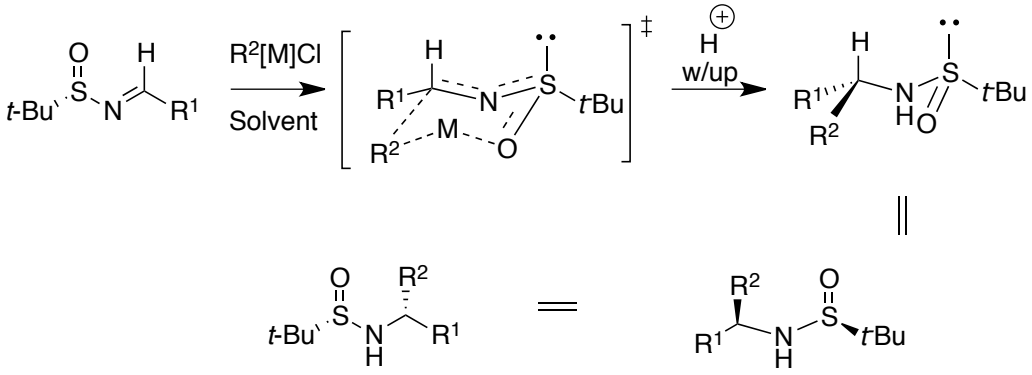

Scheme 2.5: Diastereoselectivity model for Ellman additions

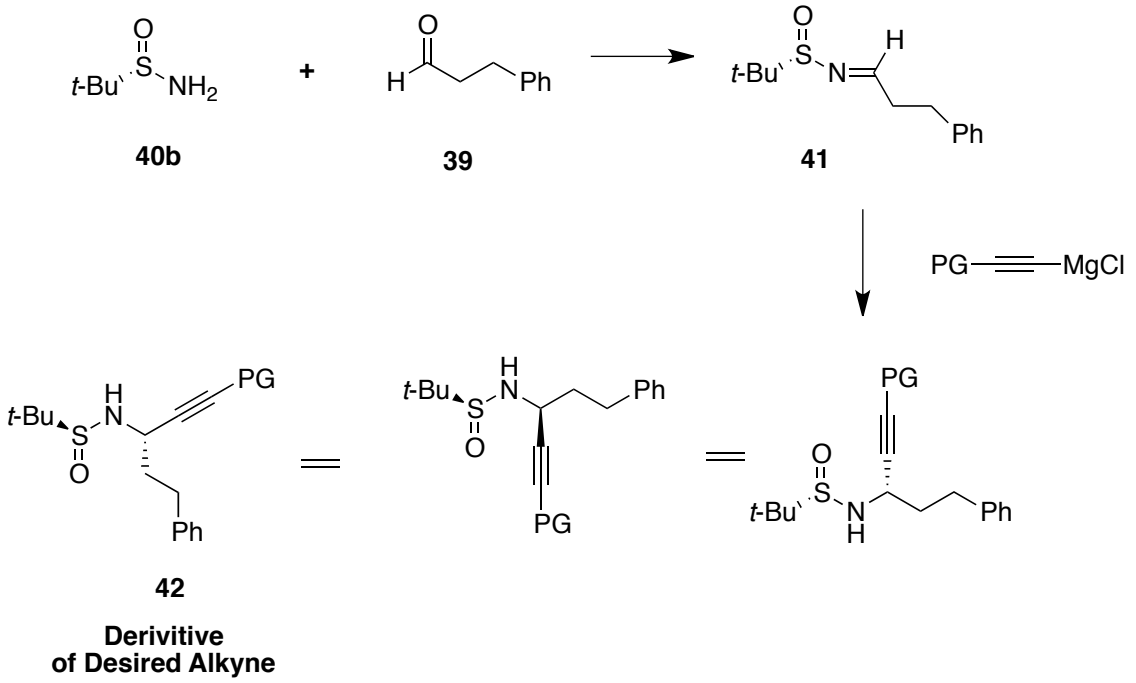

Scheme 2.6: Proposed method to derivative of desired alkyne

In order to test the methodology of metal-catalyzed alkyne hydrothiolation on our substrate, we first synthesized the desired racemic alkyne.

2.2 Results and Discussion

2.2.1 Synthesis of R/S Alkyne

Synthesis of the racemic alkyne begins with hydrocinnamaldehyde (**39**). Hydrocinnamaldehyde (**39**) was condensed with *tert*-butyl carbamate (**43**) and benzene sulfinic acid•sodium salt to produce alpha-amidoalkyl sulfone **44** in 68% yield. With excess alkynyl lithium reagent an *in situ* imine **45** was formed and reacted immediately to give the addition product propargyl amine **46** in 70% yield (Scheme 2.7).[109] Propargyl amine **46** was subsequently deprotected with TBAF to yield the desired alkyne **47** in 83% yield.

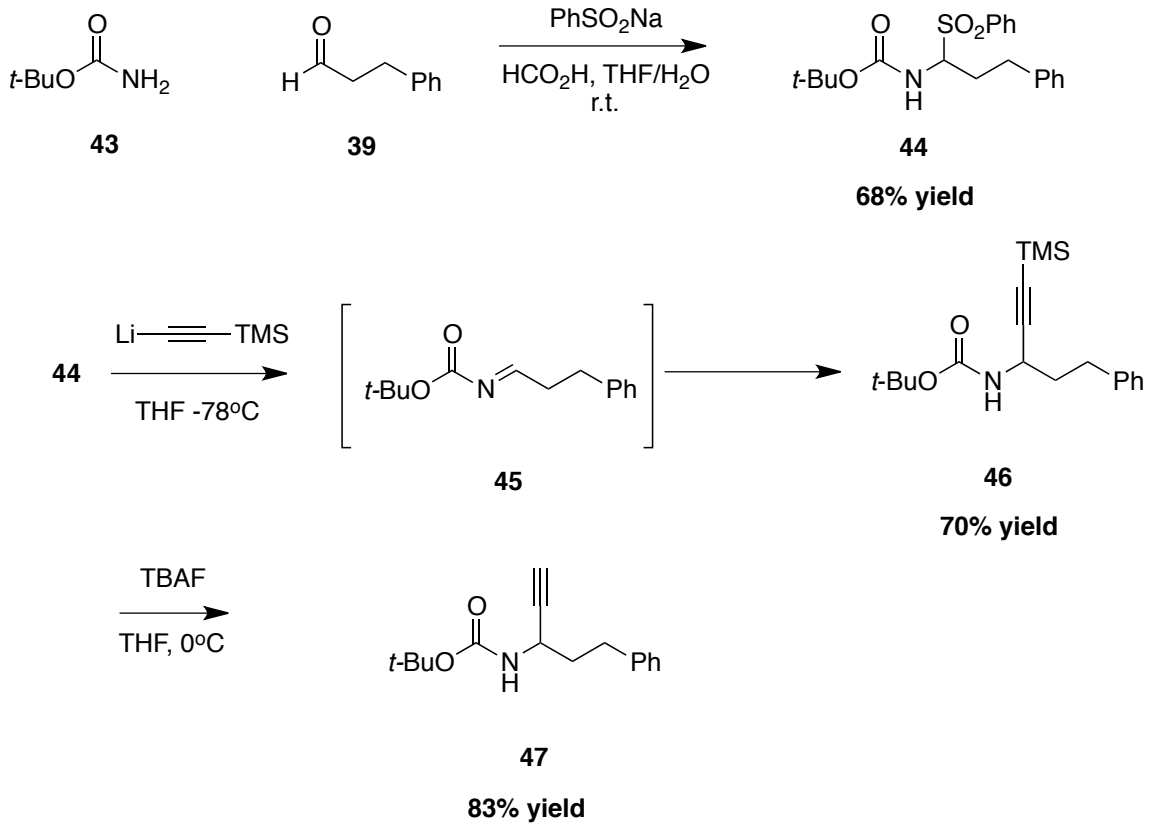

Scheme 2.7: Synthesis of R/S propargyl amine 47

2.2.2 Investigations of Alkyne Hydrothiolation and Oxidation of the R/S Alkyne

Alkyne **47** was reacted under standard conditions of the rhodium-catalyzed alkyne hydrothiolation methodology of our group using Wilkinson's catalyst. However, poor selectivity (5:2 *E*-linear:branched isomers) was observed (Scheme 2.8). Selectivity was determined by taking a ratio of the integrations of the *E*-linear vinyl protons to that of the branched product (Figure 2.2). It was postulated that the nitrogen on the propargyl amine could coordinate to the metal. Such an interaction would direct the reaction to the internal position of the alkyne, over-riding Wilkinson's catalyst's typical preference for generating the *E*-linear alkyne. Thus, we added another *tert*-butoxycarbonyl protecting group to the propargyl amine nitrogen functionality, which should minimize coordination of the nitrogen atom for both steric and electronic reasons (Scheme 2.9)

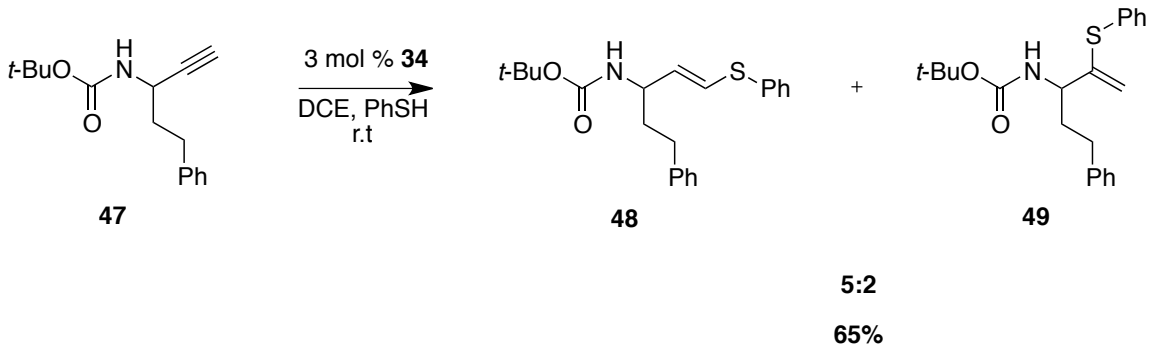

Scheme 2.8: Rhodium-catalyzed-alkyne hydrothiolation of alkyne 47

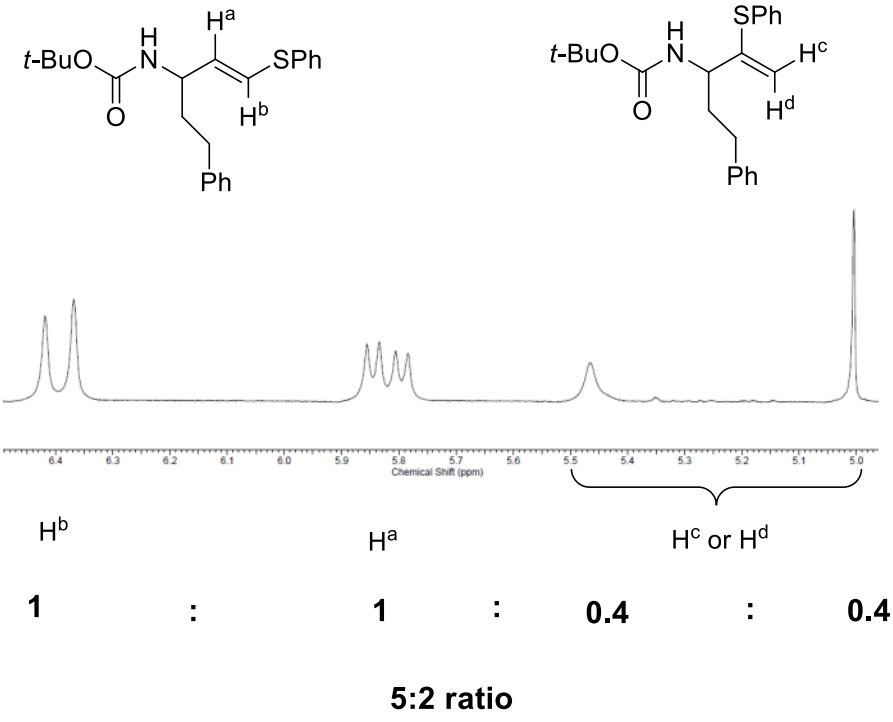

Figure 2.2: Determining selectivity of isomers by ^{1}H NMR spectroscopy

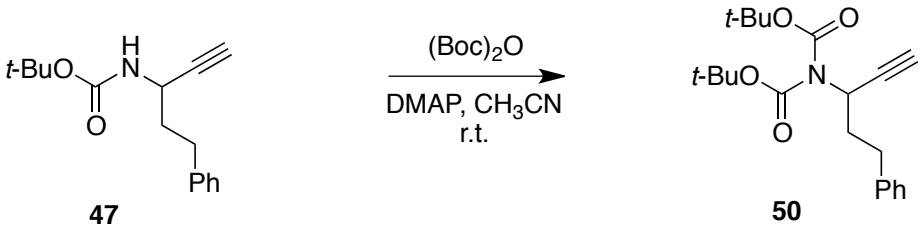

47 **50**

83% yield

Scheme 2.9: Synthesis of di-protected propargyl amine

When propargyl amine **50** was treated with 3 mol % of Wilkinson's catalyst, vinyl sulfide **51** was produced with a minimum selectivity of 25:1. (Scheme 2.10) Clearly, protection of the free amine had a considerable effect on reactivity. Table 2.1 highlights the results with differing catalytic loading. There seems to be no correlation between catalytic loading with either yield or selectivity.

Table 2.1: The effect of catalytic loading on rhodium-catalyzed alkyne hydrothiolation

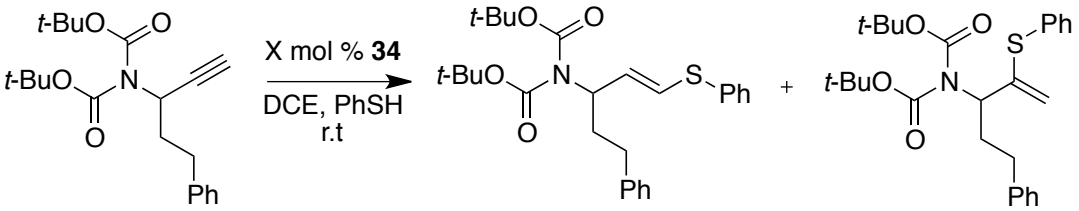

50 **51** **52**

***E*-Linear** **Branched**

Entry	Catalytic Loading	Ratio[a]	Yield[b]
1	3 mol%	>25:1	61%
2	5 mol%	>25:1	58%
3	10 mol%	>25:1	71%

[a]Ratio of *E*-Linear:Branched as determined by ^{1}H NMR spectroscopy
[b]Following purification by column chromatography

2.2.3 Synthesis of Enantioenriched Di-Protected Propargyl Amine

On the basis of these results, we proceeded to the synthesis of the chiral propargyl amine **53**. Synthesis of the chiral propargyl amine also commenced with hydrocinnamaldehyde (**39**). Hydrocinnamaldehyde ($35/mol Sigma-Aldrich) was reacted with (*S*)-(-)-2-methyl-2-propanesulfinamide ($6,900/mol TCI America) to form chiral imine **41** in 91% yield. Both starting materials are relatively cheap in comparison to the use of *tert*-butoxycarbonyl derivative of homophenylalanine **21** ($ 32,682/mol Sigma-Aldrich). This methodology is tolerant of a variety of aldehydes and thus can be used to generate analogues. Using the conditions reported by Chen and co-workers chiral imine **41** was transformed to the TMS-protected propargyl amine **54** in 92% yield and >100% *d.r*. (diastereomeric ratio) as determined by ^{1}H NMR spectroscopy.[68] Compound **54** was subsequently deprotected to yield the terminal alkyne **55**; the alkyne was used without further purification. Ellman's sulfinamide auxiliary was then removed with HCl and the

ammonium salt of the free alkyne was immediately subjected to protection conditions to yield the di-protected propargyl amine **53** in 79% yield over three steps from **55** (Scheme 2.10).

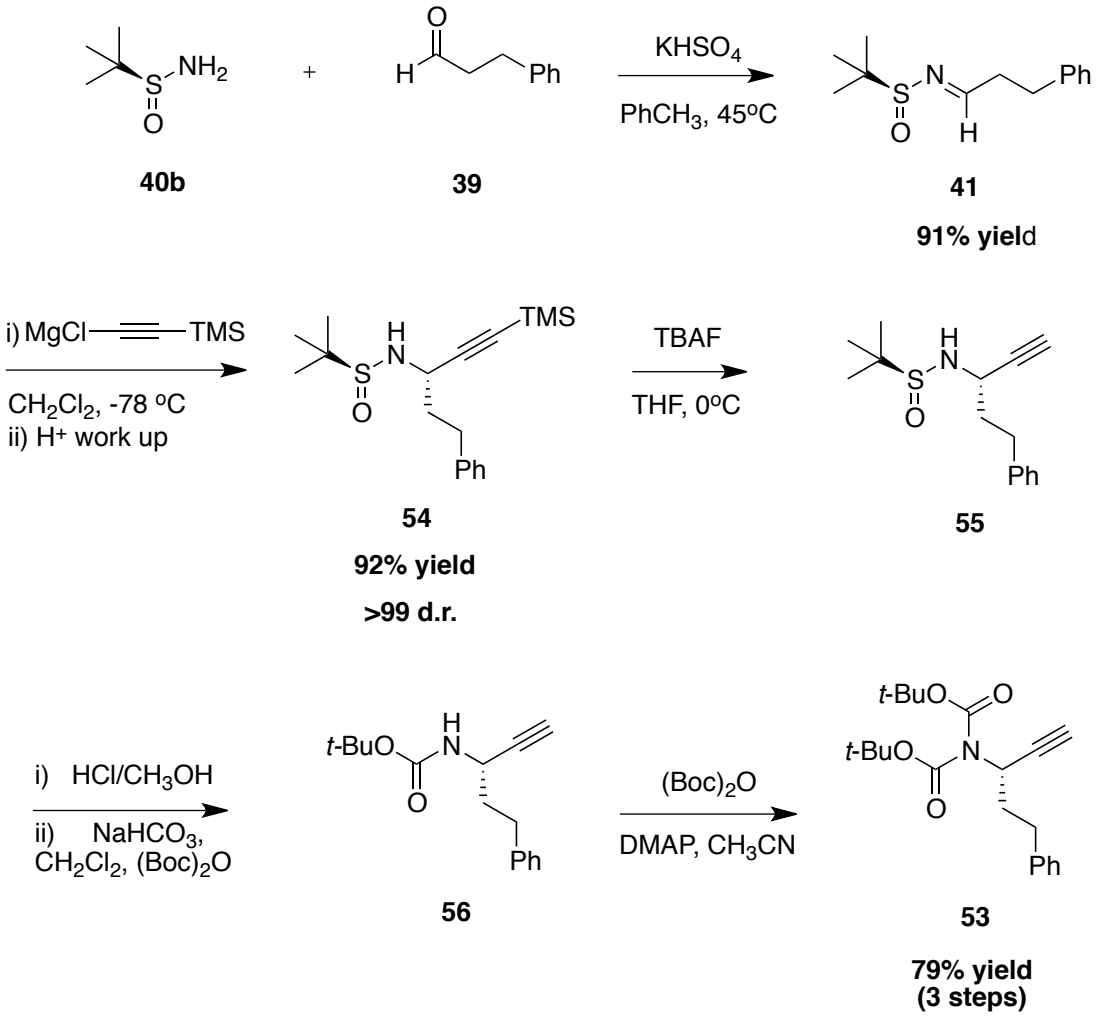

Scheme 2.10: Synthesis of enantioenriched di-protected propargyl amine 53

2.2.4 Synthesis of K777 and Analogues

Fragment **31** was synthesized using a similar procedure to the synthesis of WRR-483 (**16**), an arginine-based analogue of K777.[72] We chose this protocol over Palmer's method for the synthesis of K777 as a means to avoid the use of toxic phosgene **57**.[51] The protected salt of phenylalanine **28** was instead treated with triphosgene **58** (Figure 2.3), a safer alternative to phosgene, and coupling partner *N*-methylpiperazine to yield the urea **30**. Compound **30** was then subjected to hydrogenation to yield the free acid **31** in 66% yield over two steps (Scheme 2.11).

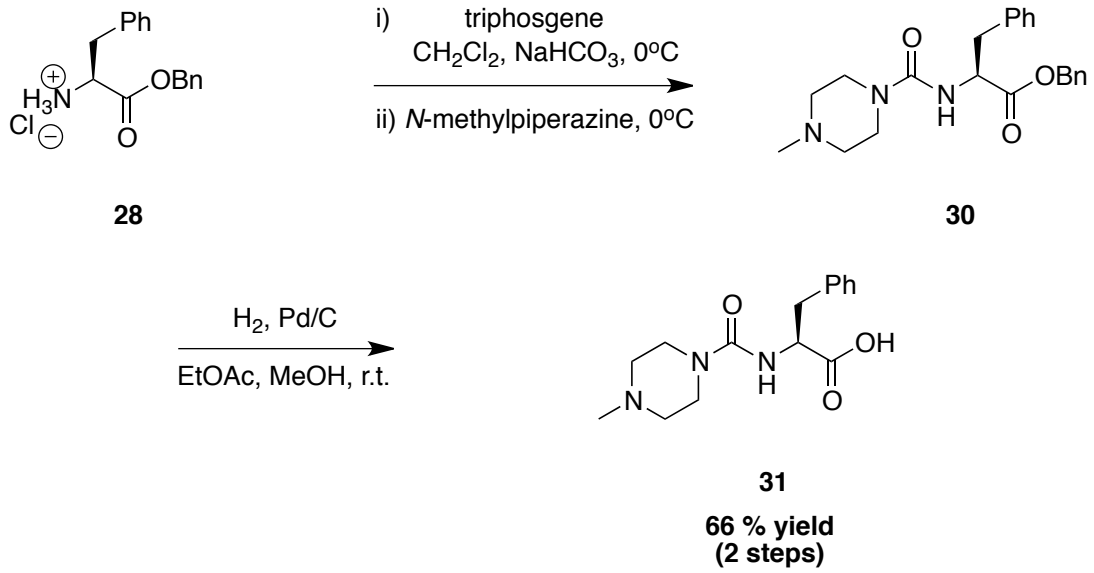

Scheme 2.11: Synthesis of peptide residue 31

Figure 2.3: Phosgene and triphosgene

Under catalytic hydrothiolation conditions, alkyne **53** yielded vinyl sulfide **59** in 91% yield, with 25:1 *E*-linear:branched isomer selectivity. Vinyl sulfide **59** was then

oxidized to vinyl sulfone **60** in 81% yield. Enantiomeric excess (*ee*) was to be determined at this stage. Originally, determination of enantiomeric excess was attempted using chiral HPLC with UV detection. Enantiomers interact differently with the chiral column and would have different elution times. However no suitable conditions were found to separate the racemic substrates (alkyne **50** and racemic sulfones). Thus, our efforts turned towards using supercritical fluid chromatography (SFC). Like chiral HPLC this method requires racemic substrates to develop the correct separation conditions (See appendix A for the separation of R/S alkyne **50** and R/S sulfone **61**). However, recently due to instrument failure we were unable to apply our conditions to our chiral substrates. We therefore, decided to employ the use of chiral shift reagents, specifically Mosher's acid chloride (α-methoxy-α-trifluoromethylphenylacetic acid or MTPA) (**62**).

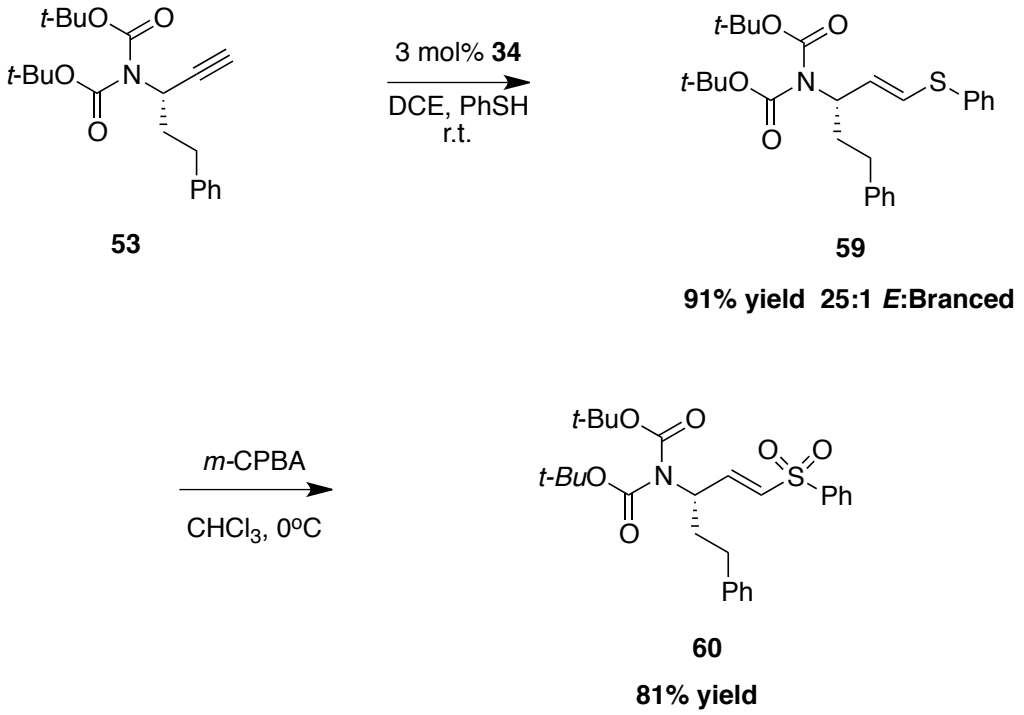

Scheme 2.12: Synthesis of enantioenriched vinyl sulfone 60

Mosher's acid chloride when reacted with chiral amines and alcohols yields chiral amides and esters, respectively.[110,111] Because Mosher's acid chloride is chiral, the products are diastereomers, which can be readily resolved in ^{1}H NMR or ^{19}F NMR spectra (Figure 2.4). Mosher's acid chloride is a good shift reagent as it lacks alpha

protons that can lead to racemization.[110,111] This strategy required the isolation and purification of **55**. Alkyne **55** was treated with HCl in ether and salt **63** was removed from the filtrate.[112] This was essential, as we needed to eliminate the possibility of our product reacting with the sulfinyl chloride of Ellman's auxiliary **64**. The ammonium chloride salt (**63**) was dissolved $CDCl_3$, reagent DIPEA was added followed by Mosher's acid chloride **62a** and transferred to an NMR tube to give alkyne **65**.[113] A ^{19}F NMR spectrum of the crude alkyne **65** was obtained immediately. Unreacted Mosher's acid chloride was observed in the spectrum along with two peaks at 100:5 ratio 90% *ee*. The relatively high *ee* was in accordance with the high *d.r.* observed in compound **54** (Scheme 2.10). If we assume that the following reactions in the synthesis conserve *ee*, our synthesis is highly selective. However, this cannot be definitively determined until the SFC is fully functional.

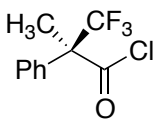

61a

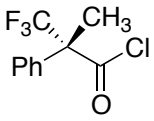

61b

Figure 2.4 Mosher's acid chlorides

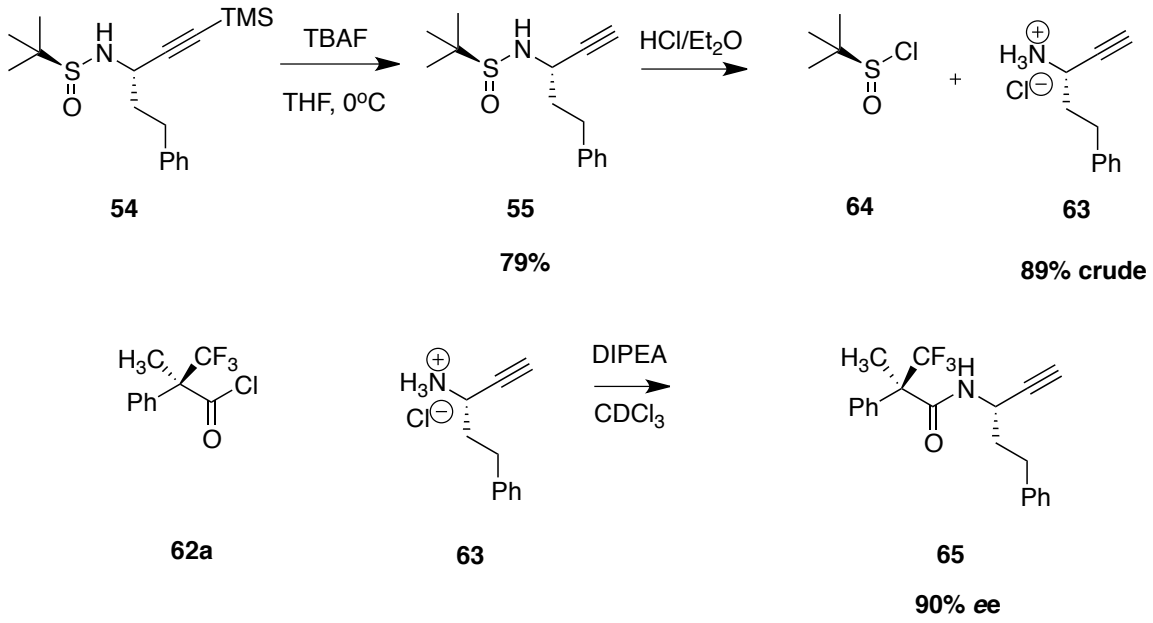

Scheme 2.13: Synthesis of alkyne derivative 65

Alkyne hydrothiolation was also tested on a propargyl amine containing one *tert*-butoxycarbonyl protecting group as well as Ellman's sulfinamide auxiliary **66**. If both the sulfinamide and protected propargyl amine could be utilized in alkyne hydrothiolation, this would eliminate two steps in the overall synthesis. Both groups could be readily removed in the same step with acid. However, it was found that this product was unreactive in our hydrothiolation protocol, possibly due to the unproductive coordination of the sulfoxide or differing electronics (Scheme 2.14).

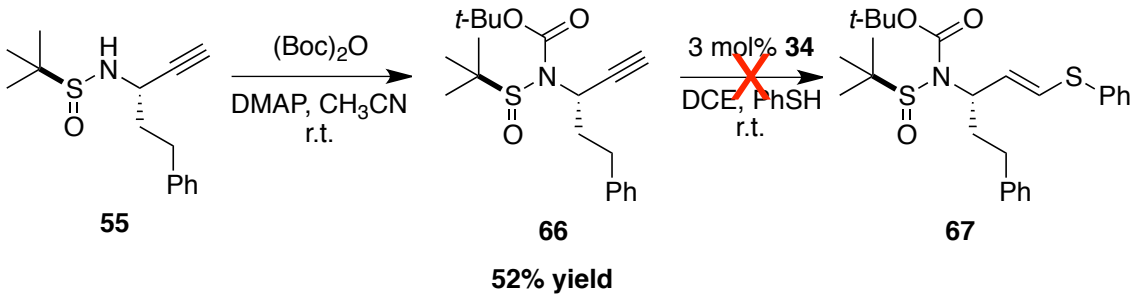

Scheme 2.14: Alkyne hydrothiolation of propargyl amine 67 containing Ellman's sulfinamide auxiliary and a *tert*-butoxycarbonyl protecting group.

We then proceeded to the coupling of fragments **60** with **31** (Scheme 2.15). Protocols for the synthesis many of the K777 analogues use a coupling partner such as EDC or DCC with HOBT (hydroxybenzotriazole) **68** as the racemization suppressor. Unfortunately, HOBT is a dangerous explosive and cannot be shipped by sea or air. HBTU (2-(1H-Benzotriazole-1-yl)-1,1,3,3-tetramethylaminium hexafluorophosphate) **69** is not only a coupling reagent but also a racemization suppressor and does not suffer from the drawbacks as HOBT. Thus HBTU was used for our coupling reaction.[114] Vinyl sulfone **60** was subsequently treated with TFA to yield the TFA salt adduct **70**. Adduct **70** was then coupled with acid **31** using HBTU to produce K777 in 64% estimated yield. In the ^{1}H NMR spectrum there are more proton signals than expected. Potentially there is a mixture of diastereomers if epimerization has occurred at this stage or racemization at previous steps prior to coupling. Enantiopurity of vinyl sulfone **60** will be further verified using SFC. One of the noticeable impurities is an ethyl group, which does not correspond to our product or to any solvent/reagent impurities in CD_2Cl_2. This potential contaminant may be triethylamine and due to interactions with our product its chemical shift may differ. The overall yield of this ten-step synthesis was 21% (ignoring minor impurities). The yield of the longest linear sequence (8 steps) was 31% (ignoring minor impurities). These yields are comparable to Palmer's eight-step synthesis at 34% overall yield (Introduction section 1.6). Our synthesis has the possibility of being more cost efficient with the elimination of homophenylalanine and safer with the elimination of phosgene for triphosgene. Although the usage of rhodium is not ideal, potential methods of rendering this catalyst recyclable are currently being developed in the Love group. It has also been reported in the literature that Ellman's auxiliary can be recycled.[108] Indeed, we have demonstrated that the auxiliary can be separated using simple filtration after removal with acid (Scheme 2.13). With the two most costly reagents (Ellman's auxiliary and Wilkinson's catalyst) of our synthesis having the possibility to be recycled our synthesis may prove to be quite advantageous. However, an area that still needs improvement is purification; column chromatography is not only tedious but solvent cost and waste is not ideal. We have shown that we can carry our synthesis through three steps without purification (Scheme 2.10) and we hope to eliminate more steps of purification upon optimization of our synthesis.

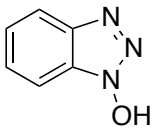

HOBT

68

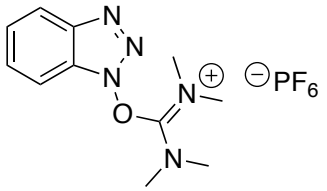

HBTU

69

Figure 2.5: Structures of HOBT and HBTU

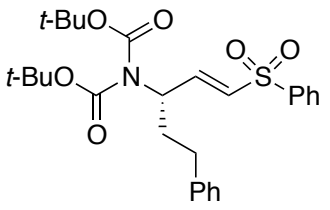

60

i)TFA/CH_2Cl_2

0°C

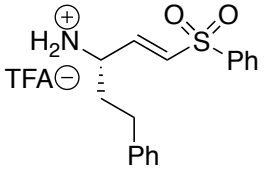

70

ii)Acid **31**, HBTU **69**

Et_3N, CH_3CN, r.t.

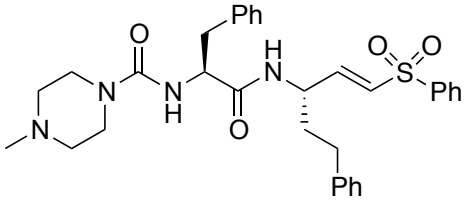

K777

64% yield

21% overall yield 10 steps

Scheme 2.15: Synthesis of K777

With the successful synthesis of K777 (although purification methods are still needed), we next turned our attention to the synthesis of analogues of K777. Our focus was a modification of the aryl vinyl sulfone moiety (P_1' site of the peptide), as this functional group is crucial for activity (acting as a Michael acceptor). In addition, few modifications of the P_1' site have been reported. We wanted to change the electronics of the aryl ring as a means to alter the reactivity of the vinyl sulfone. We had previously demonstrated the versatility of our methodology for a variety of aryl thiols. Our approach

started with the synthesis of R/S analogues as a means to test the methodology and to have a library of R/S compounds that could be used to establish separation conditions with supercritical fluid chromatography. Table 2.2 contains the results of the various R/S vinyl sulfide analogues synthesized **51**, **71**-**75**. Table 2.3 contains the results of the various R/S vinyl sulfone analogues synthesized **61**, **76**-**80**. The yields of the R/S vinyl sulfides were modest and the reaction was fairly selective for the *E*-linear isomers.

Table 2.2: Synthesis of R/S vinyl sulfide analogues

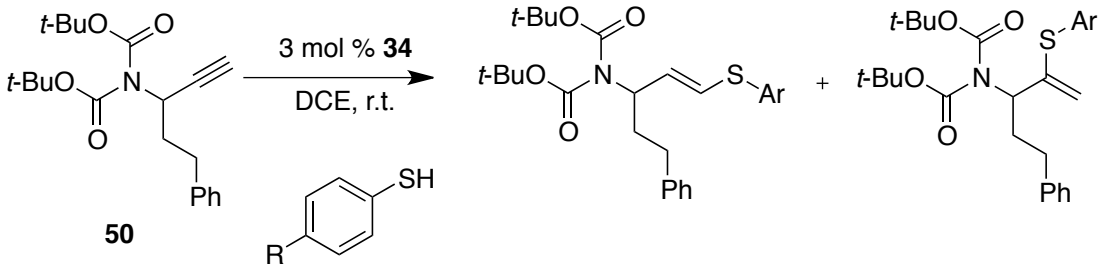

***E*-Linear** **Branched**

Entry	R Group		Ratio[a]	Yield[b]
1	H	(**51**)	>25:1	61%[c]
2	CH_3	(**71**)	30:1	77%[d]
3	OCH_3	(**72**)	17:1	65%[d]
4	Cl	(**73**)	14:1	62%[d]
5	Br	(**74**)	30:1	51%[d]
6	CF_3	(**75**)	25:1	67%[d]

[a]Ratio *E*-linear:branched isomer as determined by ^{1}H NMR spectroscopy
[b]Following purification by column chromatography
[c]Yield reported for most recent reaction
[d]Analogues **71**-**75** synthesized once.

Table 2.3: Synthesis of R/S vinyl sulfones

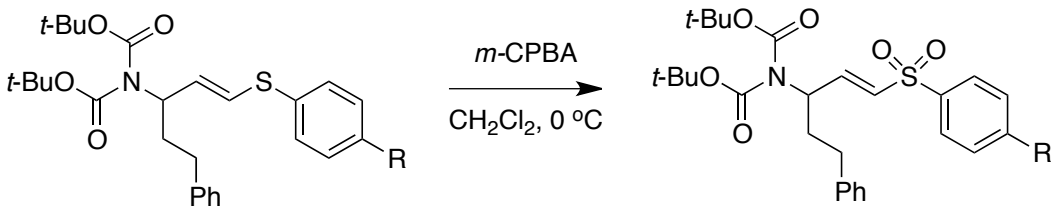

51, 71-75

Entry	R Group	Yield[a]
1	H (**61**)	40%[c]
2	CH_3 (**76**)	TBD[b,c]
3	OCH_3 (**77**)	TBD[b,c]
4	Cl (**78**)	31%[c]
5	Br (**79**)	TBD[b,c]
6	CF_3 (**80**)	33%[c]

[a]Following purification by column chromatography

[b]Yield to be determined shortly

[c]Synthesized once

After the synthesis of the R/S analogues **51**, **71-75**, the same experimental conditions were applied to the chiral propargyl amine **53** to produce enantioenriched vinyl sulfides **59**, **81-85** and subsequently vinyl sulfones **60, 86-90** (Tables 2.4-2.5). The yield and selectivities vary from their R/S analogues. These variances in the vinyl sulfides can be attributed to alkyne purity, thiol purity, increase in expertise of the methodology, and glovebox atmosphere among many other factors. The yields of the oxidation steps varied greatly. The same bottle of *m*-CPBA was used for both sets of analogues. The oxidations of the R/S analogues were completed after the oxidations of the enantioenriched analogues. The weight percent of *m*-CPBA was unknown but all

calculations were based on 77% wt. according to the label. Potential decomposition of *m*-CPBA to *meta*-chlorobenzoic acid could attribute for some of the lower yields. Also exposure to an acidic environment could cause deprotection of one or more of the *tert*-butoxycarbonyl protecting groups, as these are acid sensitive. We observed in the purification of the parent vinyl sulfone and some analogues most notably the CF_3 analogue, potential isolation of some mono-protected products. However, we were unable to confirm this at this time. If this is the case the *mono*-protected products can still be used in the next step of deprotection. The enantioenriched vinyl sulfones **60**, **86-90** were then subjected to HBTU coupling conditions and five analogues of K777 were produced (Table 2.6). Purification of these K777 analogues proved difficult. Column chromatography could not suffice as a means of purification. Many purification methods of K777 analogues currently in the literature use recrystallization methods, forming salts, column chromatography or a mixture of these methods.[51,64,72] However, on such a small scale (100mg), complex purification methods can be challenging.

Table 2.4: Synthesis of enantioenriched vinyl sulfide analogues

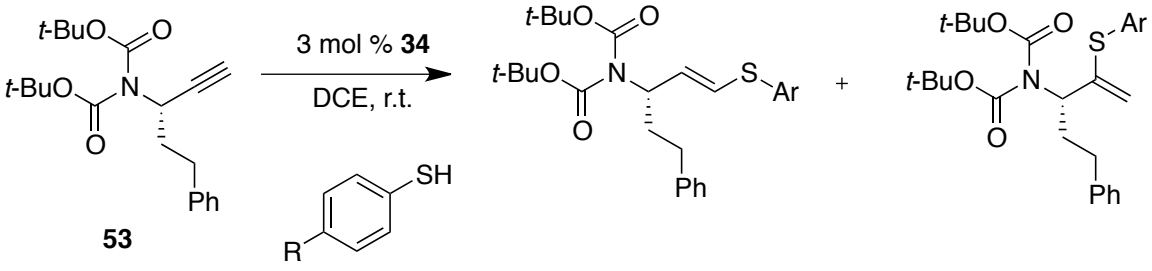

***E*-Linear** **Branched**

Entry	R Group	Ratio[a]	Yield[b]
1	H (**59**)	25:1	91%
2	CH_3 (**81**)	50:1	81%
3	OCH_3 (**82**)	50:1	52%
4	Cl (**83**)	50:1	88%
5	Br (**84**)	50:1	80%
6	CF_3 (**85**)	50:1	84%

[a]Ratio is *E*-linear:branched isomer as determined by ^{1}H NMR spectroscopy
[b]Yield after purification by column chromatography. Yield is of highest yielding reaction

Table 2.5: Synthesis of enantioenriched vinyl sulfone analogues

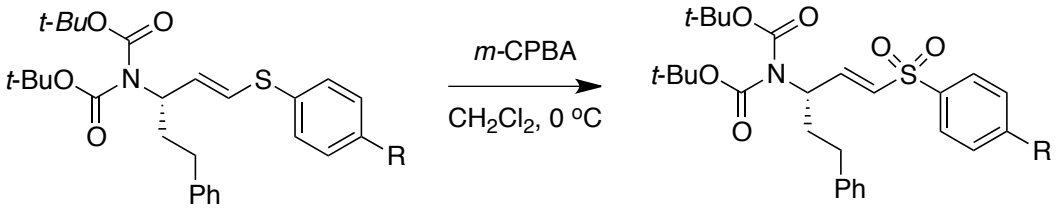

59, 81-85

Entry	R Group	Yield[a,b]	*ee*[c]
1	H (**60**)	81%	TBD
2	CH_3 (**86**)	79%	TBD
3	OCH_3 (**87**)	81%	TBD
4	Cl (**88**)	68%	TBD
5	Br (**89**)	79%	TBD
6	CF_3 (**90**)	61%	TBD

[a]Yield after purification by column chromatography
[b]Yield of compound used for characterization
[c] enantiomeric excess will be determined by super critical fluid chromatography once the instrument is back up and running

Table 2.6: Synthesis of K777 and analogues

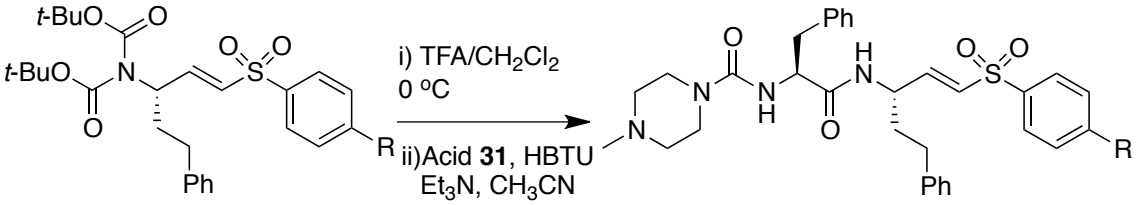

60, 86-90

Entry	R Group	Yield[a]	Overall Yield[b]	Linear Yield[c]
1	H (**13**)	64%	21%	31%
2	CH_3 (**91**)	75%	21%	32%
3	OCH_3 (**92**)	41%	8%	11%
4	Cl (**93**)	35%	9%	14%
5	Br (**94**)	70%	19%	29%
6	CF_3 (**95**)	40%	9%	15%

[a] Yield of semi-pure material after column chromatography
[b]Overal yield after ten step synthesis (includes crude yield)
[c]Yield of the eight linear step sequence (includes crude yield)

2.3 Conclusions

We have demonstrated the utility of rhodium-catalyzed alkyne hydrothiolation in the application of the total synthesis of K777, a potential therapeutic for Chagas' disease. This is the first use of alkyne hydrothiolation in total synthesis. Our synthesis avoided the use of the expensive starting material, homophenylalanine, which was employed in the original synthesis of K777. Our use of a chiral auxiliary to set the stereocenter allows us to use an aldehyde of choice, in this case hydrocinnamaldehyde, but offers room for further derivatization. Due to the versatility of the reaction scope we can use a variety of thiols, which allowed us to efficiently generate five analogues although purification methods are still needed.

2.4 Experimental

2.4.1 General Procedures

Unless otherwise stated all glassware was flame dried under vacuum and back filled with nitrogen. Manipulation of organometallic compounds was performed using standard Schlenk techniques under an atmosphere of dry nitrogen or in a nitrogen-filled MBraun drybox (O_2 < 2 ppm). Thin layer chromatography (TLC) was done using pre-coated silica gel 60 F_{254} plates containing a fluorescent indicator; purification by chromatography was done using Silica Flash P60 silica gel (230-400 mesh). The stain used for visualization was $KMnO_4$. NMR spectra were recorded on Bruker Avance 300 or Bruker Avance 400 spectrometers. ^{1}H and ^{13}C chemical shifts are reported in parts per million and referenced to residual solvent. Coupling constant values were extracted assuming first-order coupling. The multiplicities are abbreviated as follows: s = singlet, d = doublet, t = triplet, q = quartet, m = multiplet, dd = doublet of doublets, td = triplet of doublets, ddd = doublet of doublet of doublets, ddt = doublet of doublet of triplets. All spectra were obtained at 25 ^{o} C. Elemental analyses were performed using a Carlo Erba Elemental Analyzer EA 1108. High resolution mass spectra were recorded using a Bruker Esquire - LC and low resolution mass spectra were recorded on a Waters LC - MS. Enantiomeric excess studies done on racemic substrates were attempted using a Thar supercritical fluid chromatography (See Appendix II). Optical rotations were determined using a Jasco P- 2000 polarimeter. The concentrations are reported in units of 1g sample/100 mL of solvent (wt%) and specific rotation in degrees. The path length used was 100mm and the temperature was 21 ^{o}C. Four measurements were averaged to give the listed value. IR spectra were obtained from a Perkin Elmer - Frontier FTIR-ATR.

2.4.2 Materials and Methods

THF and toluene were dried by passage through solvent purification column. 1,2-Dichloroethane (DCE) was distilled from molecular sieves and degassed prior to use. Dichloromethane (DCM) and hydrocinnamaldehyde were dried over CaH_2 and distilled prior to use. All liquid thiols were freshly distilled prior to use. Ellman auxiliary (*S*)- (-)-

2-Methyl-2-propanesulfinamide and HBTU 2-(1H-Benzotriazole-1-yl)-1,1,3,3-Tetramethyluronium hexafluorophosphate were purchased from TCI America and used without further purification. Isopropyl magnesium chloride (2.0 M in THF), TBAF *tert*-butylammonium fluoride (1.0M in THF), *m*-CPBA *meta*-chloroperbenzoic acid (77% wt. - remainder a mixture of *meta*-chlorobenzoic acid and water) and *L*-phenylalanine benzyl ester hydrochloride was purchased from Sigma-Aldrich and used without further purification. Acetonitrile (anhydrous), $CDCl_3$, CD_2Cl_2, DMSO-d_6 and all other organic reagents were obtained from commercial sources and used as received.

2.4.3 General Procedure for Hydrothiolation of R/S and Enantioenriched Alkynes Using a Liquid Thiol

Wilkinson's catalyst (33 mg, 0.036 mmol, 3 mol %) was measured out in the glove box into a 10 mL round bottom flask equipped with a magnetic Teflon-coated stir bar and stoppered with a rubber septum. The flask was removed from the glove box and the catalyst was suspended in dry DCE (1.2 mL) under nitrogen to give a dark red solution. To this solution was added thiol (1.2 mmol) using a microsyringe or a 1 mL syringe where appropriate. A usual color change from the dark red solution to a lighter red-brown was observed. In a separate 10 mL pear shaped flask under nitrogen, propargyl amine **(**1.1 mmol**)** was dissolved in dry DCE (2.4 mL) and then transferred to the original 10 mL round bottom flask. Often upon addition of propargyl amine to the red brown solution varying shades of green are observed. The remaining propargyl amine was then transferred with further portions of dry DCE (2 x 0.6 mL). The flask was then covered with aluminum foil and allowed to stir for 22 hours. Solvent was removed rotary evaporation to yield a dark brown oil. The crude product was purified by silica flash column chromatography

2.4.4 General Procedure for Hydrothiolation of R/S and Enantioenriched Alkynes Using a Solid Thiol

Wilkinson's catalyst (28 mg, 0.030 mmol, 3 mol %) was measured out in the glove box into a 10 mL round bottom flask equipped with a magnetic Teflon-coated stir bar and stoppered with a rubber septum. The flask was removed from the glove box and

the catalyst was suspended in dry DCE (0.8 mL) under nitrogen to give a dark red solution. In a separate pear shaped 5 mL flask under nitrogen solid thiol (1.1 mmol) was added and dissolved in dry DCE (0.8 mL). This solution was then transferred via syringe to the original flask containing the catalyst. A usual color change from the dark red solution to a lighter red-brown was often observed. The remaining thiol was rinsed with dry DCE (0.8 mL) and transferred to the catalyst solution. In a separate 10 mL pear shaped flask, propargyl amine **(**1.0 mmol**)** was dissolved in dry DCE (0.8 mL) then transferred to the original 10 mL round bottom flask. Often upon addition of propargyl amine to the red brown solution varying shades of green are observed. The remaining propargyl amine was then transferred with further portions of dry DCE (2 x 0.5 mL). The flask was then covered with aluminum foil and allowed to stir for 22 hours. Solvent was removed by rotary evaporation to yield a dark brown oil. The crude product was purified by silica flash column chromatography

2.4.5 General Procedure for Oxidation of R/S and Enantioenriched Vinyl Sulfides

In a 50 mL round bottom flask equipped with a Teflon-coated magnetic stir bar, vinyl sulfide (0.679 mmol) was dissolved in CH_2Cl_2 (6.8 mL) and cooled to 0 ^oC. In a separate pear shaped flask, 77% wt. *m*-CPBA (0.356 g, 1.49 mmol) was dissolved in CH_2Cl_2 (2.0 mL) then added to the original flask containing the vinyl sulfide. The flask containing *m*-CPBA was further rinsed with CH_2Cl_2 (2 x 0.5 mL) and added to the vinyl sulfide solution. The solution was allowed to stir for 3 hours at 0 ^oC and a white precipitate was often observed. The solution was quenched with an equal mixture of 10 % $NaHSO_3$ and saturated $NaHCO_3$ (20 mL). The organic layer was separated and the aqueous layer was extracted with CH_2Cl_2 (3 x 20 mL). The organic layers were combined and dried over Na_2SO_4 and the drying agent was then removed by gravity filtration. Solvent was removed by rotary evaporation to give a crude light yellow solid or oil. The crude product was purified by column chromatography.

2.4.6 General Procedure for Coupling Reaction to Produce K777 and Analogues[114]

In a 10 mL round bottom flask equipped with a magnetic Teflon-coated stir bar, vinyl sulfone was added (0.41 mmol) and dissolved in a 33 % TFA:DCM solution (2.8 mL) and allowed to stir at a 0°C solution for 1.5 hours. The solvent was removed by rotary evaporation and then washed with additional toluene (2 x 10 mL) to remove the remaining TFA. Anhydrous CH_3CN (3.3 mL). acid **31** (116 mg, 0.400 mmol), Et_3N (0.11 mL, 0.796 mmol) and HBTU (0.147 g, 0.414 mmol) were added sequentially. The solution was allowed to stir overnight. The solution was quenched with brine (10 mL) and the layers separated. The aqueous layer was extracted with EtOAc (3 x 20 mL). The organic layers were combined and washed with 2N HCl (12 mL), then water (12 mL), then 5 % $NaHCO_3$ (12 mL) and finally one last water wash (12 mL). The combined organic layers were dried over $MgSO_4$ and the drying agent was removed by gravity filtration. The solvent was removed by rotary evaporation to yield a dark yellow solid. The crude product was purified by silica flash column chromatography.

2.4.7 Syntheses of the R/S and Enantioenriched Alkynes

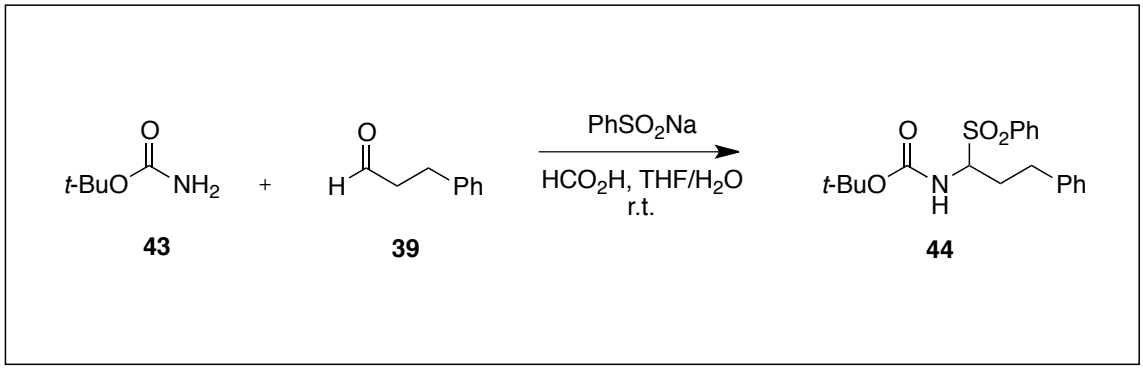

In a 100 mL round bottom flask equipped with a Teflon-coated magnetic stir bar, hydrocinnamaldehyde **39** (4.3 mL, 32.8 mmol) was dissolved in a mixture of THF (12 mL) and water (30 mL). *Tert*-butyl carbamate (**43**) (3.50g, 29.8 mmol) was added, followed by benzene sulfinic acid sodium salt (4.891g, 29.8 mmol) and formic acid (7.2 mL). The solution was allowed to stir overnight. The resulting solution contained a white precipitate, which was removed by filtration. The off-white solid obtained was then

dissolved in a minimum of warm ethyl acetate (heat gun), and then crystallized upon the addition of hexanes (4:1 ratio hexanes/EtOAc). The solid was further precipitated in an ice bath. The white solid was separated by vacuum filtration to afford **44** (7.62g, 68% yield).

Data for **44**:

^{1}H-NMR (300 MHz; $CDCl_3$): δ 7.89-7.87 (m, 2H), 7.61 (d, *J* = 7.3 Hz, 1H), 7.55-7.50 (m, 2H), 7.31-7.16 (m, 5H), 4.98 (d, *J* = 10.5 Hz, 1H), 4.89-4.80 (m, 1H), 4.77-4.66 (m, isomer), 4.66-4.53 (m, isomer), 2.92-2.53 (m, 3H), 2.14-2.01 (m, 1H), 1.22 (s, 9H), 1.10-0.98 (s, isomer).

The isomer is assumed to be due to the hindered rotation of the carbamate as the molecule hits on elemental analysis.

^{13}C{^{1}H} NMR (75 MHz; $CDCl_3$): δ 153.6, 139.7, 136.9, 133.9, 129.3, 129.1, 128.7, 128.4, 126.5, 80.9, 70.2, 31.5, 28.13, 27.99

Element Analysis calculated for $C_{20}H_{25}NO_4S$: C, 63.97; H, 6.71; N, 3.73; O, 17.04; S, 5.84. Found: C, 64.20; H, 6.72; N, 3.56.

IR (FTIR, film): ν = 3349, 2981, 2938, 1690, 1510, 1317, 1308, 1135 cm^{-1}.

HRMS, (ESI positive ion mode) m/z: calculated for $C_{20}H_{25}NO_4NaS$: 298.1402. Found: 398.1406.

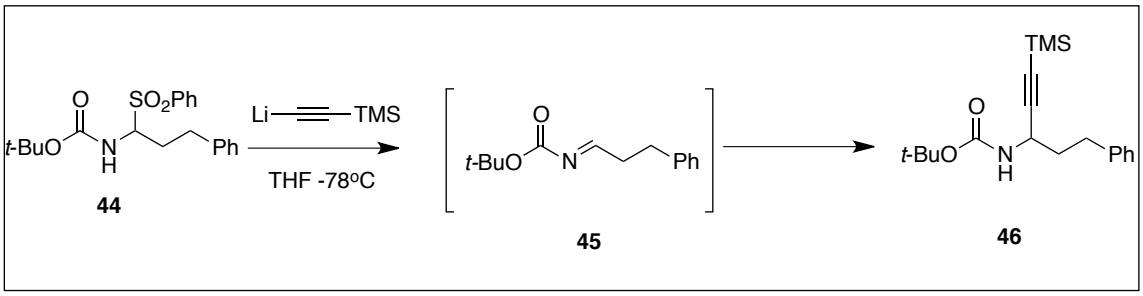

TMS-acetylene (1.5 mL, 10.7 mmol) was dissolved in dry THF (40 mL) in a 100 mL round bottom equipped with a Teflon-coated magnetic stir bar and cooled to -20 ^{o}C. Dropwise over five minutes *n*-butyllithium (1.3M in THF, 8.3 mL, 10.9 mmol) was added to the initial clear solution and turned bright orange. The Solution was allowed to stir at this temperature for 30 minutes. In a separate 250 round bottom flask equipped with a Teflon-coated magnetic stir bar, sulfone **44** was added and dissolved in dry THF (13.3 mL) and cooled to – 78 ^{o}C. The resulting TMS-acetylide was then added dropwise to the sulfone solution over five minutes. The reaction was allowed to stir at this temperature for two hours. Following two hours the reaction was quenched with NH_4Cl (50 mL) and the organic layer was separated. The aqueous layer was extracted with CH_2Cl_2 (3x50 mL) and combined. The combined organics were dried over $MgSO_4$ and filtered. The solvent was removed by rotary evaporation to yield a dark brown liquid. Crude product was purified by silica flash column chromatography (hexanes/EtOAc, 20:1, r.f. 0.2) to afford **46** as a white solid (1.33g, 70%).

Data for **46**:

^{1}H-NMR (400 MHz; $CDCl_3$): δ 7.28 (t, *J* = 7.4 Hz, 2H), 7.21-7.17 (m, 3H), 4.69 (br s, 1H), 4.45 (br s, 1H), 2.81-2.69 (m, 2H), 2.04-1.87 (m, 2H), 1.44 (s, 9H), 0.18 (s, 9H).

^{13}C{^{1}H} NMR (101 MHz; $CDCl_3$): δ 154.9, 141.41, 141.38, 128.6, 126.1, 105.2, 88.2, 77.4, 43.7, 38.2, 32.2, 28.5, 0.1

Elemental Analysis calculated for $C_{19}H_{29}NO_2Si$: C, 68.83; H, 8.82; N, 4.22; O, 9.65; Si, 8.47. Found: C, 69.17; H, 8.99; N, 4.44.

HRMS, (ESI positive ion mode) m/z: calculated for $C_{19}H_{29}NO_2NaSi$: 354.1865. Found: 354.1858.

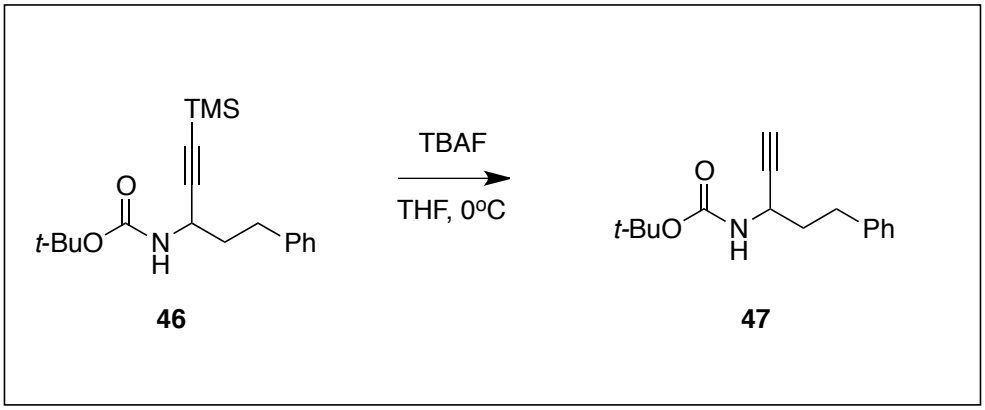

46 **47**

Alkyne **46** was transferred to a 100 mL round bottom flask equipped with a teflon magnetic stir bar, dissolved in dry THF (9.13 mL) and cooled to 0 ^{o}C. TBAF (1.0M in THF, 36 mL, 36 mmol) was added over ten minutes. The reaction was quenched with ammonium chloride and organic layers were separated. The aqueous layers were extracted with CH_2Cl_2 (3x 50 ml), combined, dried over $MgSO_4$, and solvent was removed by rotary evaporation to yield a dark brown liquid. The crude product was purified by silica flash column chromatography (hexanes/EtOAc, 12:1, r.f. 0.2) to afford free-alkyne **47** as a white solid (1.92g, 82% solvent accounted).

Data for **47**:

^{1}H-NMR (300 MHz; $CDCl_3$): δ 7.36-7.30 (m, 3H), 7.26-7.21 (m, 1H), 4.76 (br s, 1H), 4.48 (br s, 1H), 2.89-2.73 (m, 2H), 2.37 (d, *J* = 2.3 Hz, 1H), 2.11-1.92 (m, 2H), 1.49 (s, 9H).

^{13}C{^{1}H} NMR (101 MHz; $CDCl_3$): δ 154.9, 141.1, 128.62, 128.57, 126.2, 83.4, 80.1, 71.6, 42.7, 37.9, 32.0, 28.5

Elemental Analysis calculated for $C_{16}H_{21}NO_2$: C, 74.10; H, 8.16; N, 5.4; O, 12.34. Found: C, 73.72; H, 8.35; N, 5.50.

HRMS, (ESI positive ion mode) m/z: calculated for $C_{16}H_{21}NO_2Na$: 282.1470. Found: 282.1476.

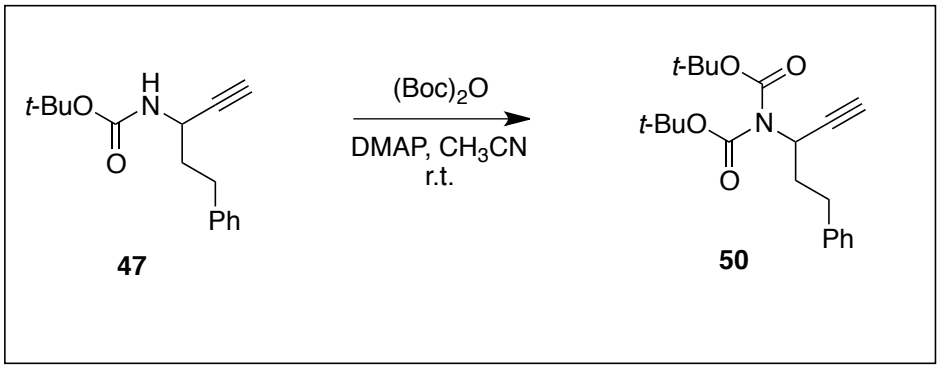

Compound **47** was dissolved in dry CH_3CN in a 100 mL round bottom flask equipped with a Teflon-coated magnetic stir bar. To this clear solution was added 4-Dimethylaminopyridine (DMAP) (0.628 g, 5.14 mmol) and di-t*ert*-butyldicarbonate (5.60g, 25.7 mmol). The solution was allowed to stir at room temperature overnight. The solvent was removed by rotary evaporation to yield a dark brown oil. The crude oil was purified by silica flash column chromatography (hexanes/EtOAc, 20:1, r.f. 0.31) to yield a clear liquid **50** (4.76g, 77%).

Data for alkyne **50**:

^{1}H-NMR (400 MHz; $CDCl_3$): δ 7.31-7.27 (m, 1H), 7.20-7.17 (m, 3H), 5.02 (ddd, *J* = 8.4, 7.1, 2.5 Hz, 1H), 2.77 (ddd, *J* = 13.9, 9.9, 5.5 Hz, 1H), 2.65 (ddd, *J* = 13.8, 9.7, 6.6 Hz, 1H), 2.35 (d, *J* = 2.5 Hz, 1H), 2.37-2.27 (m, 1H), 2.16 (ddt, *J* = 13.3, 10.0, 6.7 Hz, 1H), 1.50 (s, 18H).

^{13}C{^{1}H} NMR (101 MHz; $CDCl_3$): δ 152.1, 141.1, 128.60, 128.56, 126.2, 83.1, 81.9, 71.9, 47.9, 36.0, 32.7, 28.2

Elemental Analysis calculated for $C_{21}H_{23}NO_4$: C, 70.17; H, 8.13; N, 3.90; O, 17.80. Found: C, 70.40; H, 8.27; N, 4.15.

HRMS, (ESI positive ion mode) m/z: calculated for $C_{21}H_{29}NO_4Na$: 382.1994. Found: 382.1991.

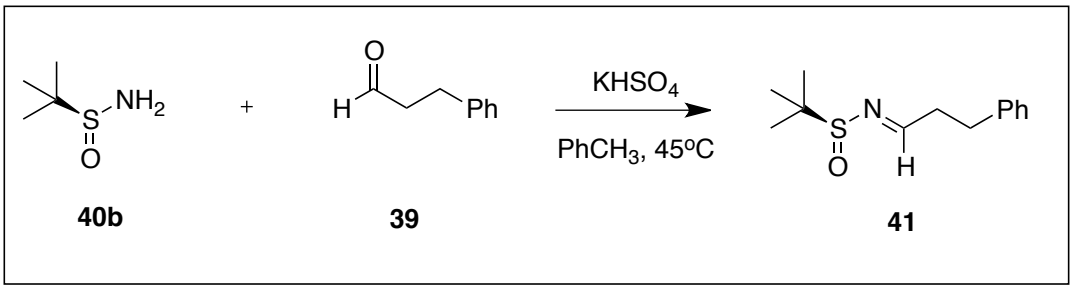

40b **39** **41**

Ellman's auxiliary **40b** (0.150 g, 1.23 mmol) was added to a 25 mL round bottom flask equipped with a Teflon-coated magnetic stir bar, followed by toluene (13 mL), $KHSO_4$ (0.336 g, 2.47 mmol) and hydrocinnamaldehyde **39** (0.33 mL, 2.47 mmol). The solution was then heated at 45 ^oC for 24 hours. The solution was filtered to remove $KHSO_4$ and the filtrate was concentrated by rotary evaporation to provide crude **41**. Crude **41** was purified by silica flash column chromatography (hexanes/eEtOAc, 9:2, r.f. 0.31) to yield a clear liquid (0.265 g, 91% yield).

Data for **41**:

^{1}H-NMR (300 MHz; $CDCl_3$): δ 8.16 (t, *J* = 4.2 Hz, 1H), 7.36-7.30 (m, 2H), 7.26-7.21 (m, 3H), 3.04-2.99 (m, 2H), 2.94-2.87 (m, 2H), 1.17 (s, 9H).

^{13}C{^{1}H} NMR (75 MHz; $CDCl_3$): δ 168.6, 140.4, 128.7, 128.4, 126.4, 56.7, 37.6, 31.5, 22.4

IR (FTIR, film): ν = 3028, 2959, 2926, 1622, 1363, 1079 cm^{-1}.

HRMS, (ESI positive ion mode) m/z: calculated for $C_{13}H_{20}NOS$: 238.1266. Found: 238.1267.

$[\alpha]_D^{21}$: + 1.7 (c 0.6, CH_2Cl_2)

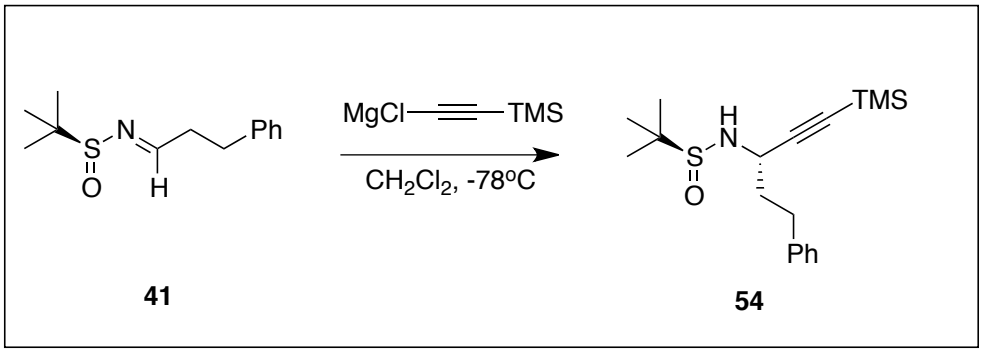

In a 25 mL two neck round bottom flask equipped with a Teflon-coated magnetic stir bar, isopropyl magnesium chloride (2.0 M in THF, 10.2 mL, 20.36 mmol) was added and cooled to 0 ^{o}C. [68] Tetramethylsilylacetylene (2.9 mL, 20.36 mmol) was then added dropwise. The solution was allowed to stir at 0 ^{o}C for 2 hours to form the Grignard reagent**.** In a 100 mL round bottom flask equipped with a Teflon-coated magnetic stir bar, **41** (1.610 g, 6.79 mmol) and dry CH_2Cl_2 (20 mL) were added and cooled to – 78 ^{o}C. The Grignard reagent was then added drop wise over five minutes and CH_2Cl_2 was used to transfer the remaining (2 x 7 mL). The solution remained at – 78 ^{o}C for another 2 hours and was allowed to warm to room temperature overnight. The solution was quenched with NH_4Cl (50 mL) and extracted with EtOAc (3 x 40 mL). The organic layers were combined, washed with brine (100 mL) and dried over Na_2SO_4. The drying agent was removed by gravity filtration, and the solvent was removed by rotary evaporation to yield a crude yellow oil. Crude **54** was purified by silica flash column chromatography (hexanes/EtOAc, 3:1, r.f. 0.3) to yield a light yellow liquid of **54** (2.086 g, 92% yield).

Data for **54**:

^{1}**H-NMR** (300 MHz; $CDCl_3$): δ 7.37-7.32 (m, 2H), 7.27-7.23 (m, 3H), 4.21-4.11 (m, 1H), 3.41 (d, *J* = 5.3 Hz, 1H), 2.92-2.76 (m, 2H), 2.18-1.98 (m, 2H), 1.27 (s, 9H), 0.24 (s, 9H).

^{13}C{^{1}H} NMR (75 MHz; $CDCl_3$): δ 141.2, 128.61, 128.56, 126.2, 105.1, 90.2, 56.2, 47.6, 38.6, 31.9, 22.6, 0.0.

IR (FTIR, film): ν =3499, 3170, 2957, 1654, 1044, 845 cm^{-1}.

HRMS, (ESI positive ion mode) m/z: calculated for $C_{18}H_{30}NOSiS$: 336.1817. Found: 336.1819.

$[\alpha]_D^{21}$: + 0.47 (c 0.23, CH_2Cl_2)

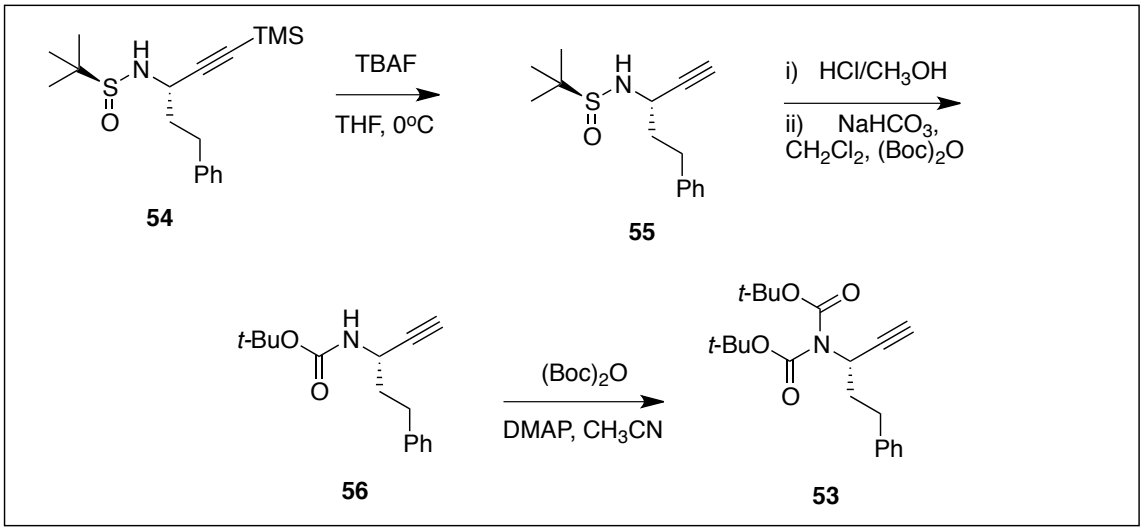

In a 100 mL round bottom flask equipped with a Teflon-coated magnetic stir bar, **54** was added (4.113 g, 12.26 mmol) and dissolved in dry THF (12.3 mL) and a light yellow solution was observed. The solution was cooled to 0 ^oC and tetrabutylammonium fluoride (TBAF) (14.7 mL of a 1.0 M solution in THF, 14.7 mmol) was added drop wise over five minutes and a red solution was observed. After stirring at room temperature for 30 minutes, the solution was quenched with water (20 mL) and the organic layer was separated. The aqueous layer was extracted with EtOAc (3 x 20 mL). The combined organic layers were washed with saturated $NaHCO_3$ and dried over Na_2SO_4. The dying agent was removed via gravity filtration and the solvent was removed by evaporation to yield a crude yellow oil **55** that was used in the next step without purification.

In a 250 mL round bottom flask equipped with a Teflon-coated magnetic stir bar, **55** (12.26 mmol assume completion) was added and dissolved in MeOH (79 mL), and HCl in MeOH (16.0 mL) was added. The resulting solution was allowed to stir at room

temperature for 4 hours. The volatiles were removed by rotary evaporation and the remaining product was transferred to a 500 mL round bottom flask equipped with a Teflon-coated magnetic stir bar and dissolved in dry CH_2Cl_2 (203 mL). $NaHCO_3$ (3.576 g, 42.6 mmol) was added followed by di-*tert*-butyldicarbonate (6.975 g, 31.9 mmol). The mixture was allowed to stir at room temperature overnight then diluted with CH_2Cl_2 and filtered by gravity filtration. The remaining filtrate was concentrated by rotary evaporation and transferred to a 50 mL round bottom flask. The crude mono-protected product was dissolved in anhydrous CH_3CN (71.3 mL) and 4-Dimethylaminopyridine (DMAP) (0.784 g, 6.39 mmol) and di-tert butyl di-carbonate (5.668 g, 25.61 mmol) were sequentially added to the flask and the solution was allowed to stir overnight. The solution was concentrated by rotary evaporation to yield a crude brown oil. The crude product was purified by silica flash column chromatography (hexanes:EtOAc, 12:1, r.f. 0.5) to yield a colorless liquid **53** (3.432 g, 79 % yield over 3 steps).

Data for **53**:

^{1}H-NMR (300 MHz; $CDCl_3$): δ 7.36-7.31 (m, 2H), 7.26-7.22 (m, 3H), 5.11-5.05 (m, 1H), 2.87-2.66 (m, 2H), 2.41 (d, *J* = 2.5 Hz, 1H), 2.44-2.32 (m, 1H), 2.22 (ddt, *J* = 13.3, 9.8, 6.8 Hz, 1H), 1.55 (s, 18H).

^{13}C{^{1}H} NMR (101 MHz; $CDCl_3$): δ 152.1, 141.1, 128.58, 128.56, 126.2, 83.1, 81.9, 71.9, 47.9, 36.0, 32.7, 28.2

IR (FTIR, film): ν = 2986, 2947, 1743, 1703, 1137 cm^{-1}.

HRMS, (ESI positive ion mode) m/z: calculated for $C_{21}H_{29}NO_4Na$: 382.1994. Found: 382.2004.

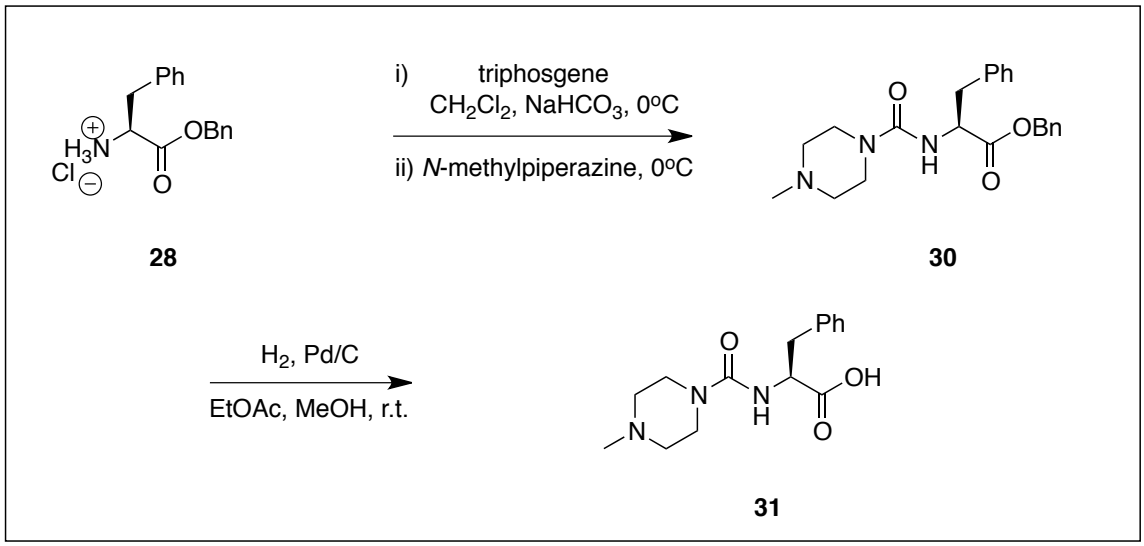

In a 500 mL round bottom flask equipped with a magnetic Teflon-coated stir bar, **28** (2.50 g, 8.56 mmol) was added, dissolved in CH_2Cl_2 (135 mL) and cooled to 0 ^oC. Saturated Na_2CO_3 (135 mL) was added to the solution and the solution was allowed to stir for 30 minutes at 0^oC. In a separate 10 mL round bottom flask, triphosgene (0.840 g, 2.84 mmol) was added and dissolved in dry CH_2Cl_2 (3.5 mL). The triphosgene solution was added dropwise to the original solution. The triphosgene flask was rinsed with more CH_2Cl_2 (2 x 1.8 mL) and these wasjed were added to the original 500 mL round bottom flask. The solution was allowed to stir for an additional 30 minutes at 0 ^oC. The layers of the solution were then separated and the aqueous layer was further extracted with CH_2Cl_2 (3 x 60 mL). The combined organic layers were dried over Na_2SO_4 and the drying agent was removed by gravity filtration. The filtrate was cooled back to 0 ^oC and *N*-methylpiperazine (0.94 mL, 8.47 mmol) was added to the solution. The mixture was stirred overnight, then the solvent was removed to yield a a white solid, **30** which was used without further purification.

In a 500 mL round bottom flask equipped with a magnetic Teflon-coated stir bar, **30** (3.195 g, ~ 8.38 mmol) was dissolved in a mixture of EtOAc (177 mL) and MeOH (71 mL). To this solution was added 10 % palladium on carbon (1.10 g) and the reaction was stirred under a hydrogen atmosphere using a balloon filled with hydrogen gas overnight. The catalyst was removed by filtration through a pad of CELITE^{TM} and the filtrate was concentrated by rotary evaporation to yield a white foam. Ethyl ether anhydrous was

added to the white foam to form a white powder. The precipitate **31** was isolated from vacuum filtration (2.139 g, 66 % yield over two steps).

Data for **31:**

^{1}H-NMR (400 MHz; DMSO-d_6): δ 7.28-7.22 (m, 4H), 7.21-7.17 (m, 1H), 6.51 (d, *J* = 8.2 Hz, 1H), 4.26 (td, *J* = 8.8, 4.8 Hz, 1H), 3.30-3.19 (m, 4H), 3.04 (dd, *J* = 13.8, 4.8 Hz, 1H), 2.93 (dd, *J* = 13.6, 9.7 Hz, 1H), 2.23-2.16 (m, 4H), 2.16 (s, 3H).

^{13}C{^{1}H} NMR (101 MHz; DMSO): δ 173.8, 156.9, 138.2, 128.9, 127.8, 125.9, 55.0, 54.1, 45.4, 43.2, 36.6

HRMS, (ESI positive ion mode) m/z: calculated for $C_{15}H_{22}N_3O_3$: 292.1661. Found: 292.1659.

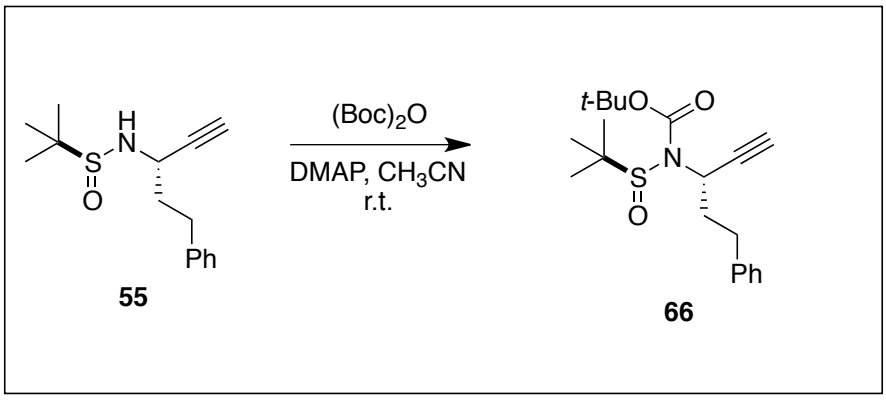

In a 10 ml round bottom flask equipped with a Teflon-coated stir bar alkyne **55** (0.201 g, 0.76 mmol) was added and dissolved in dry CH_3CN (2.5 mL). DMAP (0.0280g, 0.23 mmol), followed by di-*tert*-butyldicarbonate (0.212 g, 0.91 mmol) were added and the resulting solution was allowed to stir overnight. Solvent was removed by rotary evaporation the next morning and the resultant yellow oil was purified by flash column chromatography (hexanes/EtOAc 12:1, r.f. 0.25) to afford a colorless liquid **66** (0.145 g, 52% yield).

Data for **66:**

^{1}H-NMR (400 MHz; $CDCl_3$): δ 7.29-7.25 (m, 2H), 7.21-7.16 (m, 3H), 4.44 (ddd, *J* = 8.8, 6.5, 2.4 Hz, 1H), 2.77 (ddd, *J* = 13.5, 11.5, 4.6 Hz, 1H), 2.59 (ddd, *J* = 13.7, 11.1, 6.1 Hz, 1H), 2.44-2.37 (m, 1H), 2.36 (d, *J* = 2.4 Hz, 1H), 2.08 (ddt, *J* = 12.7, 11.5, 6.3 Hz, 1H), 1.50 (s, 9H), 1.28 (s, 9H).

^{13}C{^{1}H} NMR (101 MHz; $CDCl_3$): δ 141.3, 128.59, 128.50, 126.0, 83.3, 82.3, 71.7, 60.9, 40.8, 36.4, 32.9, 28.4, 22.8.

HRMS, (ESI positive ion mode) m/z: calculated for $C_{20}H_{29}NO_3NaS$: 386.1766. Found: 386.1760.

2.4.8 ^{19}F NMR Experiment Using Mosher's Acid Chloride to Determine Enantioselectivity

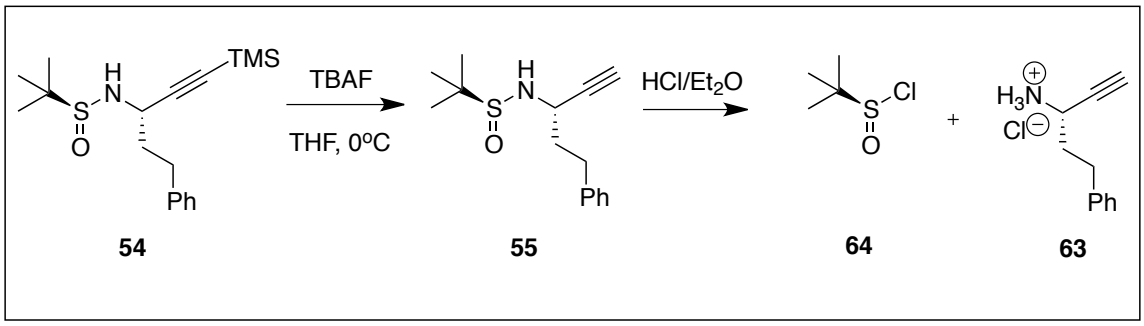

In a 10 ml round bottom flask equipped with a Teflon-coated stir bar alkyne 54 (0.795 g, 2.37 mmol) was added , followed by THF (2.4 mL). The light yellow solution was cooled to 0 ^{o}C and TBAF (3.6 mL of 1.0 M solution in THF, 3.60 mmol) was added over two minutes to produce a reddish-brown solution. After 10 minutes the solution was quenched with water (10 mL) and the organic layer was separated. The water layer was extracted with EtOAc (3 x 10 mL). The organic phases were combined and washed with $NaHCO_3$ (30 mL), dried over Na_2SO_4 and drying reagent was removed via gravity filtration. The solvent was removed by rotary evaporation to give a crude orange oil. The crude oil was purified by flash column chromatography (hexanes/EtOAc 2:1, r.f. 0.23) to yield a clear liquid **55** (0.496 g, 79% yield).

Data for **55**:

^{1}H-NMR (300 MHz; $CDCl_3$): δ 7.32-7.27 (m, 2H), 7.22-7.19 (m, 3H), 4.05 (ddd, *J* = 6.9, 2.4, 2.1 Hz, 1H), 3.36 (d, *J* = 6.7 Hz, 1H), 2.89-2.73 (m, 2H), 2.48 (d, *J* = 2.3 Hz, 1H), 2.14-1.96 (m, 2H), 1.21 (s, 9H).

^{13}C{^{1}H} NMR (75 MHz; $CDCl_3$): δ 141.0, 128.69, 128.59, 126.3, 83.5, 73.7, 56.3, 47.2, 38.5, 31.8, 22.7

Elemental Analysis calculated for $C_{18}H_{29}NOSSi$: C, 64.42; H, 8.71; N, 4.17; O, 4.77; S, 9.56; Si, 8.37. Found: C, 64.64; H, 8.87; N, 4.27.

IR (FTIR, film): ν = 3209, 3287, 2926, 2954, 1455, 1053 cm^{-1}.

HRMS, (ESI positive ion mode) m/z: calculated for $C_{15}H_{22}NOS$: 264.1422. Found: 264.1426.

$[\alpha]_D^{21}$: + 0.371 (c 0.2, CH_2Cl_2)

In a 20 mL vial alkyne **55** (0.050 g, 0.189 mmol) was dissolved in Et_2O. HCl/Et_2O (0.4 mL 1.0M) was added in one portion, immediately an off-white precipitate was formed. The precipitate was isolated by vacuum filtration and washed with Et_2O (3x 5 mL). The resulting off white powder **63** was used without further purification.

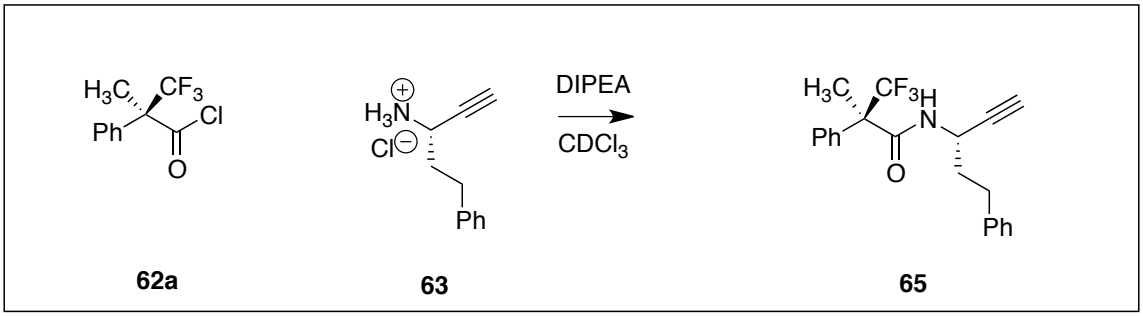

Alkyne salt **63** (5 mg, 0.025 mmol) was dissolved in $CDCl_3$ (0.4 mL) in a small vial and DIPEA (0.013 mL) was added via microsyringe. To this solution Mosher's acid chloride **62a** (77 mg, 0.031 mmol) was added and then the entire solution was transferred to an NMR test tube. ^{19}F NMR spectrum was recorded immediately.

Data for **65**:

$^{19}F\{^{1}H\}$ NMR (282 MHz; CDCl3): δ -69.22 (minor isomer), -69.39, -70.4 (Mosher's Acid Chloride).

2.4.9 Analytical Data

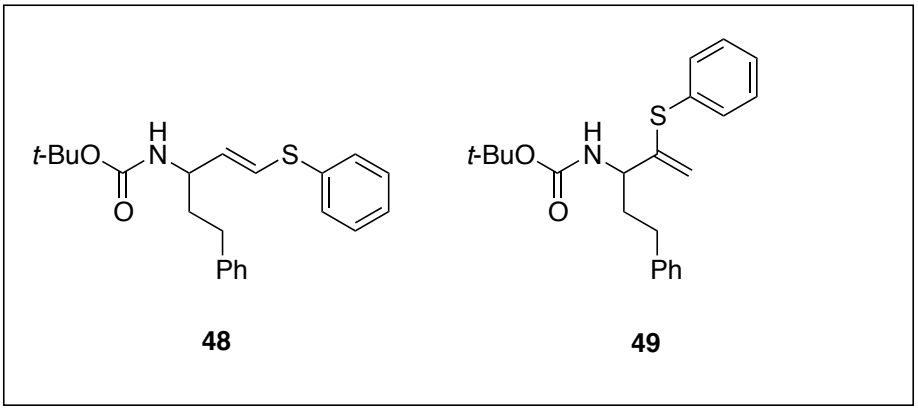

Followed general procedure **2.4.3**. Prepared from alkyne **50**. Colorless liquid, 65% yield, 5:2 ratio of *E*-linear:branched isomers. Purification was completed using flash column chromatography (hexanes/EtOAc 20:1, r.f. 0.25).

Data for mixture of **48**/**49**:

^{1}H-NMR (400 MHz; $CDCl_3$): δ 7.49 (m, *J* = 7.2 Hz, branched impurity), 7.38-7.19 (m, 10H), 6.37 (d, *J* = 15.1 Hz, 1H), 5.80 (dd, *J* = 15.1, 6.4 Hz, 1H), 5.45 (s, branched impurity), 4.99 (s, branched impurity), 4.86-4.83 (m, branched impurity), 4.57 (d, *J* = 6.2 Hz, 1H), 4.26 (br s, 1H), 2.76-2.63 (m, 2H), 2.12-1.90 (m, branched impurity), 1.93-1.81 (m, 2H), 1.48 (s, 9H).

^{13}C{^{1}H} NMR (101 MHz; $CDCl_3$): δ 155.2, 146.6, 141.4, 135.9, 135.3, 134.0, 133.3, 132.8, 129.6, 129.37, 129.17, 129.13, 128.58, 128.47, 128.1, 126.8, 126.13, 126.07, 115.1, 79.6, 56.1, 52.5, 37.3, 37.0, 36.1, 32.42, 32.29, 29.8, 28.69, 28.56, 28.51, 28.3

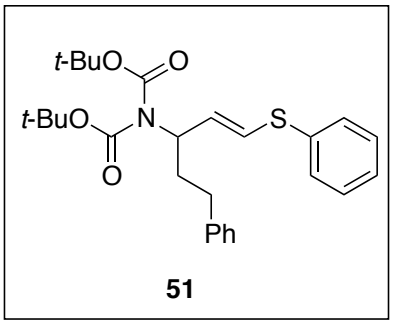

51

Followed general procedure **2.4.3**. Prepared from alkyne **50**. Colorless liquid, 61% yield, >25:1 ratio of *E*-linear:branched isomers. Purification was completed using flash column chromatography (hexanes/ EtOAc 20:1, r.f. 0.29). For full characterization see chiral analogue **59**.

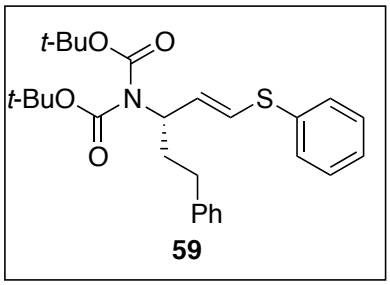

59

Followed general procedure **2.4.3**. Prepared from alkyne **53**. Colorless liquid, 89% yield (corrected for solvent). Purification was completed using flash column chromatography (hexanes/ EtOAc 20:1, r.f. 0.29).

Data for **59**:

^{1}H-NMR (300 MHz; $CDCl_3$): δ 7.43-7.24 (m, 10H), 6.44 (dd, *J* = 15.2, 1.0 Hz, 1H), 6.14 (dd, *J* = 15.2, 7.6 Hz, 1H), 4.89-4.81 (m, 1H), 2.70 (t, *J* = 16.0 Hz, 2H), 2.36-2.23 (m, 1H), 2.20-2.06 (m, 1H), 1.57 (s, 18H).

^{13}C{^{1}H} NMR (75 MHz; $CDCl_3$): δ 152.9, 141.5, 135.1, 132.1, 129.8, 129.2, 128.52, 128.49, 126.9, 126.21, 126.06, 82.5, 58.3, 34.8, 32.9, 28.2

IR (FTIR, film): ν = 2987, 2940, 1736, 1698, 1392, 1368, 1140, 906 cm^{-1}.

HRMS, (ESI positive ion mode) m/z: calculated for $C_{27}H_{35}NO_4NaS$: 492.2185. Found: 492.2193.

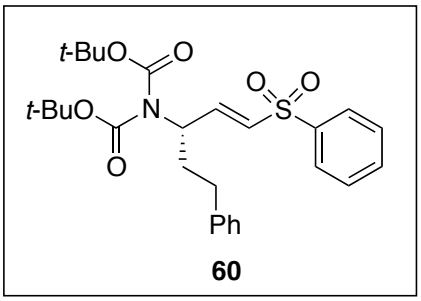

60

Followed general procedure **2.4.5**. Prepared from vinyl sulfide **59**. White solid, 80% yield (corrected for solvent). Purification was completed using flash column chromatography (hexanes/ EtOAc 7:1, r.f. 0.3)

Data for **60**:

^{1}**H-NMR** (400 MHz; $CDCl_3$): δ 7.87 (dd, *J* = 8.5, 1.1 Hz, 2H), 7.63-7.58 (m, 1H), 7.54-7.50 (m, 2H), 7.28-7.25 (m, 2H), 7.20-7.17 (m, 1H), 7.14-7.12 (m, 2H), 7.08 (dd, *J* = 15.3, 5.0 Hz, 1H), 6.35 (dd, *J* = 15.3, 1.8 Hz, 1H), 4.96-4.90 (m, 1H), 2.68-2.56 (m, 2H), 2.28 (dtd, *J* = 13.7, 9.3, 6.4 Hz, 1H), 2.09-2.00 (m, 1H), 1.44 (s, 18H).

^{13}C{^{1}H} NMR (101 MHz; $CDCl_3$): δ 152.3, 146.0, 140.7, 140.5, 133.5, 130.7, 129.4, 128.7, 128.4, 127.8, 126.4, 83.4, 55.8, 33.9, 32.4, 28.1

IR (FTIR, film): ν = 2987, 2940, 1732, 1688, 1342, 1309, 1334 cm^{-1}.

HRMS, (ESI positive ion mode) m/z: calculated for $C_{27}H_{35}NO_6NaS$: 524.2083. Found: 524.2079.

$[\alpha]_D^{21}$: + 0.0835 (c 0.2, CH_2Cl_2)

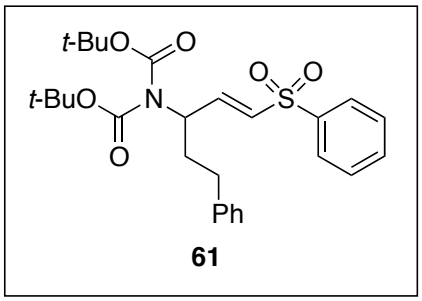

61

Followed general procedure **2.4.5**. Prepared from vinyl sulfide **51**. White solid, 40% yield. Purification was completed using flash column chromatography (hexanes/ EtOAc 7:1, r.f. 0.30). For full characterization see analogue **60**.

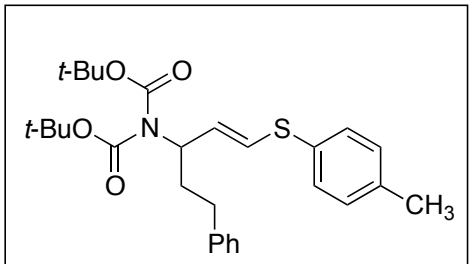

71

Followed general procedure **2.4.3**. Prepared from alkyne **50**. Colorless liquid, 71% yield, 30:1 ratio of *E*-linear:branched isomer. Purification was completed using flash column chromatography (hexanes/EtOAc 20:1, r.f. 0.20). For full characterization see analogue **81**.

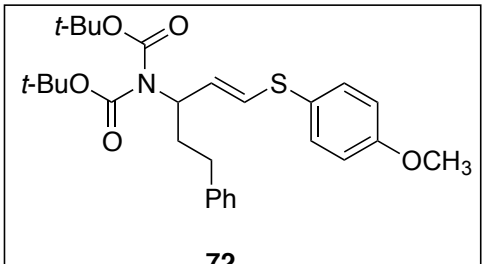

72

Followed general procedure **2.4.3**. Prepared from alkyne **50**. Colorless liquid, 65% yield. 17:1 ratio of *E*-linear:branched isomer. Purification was completed using flash

column chromatography (hexanes/ethyl acetate 25:1, r.f. 0.18). For full characterization see analogue **82**.

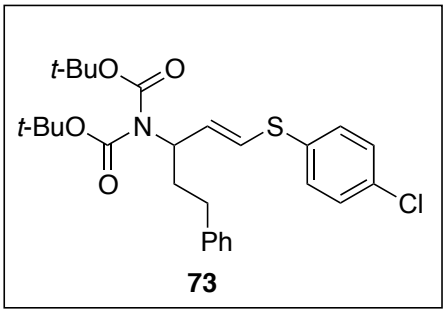

73

Followed general procedure **2.4.4**. Prepared from alkyne **50**. Colorless liquid, 62% yield, 14:1 ratio of *E*-linear:branched isomer. Purification was completed using flash column chromatography (hexanes/ EtOAc 30:1, r.f. 0.26) For full characterization see chiral analogue **83**.

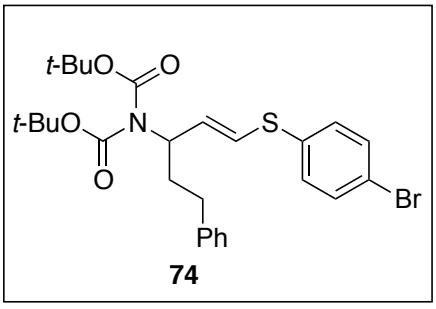

74

Followed general procedure **2.4.4**. Prepared from alkyne **50**. Colorless liquid, 51% yield, 30:1 ratio of *E*-linear:branched isomer. Purification was completed using flash column chromatography (hexanes/EtOAc 30:1, r.f. 0.30). For full characterization see analogue **86**.

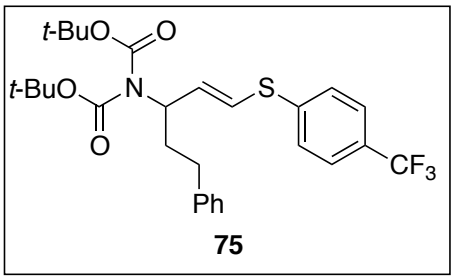

75

Followed general procedure **2.4.3**. Prepared from alkyne **50**. White solid, 67% yield, 30:1 ratio of *E*-linear:branched isomer. Purification was completed using flash column chromatography (hexanes/EtOAc 30:1, r.f. 0.40). For full characterization see analogue **85**.

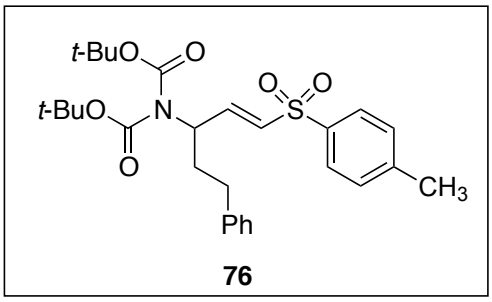

76

Followed general procedure **2.4.5**. Prepared from vinyl sulfide **75**. Yield to be determined. For full characterization see analogue **86**.

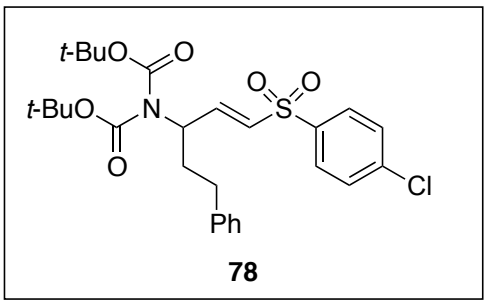

78

Followed general procedure **2.4.5**. Prepared from vinyl sulfide **73**. White solid, 31% yield. Purification was completed using flash column chromatography (hexanes/EtOAc 30:1, r.f. 0.40). For full characterization see analogue **88**.

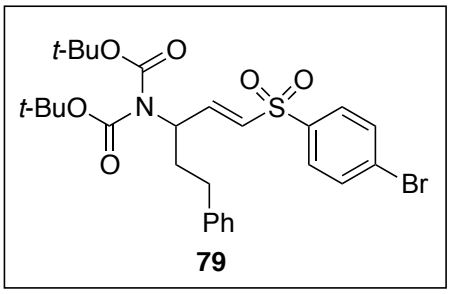

79

Followed general procedure **2.4.5**. Prepared from vinyl sulfide **74**. Yield to be determined. For full characterization see analogue **89.**

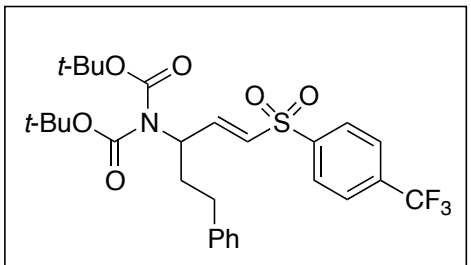

80

Followed general procedure **2.4.5**. Prepared from vinyl sulfide **75**. Yield to be determined. For full characterization see analogue **90**.

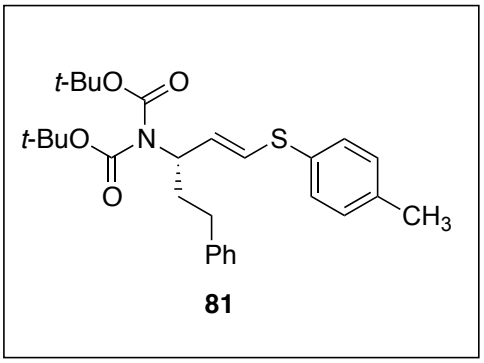

81

Followed general procedure **2.4.4**. Prepared from alkyne **53**. Colorless liquid, 81% yield, 50:1 ratio of *E*-linear:branched isomer. Purification was completed using flash column chromatography (hexanes/EtOAc 20:1, r.f. 0.2).

Data for **81**:

^{1}H-NMR (400 MHz; $CDCl_3$): δ 7.30-7.25 (m, 5H), 7.22-7.17 (m, 3H), 7.13 (d, *J* = 7.9 Hz, 2H), 6.34 (d, *J* = 15.2 Hz, 1H), 5.97 (dd, *J* = 15.1, 7.7 Hz, 1H), 4.75 (q, *J* = 7.7 Hz, 1H), 2.62 (t, *J* = 8.0 Hz, 2H), 2.34 (s, 3H), 2.25-2.16 (m, 2H), 2.00-1.99 (m, 1H), 1.49 (s, 18H).

^{13}C{^{1}H} NMR (101 MHz; $CDCl_3$): δ 154.0, 152.4, 145.3, 144.5, 137.5, 131.1, 130.0, 128.7, 128.4, 127.9, 126.4, 83.3, 55.8, 33.9, 32.5, 28.1, 21.7

IR (FTIR, film): ν = 2977, 2934, 1738, 1700, 1367, 1340, 1138 cm^{-1}.

HRMS, (ESI positive ion mode) m/z: calculated for $C_{28}H_{37}NO_4NaS$: 506.2341. Found: 506.2335.

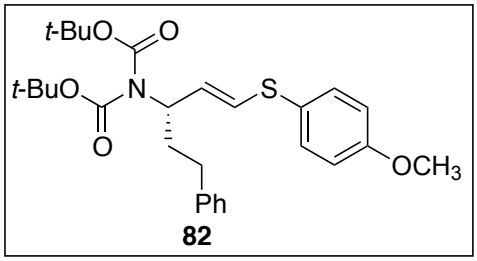

82

Followed general procedure **2.4.3**. Prepared from alkyne **53**. Colorless liquid, 52% yield, 50:1 ratio of *E*-linear:branched isomer. Purification was completed using flash column chromatography (hexanes/EtOAc 20:1 r.f. 0.2).

Data for **82**:

^{1}H-NMR (400 MHz; $CDCl_3$): δ 7.35-7.31 (m, 2H), 7.27 (t, *J* = 7.4 Hz, 3H), 7.18 (t, *J* = 7.0 Hz, 3H), 6.89-6.85 (m, 2H), 6.31 (dd, *J* = 15.1, 0.7 Hz, 1H), 5.85 (dd, *J* = 15.1, 7.7 Hz, 1H), 4.73 (q, *J* = 7.6 Hz, 1H), 3.81 (s, 3H), 2.61 (t, *J* = 8.0 Hz, 2H), 2.24-2.15 (m, 1H), 2.07-1.98 (m, 1H), 1.49 (s, 19H).

^{13}C{^{1}H} NMR (101 MHz; CDCl3): δ 159.6, 152.9, 141.6, 136.1, 133.5, 129.2, 128.50, 128.42, 126.0, 124.6, 115.0, 82.4, 58.4, 55.5, 35.0, 32.9, 28.2

IR (FTIR, film): ν = 2986, 2934, 1738, 1699, 1367, 1340, 1244 cm^{-1}.

HRMS, (ESI positive ion mode) m/z: calculated for $C_{28}H_{37}NO_5NaS$: 522.2290. Found: 522.2271.

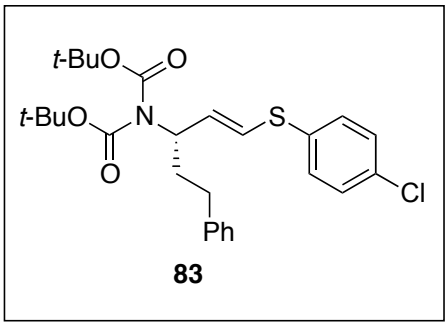

83

Followed general procedure **2.4.4**. Prepared from alkyne **53.** Colorless liquid, 88% yield, 50:1 ratio of *E*-linear:branched isomer. Purification was completed using flash column chromatography (hexanes/EtOAc 30:1, r.f. 0.26).

Data for **83**:

^{1}H-NMR (400 MHz; $CDCl_3$): δ 7.30-7.23 (m, 7H), 7.20-7.16 (m, 3H), 6.30 (dd, *J* = 15.1, 0.9 Hz, 1H), 6.08 (dd, *J* = 15.1, 7.5 Hz, 1H), 4.76 (q, *J* = 7.6 Hz, 1H), 2.62 (t, *J* = 8.0 Hz, 2H), 2.27-2.18 (m, 1H), 2.10-1.99 (m, 1H), 1.49 (s, 18H).

^{13}C{^{1}H} NMR (101 MHz; $CDCl_3$): δ 152.9, 141.4, 133.8, 133.2, 132.9, 131.0, 129.4, 128.57, 128.52, 126.1, 125.4, 82.6, 58.2, 34.7, 32.9

Elemental Analysis calculated for $C_{27}H_{34}ClNO_4S$: C, 64.33; H, 6.80; Cl, 7.03; N, 2.78; O, 12.70; S, 6.36. Found: C, 64.17; H, 6.76; N, 2.73.

IR (FTIR, film): ν = 2983, 2944, 1739, 1699, 1368, 1323, 1086 cm^{-1}.

HRMS, (ESI positive ion mode) m/z: calculated for $C_{27}H_{34}NO_4NaSCl$: 526.1795 Found: 526.1785.

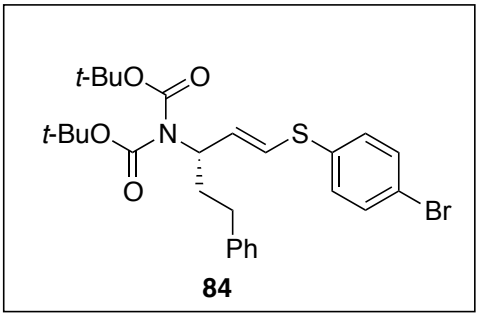

84

Followed general procedure **2.4.4**. Prepared from alkyne **53**. Colorless liquid, 80% yield, 50:1 ratio of *E*-linear:branched isomer. Purification was completed using flash column chromatography (hexanes/EtOAc 30:1, r.f. 0.30).

Data for **84**:

^{1}H-NMR (400 MHz; $CDCl_3$): δ 7.43-7.39 (m, 2H), 7.30-7.26 (m, 3H), 7.20-7.16 (m, 5H), 6.30 (dd, *J* = 15.1, 0.9 Hz, 1H), 6.09 (dd, *J* = 15.1, 7.5 Hz, 1H), 4.76 (q, *J* = 7.5 Hz, 1H), 2.62 (t, *J* = 8.0 Hz, 2H), 2.27-2.18 (m, 1H), 2.08-1.99 (m, 1H), 1.49 (s, 18H).

^{13}C{^{1}H} NMR (101 MHz; $CDCl_3$): δ 152.9, 141.4, 134.5, 133.5, 132.2, 131.1, 128.57, 128.52, 126.1, 125.1, 120.8, 82.6, 58.2, 34.6, 32.9, 28.2

HRMS, (ESI positive ion mode) m/z: calculated for $C_{27}H_{34}NO_4NaSBr$: 570.1290. Found: 570.1291.

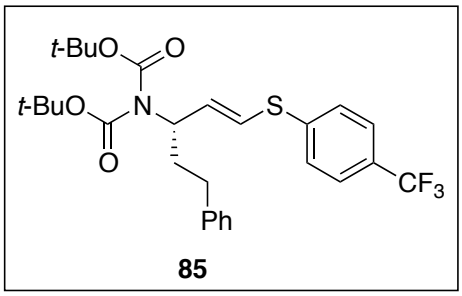

85

Followed general procedure **2.4.3**. Prepared from alkyne **53**. Colorless liquid, 84% yield, 50:1 ratio of *E*-linear:branched isomer. Purification was completed using column chromatography (hexanes/EtOAc 30:1, r.f. 0.4).

Data for **85**:

^{1}H-NMR (300 MHz; $CDCl_3$): δ 7.52 (d, *J* = 8.6 Hz, 2H), 7.37 (d, *J* = 8.6 Hz, 2H), 7.31-7.26 (m, 3H), 7.22-7.17 (m, 3H), 6.35 (d, *J* = 15.2 Hz, 1H), 6.25 (dd, *J* = 15.2, 6.9 Hz, 1H), 4.81 (q, *J* = 7.7 Hz, 1H), 2.64 (t, *J* = 8.0 Hz, 2H), 2.33-2.20 (m, 1H), 2.13-2.01 (m, 1H), 1.51 (s, 18H).

^{13}C{^{1}H} NMR (75 MHz; $CDCl_3$): δ 129.6, 117.96, 117.82, 112.7, 105.25 (2C), 105.17 (2C), 104.8, 102.8, 102.6, 100.0, 59.4, 34.8, 11.1, 9.5, 4.8

^{19}F{^{1}H} NMR (282 MHz; $CDCl_3$): δ -62.8

Elemental Analysis calculated for $C_{28}H_{34}F_3NO_4S$: C, 62.55; H, 6.37; F, 10.60; N, 2.61; O, 11.90; S, 5.96. Found: C, 62.28; H, 6.28; N, 2.55.

IR (FTIR, film): ν =2981, 2934, 1735, 1713, 1699, 1338, 1138 cm^{-1}.

HRMS, (ESI positive ion mode) m/z: calculated for $C_{28}H_{34}NO_4F_3NaS$: 560.2058. Found: 560.2066.

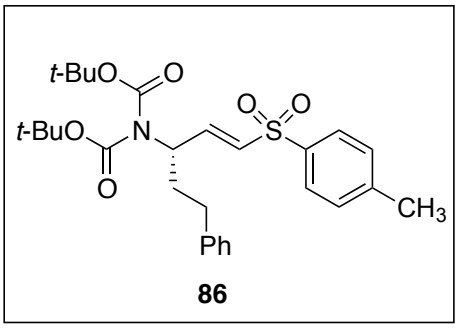

86

Followed general procedure **2.4.5**. Prepared from vinyl sulfide **81**. White solid, 79% yield. Purification was completed using flash column chromatography (hexanes/EtOAc 7:1, r.f. 0.25).

Data for **86**:

^{1}H-NMR (400 MHz; $CDCl_3$): δ 7.74 (d, *J* = 8.3 Hz, 2H), 7.31 (d, *J* = 8.0 Hz, 2H), 7.28-7.24 (m, 3H), 7.20-7.16 (m, 1H), 7.12 (d, *J* = 7.0 Hz, 2H), 7.04 (dd, *J* = 15.3, 5.0 Hz, 1H), 6.34 (dd, *J* = 15.3, 1.8 Hz, 1H), 4.94-4.89 (m, 1H), 2.67-2.55 (m, 2H), 2.42 (s, 3H), 2.32-2.22 (m, 1H), 2.04 (ddt, *J* = 13.7, 9.7, 6.7 Hz, 1H), 1.45 (s, 18H).

^{13}C{^{1}H} NMR (75 MHz; $CDCl_3$): δ 152.3, 145.3, 144.5, 10.8, 137.5, 131.1, 130.0, 128.71, 128.45, 127.9, 126.3, 83.3, 55.8, 34.0, 32.4, 28.1, 21.7

Elemental Analysis calculated for $C_{28}H_{37}NO_6S$: C, 65.22; H, 7.23; N, 2.72; O, 18.62; S, 6.22. Found: C, 64.41; H, 7.16; N, 2.83.

HRMS, (ESI positive ion mode) m/z: calculated for $C_{28}H_{37}NO_6NaS$: 538.2239 Found: 538.2251.

$[\alpha]_D^{21}$: - 0.0260 (c 0.2, CH_2Cl_2)

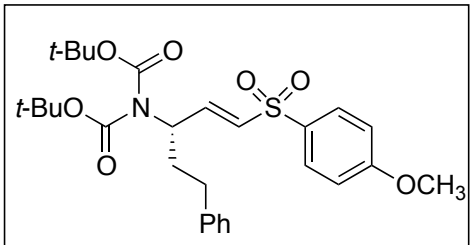

87

Followed general procedure **2.4.5**. Prepared from vinyl sulfide **82**. White solid, 81% yield. Purification was completed using flash column chromatography (hexanes/EtOAc 7:1, r.f. 0.26).

Data for **87**:

^{1}H-NMR (400 MHz; $CDCl_3$): δ 7.79 (d, *J* = 9.0 Hz, 2H), 7.28-7.25 (m, 3H), 7.18 (t, *J* = 7.4 Hz, 1H), 7.14-7.12 (m, 2H), 7.04-6.96 (m, 3H), 6.33 (dd, *J* = 15.3, 1.8 Hz, 1H), 4.94-4.88 (m, 1H), 3.86 (s, 3H), 2.68-2.55 (m, 2H), 2.32-2.22 (m, 1H), 2.08-1.99 (m, 1H), 1.45 (s, 18H).

^{13}C{^{1}H} NMR (101 MHz; $CDCl_3$): δ 163.7, 152.4, 144.7, 140.8, 134.0, 131.4, 130.1, 128.7, 128.5, 126.3, 114.6, 83.3, 55.83, 55.80, 34.0, 32.5, 28.1

Elemental Analysis calculated for $C_{28}H_{37}NO_7S$: C, 63.25; H, 7.01; N, 2.63; O, 21.07; S, 6.03. Found: C, 63.04; H, 6.94; N, 2.61.

IR (FTIR, film): ν =2983, 2927, 1736, 1697, 1368, 1339, 1138 cm^{-1}.

HRMS, (ESI positive ion mode) m/z: calculated for $C_{28}H_{37}NO_7NaS$: 554.2188. Found: 554.2185.

$[\alpha]_D^{21}$: + 0.009 (c 0.2, CH_2Cl_2)

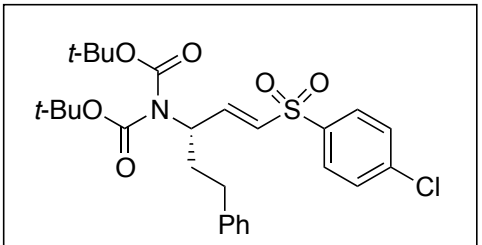

88

Followed general procedure **2.4.5**. Prepared from vinyl sulfide **83**. White solid, 68% yield. Purification was completed using flash column chromatography (hexanes/EtOAc 7:1, r.f. 0.25).

Data for **88**:

^{1}H-NMR (400 MHz; $CDCl_3$): δ 7.80 (d, *J* = 8.5 Hz, 2H), 7.49 (d, *J* = 8.5 Hz, 2H), 7.27 (d, *J* = 10.3 Hz, 3H), 7.19 (t, *J* = 7.3 Hz, 1H), 7.14-7.07 (m, 3H), 6.32 (dd, *J* = 15.3, 1.8 Hz, 1H), 4.96-4.90 (m, 1H), 2.68-2.56 (m, 2H), 2.28 (dtd, *J* = 13.6, 9.5, 6.1 Hz, 1H), 2.08-1.99 (m, 1H), 1.46 (s, 18H).

^{13}C{^{1}H} NMR (101 MHz; $CDCl_3$): δ 152.4, 146.8, 140.7, 140.3, 139.0, 130.3, 129.7, 129.3, 128.7, 128.4, 126.4, 83.5, 55.8, 33.8, 32.4, 28.1

IR (FTIR, film): ν = 2981, 2938, 1742, 1700, 1094 cm^{-1}.

HRMS, (ESI positive ion mode) m/z: calculated for $C_{27}H_{34}NO_6NaSCl$: 558.1693. Found: 558.1698.

$[\alpha]_D^{21}$: - 0.1010 (c 0.2, CH_2Cl_2)

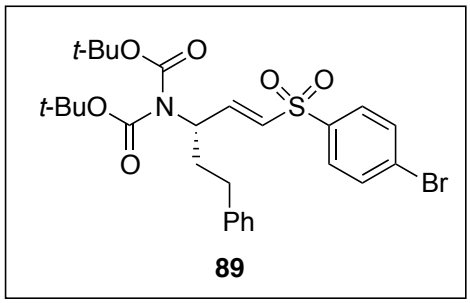

89

Followed general procedure **2.4.5**. Prepared from vinyl sulfide **84**. White solid, 79% yield. Purification was completed using flash column chromatography (hexanes/EtOAc 7:1, r.f. 0.3).

Data for **89**:

^{1}H-NMR (400 MHz; $CDCl_3$): δ 7.72 (d, *J* = 8.7 Hz, 2H), 7.66 (d, *J* = 8.8 Hz, 2H), 7.29-7.25 (m, 3H), 7.21-7.17 (m, 1H), 7.14-7.07 (m, 3H), 6.32 (dd, *J* = 15.3, 1.8 Hz, 1H), 4.95-4.90 (m, *J* = 1.6 Hz, 1H), 2.69-2.55 (m, 2H), 2.28 (dtd, *J* = 13.6, 9.5, 6.2 Hz, 1H), 2.04 (ddt, *J* = 13.4, 9.4, 6.6 Hz, 1H), 1.46 (s, 16H).

^{13}C{^{1}H} NMR (101 MHz; $CDCl_3$): δ 152.4, 146.9, 140.7, 139.6, 132.7, 130.3, 129.4, 128.82, 128.71, 128.4, 126.4, 83.5, 55.8, 33.8, 32.4, 28.1

Elemental Analysis calculated for $C_{27}H_{34}BrNO_4S$: C, 59.12; H, 6.25; Br, 14.57; N, 2.55; O, 11.67; S, 5.85. Found: C, 59.45; H, 6.22; N, 2.49.

IR (FTIR, film): ν =2981, 2938, 1742, 1700, 1111, 1090 cm^{-1}.

HRMS, (ESI positive ion mode) m/z: calculated for $C_{27}H_{34}NO_6NaSBr$: 602.1188. Found: 602.1194.

$[\alpha]_D^{21}$: + 0.05 (c 0.2, CH_2Cl_2)

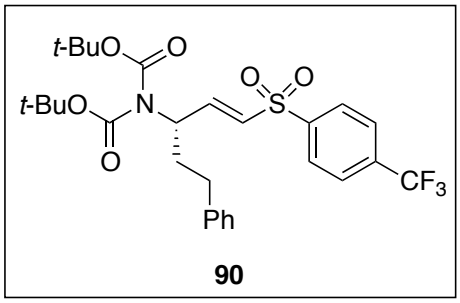

90

Followed general procedure **2.4.5**. Prepared from vinyl sulfide **85**. White solid, 61% yield. Purification was completed using flash column chromatography (hexanes/EtOAc 7:1, r.f. 0.3).

Data for **90**:

^{1}H-NMR (400 MHz; $CDCl_3$): δ 7.99 (d, *J* = 8.2 Hz, 2H), 7.78 (d, *J* = 8.2 Hz, 2H), 7.28-7.24 (m, 3H), 7.20-7.11 (m, 4H), 6.33 (dd, *J* = 15.3, 1.8 Hz, 1H), 4.96-4.91 (m, 1H), 2.69-2.56 (m, 2H), 2.33-2.24 (m, 1H), 2.04 (ddt, *J* = 13.5, 9.3, 6.6 Hz, 1H), 1.44 (s, 18H).

^{13}C{^{1}H} NMR (101 MHz; $CDCl_3$): δ 152.3, 148.0, 144.1, 140.6, 135.3, 129.7, 128.7, 128.4, 126.50, 126.39, 124.6, 121.9, 83.5, 55.8, 33.8, 32.4, 28.1

^{19}F {^{1}H} NMR (282 MHz; $CDCl_3$): δ -63.5

IR (FTIR, film): ν = 2983, 2928, 1738, 1699, 1347, 1303, 1084 cm^{-1}.

HRMS, (ESI positive ion mode) m/z: calculated for $C_{28}H_{34}NO_6F_3NaS$: 592.1957. Found: 592.1959.

$[\alpha]_D^{21}$: + 0.0485 (c 0.2, CH_2Cl_2)

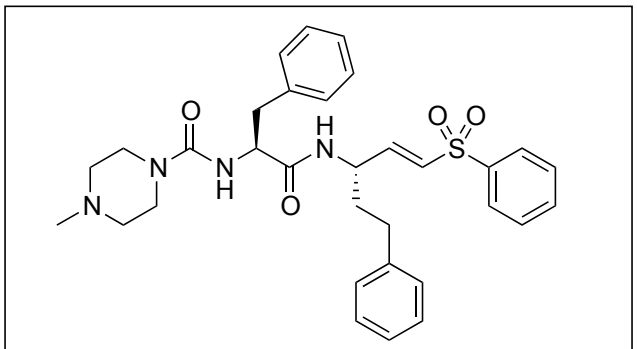

13

Followed general procedure **2.4.6**. Prepared from vinyl sulfone **60**. Off-white foam, 64% yield with slight impurities. Purification was completed using flash column chromatography (CH_2Cl_2/MeOH 20:1, r.f. 0.28).

Data for **13**:

^{1}H-NMR (400 MHz; $CDCl_3$): δ 7.79 (d, *J* = 7.6 Hz, 2H), 7.61 (t, *J* = 7.6 Hz, 1H), 7.52 (t, *J* = 7.5 Hz, 2H), 7.25-7.13 (m, 10H), 7.06 (d, *J* = 7.5 Hz, 2H), 6.80-6.75 (m, 2H), 6.30 (d, *J* = 14.8 Hz, 1H), 5.53 (br s, 1H), 4.55-4.47 (m, 1H), 4.32-4.23 (m, 1H), 3.57-3.38 (m, 4H), 3.16-3.05 (m, 1H), 3.04-2.94 (m, 1H), 2.91-2.71 (m, 4H), 2.67-2.46 (m, 3H), 1.86-1.79 (m, 2H).

^{13}C{^{1}H} NMR (101 MHz; CD_2Cl_2): δ 173.1, 157.2, 146.6, 141.0, 140.3, 137.1, 134.1, 131.3, 130.8, 129.9, 129.61, 129.48, 129.1, 128.84, 128.77, 127.8, 127.5, 126.5, 58.2, 49.8, 47.6, 44.6, 42.2, 37.9, 35.3, 32.2, 8.9

IR (FTIR, film): ν = 2927, 2875, 1629 cm^{-1}.

HRMS, (ESI positive ion mode) m/z: calculated for $C_{32}H_{39}N_4O_4S$: 575.2692. Found: 575.2690.

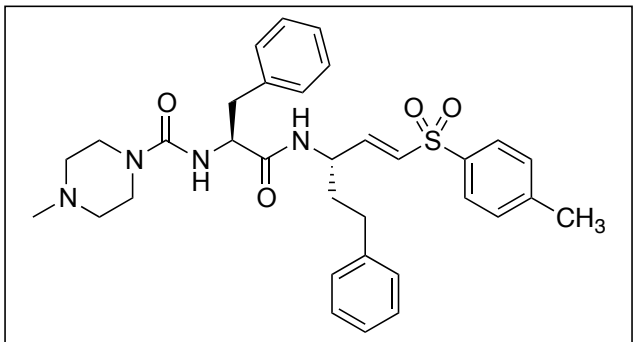

91

Followed general procedure **2.4.6**. Prepared from vinyl sulfone **86**. Off-white foam, 75% yield with slight impurities. Purification was completed using flash column chromatography (CH_2Cl_2/MeOH, 20:1, r.f.0.29).

Data for **91**:

^{1}**H-NMR** (400 MHz; CD_2Cl_2): δ 7.66 (d, *J* = 8.3 Hz, 2H), 7.44 (d, *J* = 8.3 Hz,), 7.32 (d, *J* = 8.0 Hz, 2H), 7.29-7.12 (m, 10H), 7.07-7.05 (m, 2H), 7.01-6.99 (m,), 6.73 (dd, *J* = 15.1, 4.7 Hz, 1H), 6.69 (d, *J* = 8.4 Hz, 1H), 6.30 (dd, *J* = 15.1, 1.7 Hz, 1H), 5.41 (d, *J* = 6.0 Hz, 1H), 4.53-4.46 (m, 1H), 4.25-4.20 (m, 1H), 3.65-3.58 (m, 1H), 3.49-3.38 (m, 4H), 3.22-3.11 (m,), 3.13-3.06 (m, 1H), 3.01-2.90 (m, 1H), 2.84-2.74 (m, 4H), 2.65-2.47 (m, 1H), 2.57-2.53 (m, 3H), 2.39 (s, 3H), 1.87-1.80 (m, 2H).

^{13}C{^{1}H} NMR (101 MHz; CD_2Cl_2): δ 198.8, 172.6, 157.0, 145.5, 145.0, 140.8, 137.3, 136.9, 131.42, 131.24, 130.13, 129.96, 129.30, 129.21, 129.02, 128.88, 128.56, 128.48, 128.42, 128.27, 127.6, 127.29, 127.20, 126.25, 126.08, 57.8, 57.4, 49.5, 47.9, 44.8, 42.3, 42.0, 38.5, 37.67, 37.50, 35.1, 33.8, 32.0, 21.3, 8.7

IR (FTIR, film): ν =3042, 2929, 1662, 1627, 1525, 831 cm^{-1}.

HRMS, (ESI positive ion mode) m/z: calculated for $C_{33}H_{41}N_4O_4S$: 589.2849. Found: 589.2847.

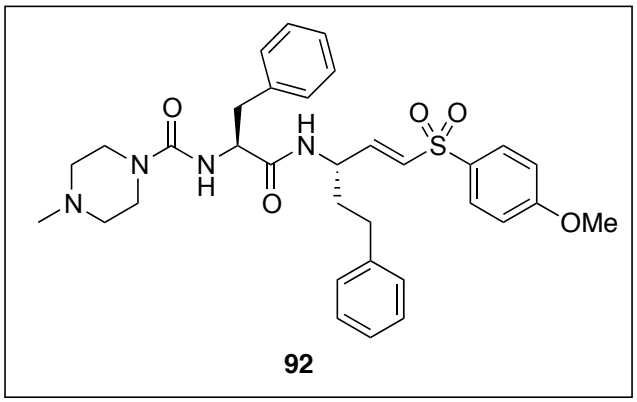

92

Followed general procedure **2.4.6**. Prepared from vinyl sulfone **87**. White foam, 41% yield with slight impurities. Purification was completed using flash column chromatography (CH_2Cl_2/MeOH 15:1 r.f. 0.2). Appears to be much cleaner than other analogues (See Appendix II).

Data for **92**:

^{1}H-NMR (400 MHz; CD_2Cl_2): δ 7.69 (d, *J* = 8.9 Hz, 2H), 7.26-7.12 (m, 8H), 7.04 (d, *J* = 6.9 Hz, 2H), 6.96 (d, *J* = 9.0 Hz, 2H), 6.74 (d, *J* = 8.6 Hz, 1H), 6.68 (dd, *J* = 15.2, 4.9 Hz, 1H), 6.30 (d, *J* = 14.8 Hz, 1H), 5.61 (d, *J* = 5.4 Hz, 1H), 4.52-4.44 (m, 1H), 4.25-4.19 (m, 1H), 3.80 (s, 3H), 3.52 (s, 4H), 3.13-3.08 (m, 1H), 3.02-2.93 (m, 4H), 2.68 (s, 3H), 2.65-2.56 (m, 1H), 2.52-2.44 (m, 1H), 1.85-1.79 (m, 2H).

^{13}C{H} NMR (101 MHz; CD2Cl2): δ 173.3, 164.4, 157.2, 145.4, 141.0, 136.9, 131.5, 131.2, 130.2, 129.4, 129.2, 128.83, 128.76, 127.5, 126.5, 115.1, 65.7, 58.8, 56.2, 49.8, 44.4, 41.7, 37.9, 35.1, 32.3

IR (FTIR, film): ν = 3033, 2938, 1639, 1525, 832 cm^{-1}.

HRMS, (ESI positive ion mode) m/z: calculated for $C_{33}H_{41}N_4O_5S$: 605.2798. Found: 605.2797.

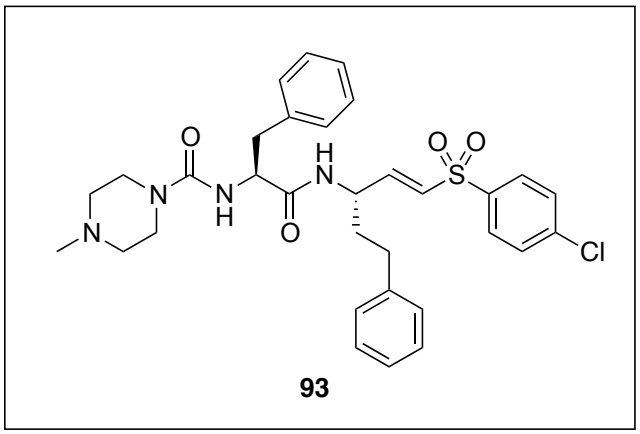

93

Followed general procedure **2.4.6**. Prepared from vinyl sulfone **88**. White foam, 35% yield with slight impurities. Purification was completed using flash column chromatography (CH_2Cl_2/MeOH 20:1, r.f. 0.28). Appears to be much cleaner than other analogues (See Appendix II).

Data for **93**:

^{1}H-NMR (400 MHz; CD_2Cl_2): δ 7.69 (d, *J* = 8.9 Hz, 2H), 7.26-7.12 (m, 8H), 7.04 (d, *J* = 6.9 Hz, 2H), 6.96 (d, *J* = 9.0 Hz, 2H), 6.74 (d, *J* = 8.6 Hz, 1H), 6.68 (dd, *J* = 15.2, 4.9 Hz, 1H), 6.30 (d, *J* = 14.8 Hz, 1H), 5.61 (d, *J* = 5.4 Hz, 1H), 4.52-4.44 (m, 1H), 4.25-4.19 (m, 1H), 3.80 (s, 3H), 3.52 (s, 4H), 3.13-3.08 (m, 1H), 3.02-2.93 (m, 4H), 2.68 (s, 3H), 2.65-2.56 (m, 1H), 2.52-2.44 (m, 1H), 1.85-1.79 (m, 2H).

^{13}C{^{1}H} NMR (101 MHz; CD_2Cl_2): δ 173.1, 157.4, 147.2, 141.2, 140.8, 139.3, 137.2, 131.1, 130.3, 129.65, 129.62, 129.4, 129.06, 128.90, 127.7, 126.8, 58.3, 50.1, 48.3, 45.0, 42.4, 38.2, 35.5, 32.4, 9.1

IR (FTIR, film): ν = 3042, 2934, 1632, 1521, 1476, 835 cm^{-1}.

HRMS, (ESI positive ion mode) m/z: calculated for $C_{32}H_{38}N_4Q_4SCl$: 609.2302. Found: 609.2310.

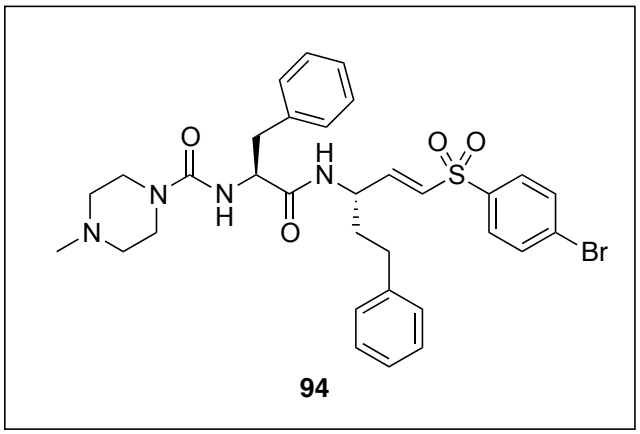

94

Followed general procedure **2.4.6**. Prepared from vinyl sulfone **89**. Off-white foam, 70% yield with slight impurities. Purification was completed using flash column chromatography (CH_2Cl_2/MeOH 20:1, r.f. 0.4).

Data for **94**:

^{1}H-NMR (400 MHz; CD_2Cl_2): δ 7.66 (s, 5H), 7.27-7.14 (m, 10H), 7.08-7.06 (m, 2H), 6.79 (dd, *J* = 15.1, 4.6 Hz, 1H), 6.71 (d, *J* = 8.3 Hz, 1H), 6.29 (dd, *J* = 15.1, 1.7 Hz, 1H), 5.29 (s, 1H), 4.56-4.49 (m, 1H), 4.31-4.23 (m, 1H), 3.46-3.33 (m, 4H), 3.09 (dd, *J* = 13.9, 7.0 Hz, 1H), 2.98 (dd, *J* = 13.8, 8.1 Hz, 1H), 2.70-2.59 (m, 4H), 2.55-2.50 (m, 2H), 2.48 (s, 3H), 1.88-1.77 (m, 2H).

^{13}C{^{1}H} NMR (101 MHz; CD_2Cl_2): δ 173.0, 157.3, 147.2, 141.0, 139.4, 137.1, 130.4, 129.57, 129.48, 129.14, 128.95, 128.86, 128.75, 127.5, 126.6, 91.3, 66.2, 57.9, 49.8, 47.9, 45.2, 42.8, 37.9, 35.3, 32.2, 9.0

IR (FTIR, film): ν =3033, 2934, 1627.77, 1526, 1142, 834 cm^{-1}.

HRMS, (ESI positive ion mode) m/z: calculated for $C_{32}H_{38}N_4O_4SBr$: 653.1797. Found: 653.1790.

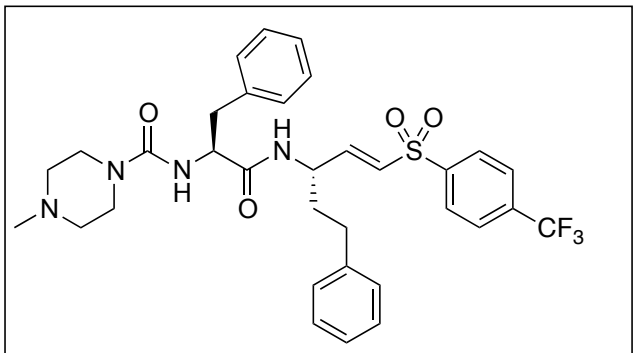

95

Followed general procedure **2.4.6**. Prepared from vinyl sulfone **90**. Off-white foam, 40% yield with slight impurities. Purification was completed using flash column chromatography (CH_2Cl_2/MeOH 20:1, r.f. 0.25).

Data for **95**:

^{1}H-NMR (400 MHz; CD_2Cl_2): δ 7.96 (d, *J* = 8.2 Hz, 2H), 7.80 (d, *J* = 8.3 Hz, 2H), 7.33-7.14 (m, 8H), 7.09-7.07 (m, 2H), 6.87 (dd, *J* = 15.1, 4.5 Hz, 1H), 6.72 (d, *J* = 8.4 Hz, 1H), 6.32 (dd, *J* = 15.1, 1.7 Hz, 1H), 5.29-5.28 (m, 1H), 4.59-4.53 (m, 1H), 4.36-4.30 (m, 1H), 3.47-3.35 (m, 4H), 3.11 (dd, *J* = 13.1, 6.2 Hz, 1H), 2.99 (dd, *J* = 13.9, 8.1 Hz, 1H), 2.67-2.58 (m, 4H), 2.56-2.51 (m, 2H), 2.46-2.42 (m, 3H), 1.93-1.76 (m, 2H).

^{13}C{^{1}H} NMR (101 MHz; CD_2Cl_2): δ 172.7, 157.3, 148.2, 144.3, 141.0, 137.2, 135.4, 130.0, 129.5, 129.12, 128.98, 128.86, 128.70, 127.4, 126.86, 126.82, 126.6, 125.0, 57.6, 49.7, 47.7, 45.2, 42.9, 37.9, 35.4, 32.2, 9.0

^{19}F{^{1}H} NMR (282 MHz; CD_2Cl_2): δ -63.8, -70.2, -72.7

IR (FTIR, film): ν = 3039, 2931, 1625, 1321 cm^{-1}.

HRMS, (ESI positive ion mode) m/z: calculated for $C_{33}H_{38}N_4O_4F_3S$: 643.2566. Found: 643.2560.

3 Conclusions and Future Work

We have demonstrated the first utility of metal-catalyzed-alkyne hydrothiolation in total synthesis. We successfully synthesized K777 in a ten step convergent synthesis in 21% overall yield and 31% yield over 8 linear steps. However these yields are only an estimate at this time until we can improve on the method of purification. Due to the wide substrate scope of our methodology we were able to synthesize five analogues of K777 that differed in the P_1' site of K777 however these analogues also suffered from the same purification problems with the exception of the chloride **94** and methoxy **92** analogues which were produced much more cleanly.

We require ample amount of K777 analogues for proper purification. We will be starting to increase our scale shortly. Also at this time we will explore alternative protocols for oxidizing vinyl sulfides to sulfones to improve the yield of this step and make it more atom economic.

We were able to improve on the cost of the synthesis by avoiding the use of the expensive unnatural amino acid homophenylalanine. Instead we used hydrocinnamaldehyde **39** and an Ellman auxiliary **40b** to form a chiral imine **41** (See Scheme 2.10 p. 37). The addition reaction of Grignard to this chiral imine **41** proceeded with high disastereselectivity and the selectivity was determined again after the removal of the Ellman auxiliary with the use of Mosher's acid chloride **62a**. The exact enantiomeric excess at various stages will be examined with supercritical fluid chromatography in due course.

The use of Ellman's auxiliary can lead to a wide range of analogues, as this is a way to manipulate the P_1 site. Using a different starting aldehyde could potentially lead to ways of incorporating complex unnatural side chains (Scheme 3.1). Since we have demonstrated the utility of metal-catalyzed alkyne hydrothiolation to reach five analogues, we hope to produce more analogues by using a wider range of aryl thiols with various substitutions (Scheme 3.1).

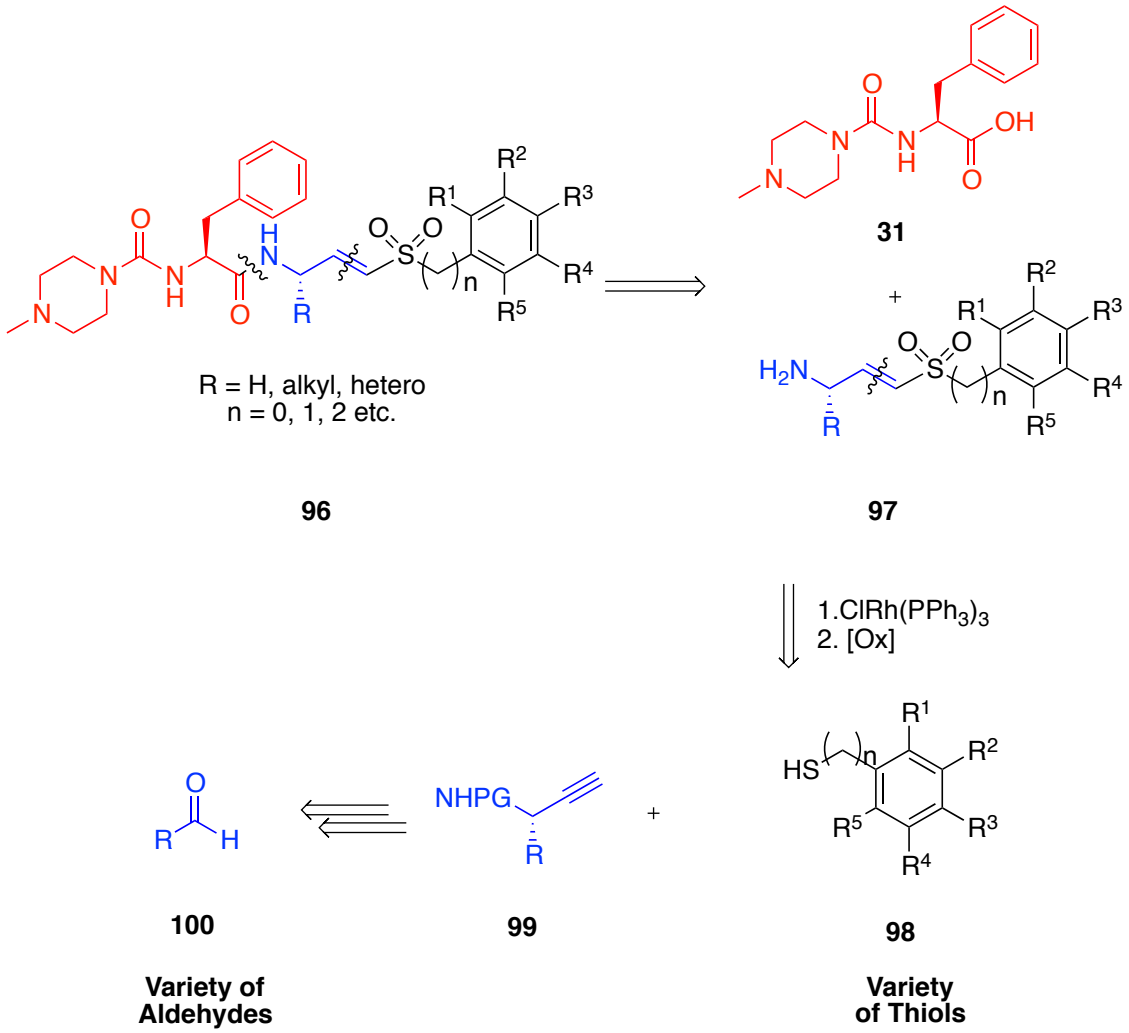

Scheme 3.1: Proposed method to accessing various K777 analogues

In order to demonstrate the reactivity of our current analogues **91-95** we will run a proof of principle kinetic study according to a procedure done by Roush.[115] The relative rates of Michael additions of 2'-(phenethyl) thiol to acceptors **13**, **91-95** can be monitored using ^{1}H NMR spectroscopy. The reaction will be done in CD_3OD, and CH_2Cl_2 will be used as an internal standard. The relative reaction rates can be determined from the disappearance of vinyl proton signal of the starting material against an internal standard. A large excess of 2'-(phenethyl) thiol will be used to promote pseudo-first-order kinetics (Scheme 3.2). This will demonstrate the electronic capabilities of our analogues. An *In-vitro* analysis with a collaborator through UBC's Neglected Global disease initiative will

be sought out. Although it is postulated that electron deficient ring systems should increase the Michael acceptor reactivity of our analogues, minimal reactivity is essential to avoiding reactivity with host cell cysteine proteases.

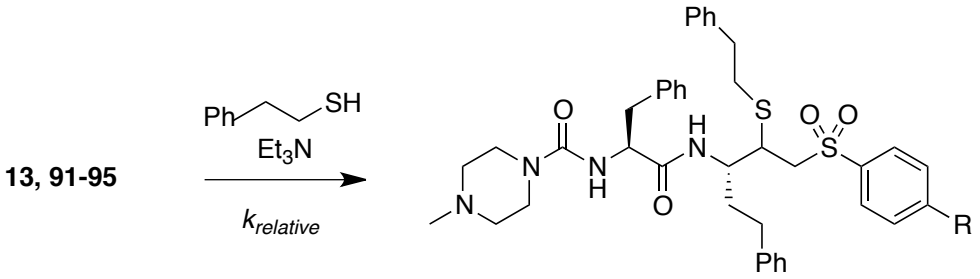

Scheme 3.2: Proposed kinetic study of K777 and analogues 91-95

In successfully demonstrating our ability to apply metal-catalyzed alkyne hydrothiolation to total synthesis we would like to start applying our methodology to more systems. A substrate of interest is griseoviridin (**101**) a promising antibiotic that contains a branched vinyl sulfide and would showcase our other methodology for synthesizing branched analogues using Tp*Rh(PPh_3)$_2$ as a catalyst (see Scheme 1.6 p. 21).[116] Finally another set of irreversible cysteine protease inhibitors being explored in our group is shown in figure 3.2. These cysteine protease inhibitors inhibit falcipain 2. Like cruzain, falicipain 2, is crucial to the life cycle of an organism, specifically of Plasmodium *falciparum* (P. *falciparum*) the causative organism of Malaria. Pursuit of these different inhibitors could lead to effective therapeutics for the treatment of malaria.[117]

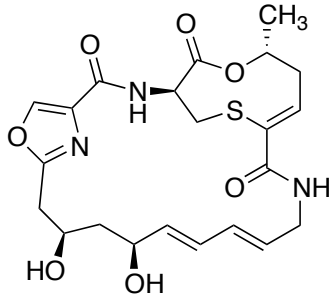

101

Figure 3.1 Griseoviridin

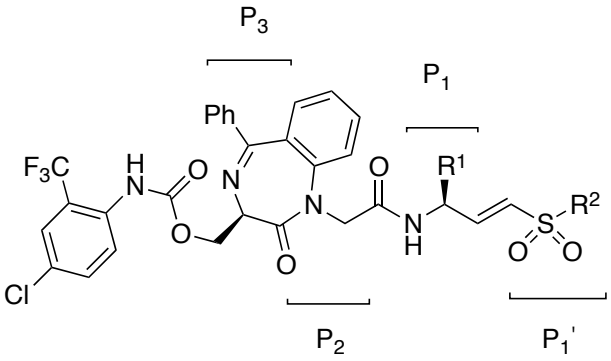

R^1= CH_2CH_2Ph or H
R^2= CH_3, C_2H_5, Ph, *p*-CH_3OPh

Figure 3.2 Falcipain 2 inhibitors

Bibliography

(1) Fenwick, A. *Public Health* **2012**, *126*, 233-236.

(2) United Nations United Nations Millennium Development Goals. http://www.un.org/millenniumgoals/ (accessed April/28, 2012).

(3) Hotez, P. J.; Molyneux, D. H.; Fenwick, A.; Kumaresan, J.; Sachs, S. E.; Sachs, J. D.; Savioli, L. *N. Engl. J. Med.* **200**7, *35*7, 1018-1027.

(4) Molyneux, D. H.; Malecela, M. N. *Parasit. Vectors* **2011**, 4, 234-3305-4-234.

(5) Trouiller, P.; Olliaro, P.; Torreele, E.; Orbinski, J.; Laing, R.; Ford, N. *Lancet* **2002**, *359*, 2188-2194.

(6) Clayton, J. *Nature* **2010**, *465*, S12-S15.

(7) Drugs for Neglected Diseases initiative DND*i* Overview. http://www.dndi.org/index.php/overview-dndi.html?ids=1 (accessed April/28, 2012).

(8) Drugs for Neglected Global Diseases initiative Product Profile - Overview. http://www.dndi.org/index.php/asaq.html?ids=3 (accessed May/13, 2012).

(9) Wasan, K. Neglected Global Diseases Initiative UBC. http://ngdi.ubc.ca/ (accessed April/28, 2012).

(10) Teixeira, A. R.; Hecht, M. M.; Guimaro, M. C.; Sousa, A. O.; Nitz, N. *Clin. Microbiol. Rev.* **2011**, *2*4, 592-630.

(11) Kirchhoff, L. V. *N. Engl. J. Med.* **1993**, *329*, 639-644.

(12) Andrade, L. O.; Andrews, N. W. *Nat Rev Micro* **2005**, 3, 819-823.

(13) Hemmige, V.; Tanowitz, H.; Sethi, A. *Int. J. Dermatol.* **2012**, *5*1, 501-508.

(14) Barcan, L.; Luna, C.; Clara, L.; Sinagra, A.; Valledor, A.; De Rissio, A. M.; Gadano, A.; Garcia, M. M.; de Santibanes, E.; Riarte, A. *Liver Transpl.* **2005**, *1*1, 1112-1116.

(15) Alarcon de Noya, B., et al *J. Infect. Dis.* **2010**, *20*1, 1308-1315.

(16) Gurtler, R.; Segura, E.; Cohen, J. *Emerg. Infec. Dis.* **2003**, 9, 29-32.

(17) Schmunis, G. A.; Cruz, J. R. *Clin. Microbiol. Rev.* **2005**, *1*8, 12-29.

(18) World Health Organization, First WHO report on neglected tropical diseases 2010: working to overcome the global impact of neglected tropical diseases **2010**, 1, 1.

(19) Schmunis, G. A.; Yadon, Z. E. *Acta Trop.* **2010**, *115*, 14-21.

(20) Schmunis, G. A. *Memórias do Instituto Oswaldo Cruz* **2007**, *102*, 75-86.

(21) Eakin, A. E.; Mills, A. A.; Harth, G.; McKerrow, J. H.; Craik, C. S. *J. Biol. Chem.* **1992**, *267*, 7411-7420.

(22) McGrath, M. E.; Eakin, A. E.; Engel, J. C.; McKerrow, J. H.; Craik, C. S.; Fletterick, R. J. *J. Mol. Biol.* **1995**, *247*, 251-259.

(23) Prata, A. *Lancet Infect. Dis.* **2001**, 1, 92-100.

(24) Boiani, M.; Piacenza, L.; Hernandez, P.; Boiani, L.; Cerecetto, H.; Gonzalez, M.; Denicola, A. *Biochem. Pharmacol.* **2010**, *79*, 1736-1745.

(25) Castro, J. A.; de Mecca, M. M.; Bartel, L. C. *Hum. Exp. Toxicol.* **2006**, *25*, 471-479.

(26) Coura, J. R.; Castro, S. L. d. *Memórias do Instituto Oswaldo Cruz* **2002**, *97*, 3-24.

(27) Bern, C.; Montgomery, S. P.; Herwaldt, B. L.; Rassi, A.,Jr; Marin-Neto, J. A.; Dantas, R. O.; Maguire, J. H.; Acquatella, H.; Morillo, C.; Kirchhoff, L. V.; Gilman, R. H.; Reyes, P. A.; Salvatella, R.; Moore, A. C. *JAMA* **2007**, *298*, 2171-2181.

(28) Gorla, N. B.; Ledesma, O. S.; Barbieri, G. P.; Larripa, I. B. *Mutat. Res.* **1989**, *224*, 263-267.

(29) Kaneshima, E. N.; Castro-Prado, Marialba A Alves de *Memórias do Instituto Oswaldo Cruz* **2005**, *100*, 325-330.

(30) Moraga, A. A.; Graf, U. *Mutagenesis* **1989**, 4, 105-110.

(31) Vagner, J.; Qu, H.; Hruby, V. J. *Curr. Opin. Chem. Biol.* **2008**, *12*, 292-296.

(32) Smith, A. B.,3rd; Hirschmann, R.; Pasternak, A.; Yao, W.; Sprengeler, P. A.; Holloway, M. K.; Kuo, L. C.; Chen, Z.; Darke, P. L.; Schleif, W. A. *J. Med. Chem.* **1997**, *40*, 2440-2444.

(33) De Clercq, E. *Int. J. Antimicrob. Agents* **2009**, *33*, 307-320.

(34) Stoch, S. A.; Zajic, S.; Stone, J.; Miller, D. L.; Van Dyck, K.; Gutierrez, M. J.; De Decker, M.; Liu, L.; Liu, Q.; Scott, B. B.; Panebianco, D.; Jin, B.; Duong, L. T.; Gottesdiener, K.; Wagner, J. A. *Clin. Pharmacol. Ther.* **2009**, *86*, 175-182.

(35) Gauthier, J. Y., et al *Bioorg. Med. Chem. Lett.* **2008**, *18*, 923-928.

(36) Shah, F.; Mukherjee, P.; Gut, J.; Legac, J.; Rosenthal, P. J.; Tekwani, B. L.; Avery, M. A. *J. Chem. Inf. Model.* **2011**, *5*1, 852-864.

(37) Menezes, C.; Costa, G. C.; Gollob, K. J.; Dutra, W. O. *Drug Dev. Res.* **2011**, *7*2, 471-479.

(38) Urbina, J. A. *Memórias do Instituto Oswaldo Cruz* **2009**, *10*4, 311-318.

(39) Urbina, J. A.; Docampo, R. *Trends Parasitol.* **2003**, *1*9, 495-501.

(40) Pinazo, M. J.; Espinosa, G.; Gallego, M.; Lopez-Chejade, P. L.; Urbina, J. A.; Gascon, J. *Am. J. Trop. Med. Hyg.* **2010**, *8*2, 583-587.

(41) Drugs for Neglected Global Diseases initiative Eisai and DNDi Enter into a Collaboration and License Agreement to Develop a New Drug for Chagas disease. http://www.dndi.org/press-releases/532-eisai-and-dndi-enter-into-a-collaboration.html (accessed May/6, 2012).

(42) McKerrow, J. H.; Sun, E.; Rosenthal, P. J.; Bouvier, J. *Annu. Rev. Microbiol.* **1993**, *4*7, 821-853.

(43) Yang, P.; Wang, M.; He, C. Y.; Yao, S. Q. *Chem. Commun.* **2012**, *4*8, 835-837.

(44) Shenai, B. R.; Lee, B. J.; Alvarez-Hernandez, A.; Chong, P. Y.; Emal, C. D.; Neitz, R. J.; Roush, W. R.; Rosenthal, P. J. *Antimicrob. Agents Chemother.* **2003**, *4*7, 154-160.

(45) Jílková, A.; Řezáčová, P.; Lepšík, M.; Horn, M.; Váchová, J.; Fanfrlík, J.; Brynda, J.; McKerrow, J. H.; Caffrey, C. R.; Mareš, M. *Journal of Biological Chemistry* **2011**, *28*6, 35770-35781.

(46) Engel, J. C.; Doyle, P. S.; Palmer, J.; Hsieh, I.; Bainton, D. F.; McKerrow, J. H. *J. Cell. Sci.* **1998**, *111 (Pt 5*), 597-606.

(47) Bontempi, E.; Martinez, J.; Cazzulo, J. J. *Mol. Biochem. Parasitol.* **1989**, *3*3, 43-47.

(48) Rasnick, D. *Anal. Biochem.* **1985**, *14*9, 461-465.

(49) Hanzlik, R. P.; Thompson, S. A. *J. Med. Chem.* **1984**, *2*7, 711-712.

(50) Liu, S.; Hanzlik, R. P. *J. Med. Chem.* **1992**, *3*5, 1067-1075.

(51) Somoza, J. R.; Zhan, H.; Bowman, K. K.; Yu, L.; Mortara, K. D.; Palmer, J. T.; Clark, J. M.; McGrath, M. E. *Biochemistry* **2000**, *3*9, 12543-12551.

(52) McKerrow, J. H.; Engel, J. C.; Caffrey, C. R. *Bioorg. Med. Chem.* **1999**, 7, 639-644.

(53) Palmer, J. T.; Rasnick, D.; Klaus, J. L.; Bromme, D. *J. Med. Chem.* **1995**, *3*8, 3193-3196.

(54) Otto, H.; Schirmeister, T. *Chem. Rev.* **1997**, *9*7, 133-172.

(55) Hanzlik, R. P.; Jacober, S. P.; Zygmunt, J. *Biochimica et Biophysica Acta (BBA) - General Subjects* **1991**, *107*3, 33-42.

(56) Hanzlik, R. P.; Zygmunt, J.; Moon, J. B. *Biochimica et Biophysica Acta (BBA) - General Subjects* **1990**, *103*5, 62-70.

(57) Li, Z.; Patil, G. S.; Golubski, Z. E.; Hori, H.; Tehrani, K.; Foreman, J. E.; Eveleth, D. D.; Bartus, R. T.; Powers, J. C. *J. Med. Chem.* **1993**, *3*6, 3472-3480.

(58) Meirelles, M. N. L.; Juliano, L.; Carmona, E.; Silva, S. G.; Costa, E. M.; Murta, A. C. M.; Scharfstein, J. *Mol. Biochem. Parasitol.* **1992**, *5*2, 175-184.

(59) Ashall, F.; Angliker, H.; Shaw, E. *Biochem. Biophys. Res. Commun.* **1990**, *17*0, 923-929.

(60) Harth, G.; Andrews, N.; Mills, A. A.; Engel, J. C.; Smith, R.; McKerrow, J. H. *Mol. Biochem. Parasitol.* **1993**, *5*8, 17-24.

(61) Eichhold, T. H.; Hookfin, E. B.; Taiwo, Y. O.; De, B.; Wehmeyer, K. R. *J. Pharm. Biomed. Anal.* **1997**, *1*6, 459-467.

(62) Bromme, D.; Klaus, J. L.; Okamoto, K.; Rasnick, D.; Palmer, J. T. *Biochem. J.* **1996**, *315 (Pt 1*), 85-89.

(63) McGrath, M. E.; Klaus, J. L.; Barnes, M. G.; Bromme, D. *Nat Struct Mol Biol* **1997**, 4, 105-109.

(64) Roush, W. R.; Gwaltney, S. L.; Cheng, J.; Scheidt, K. A.; McKerrow, J. H.; Hansell, E. *J. Am. Chem. Soc.* **1998**, *12*0, 10994-10995.

(65) Brinen, L. S.; Hansell, E.; Cheng, J.; Roush, W. R.; McKerrow, J. H.; Fletterick, R. J. *Structure* **2000**, 8, 831-840.

(66) Jaishankar, P.; Hansell, E.; Zhao, D.; Doyle, P. S.; McKerrow, J. H.; Renslo, A. R. *Bioorg. Med. Chem. Lett.* **2008,** *1*8, 624-628.

(67) Kerr, I. D.; Lee, J. H.; Farady, C. J.; Marion, R.; Rickert, M.; Sajid, M.; Pandey, K. C.; Caffrey, C. R.; Legac, J.; Hansell, E.; McKerrow, J. H.; Craik, C. S.; Rosenthal, P. J.; Brinen, L. S. *J. Biol. Chem.* **2009**, *28*4, 25697-25703.

(68) Chen, B.; Wang, B.; Lin, G. *J. Org. Chem.* **2010**, *7*5, 941-944.

(69) Engel, J. C.; Doyle, P. S.; Hsieh, I.; McKerrow, J. H. *J. Exp. Med.* **1998**, *18*8, 725-734.

(70) Jacobsen, W.; Christians, U.; Benet, L. Z. *Drug Metab. Dispos.* **2000**, *2*8, 1343-1351.

(71) Cobo, E. R.; Reed, S. L.; Corbeil, L. B. *Int. J. Antimicrob. Agents* **2012**, *3*9, 259-262.

(72) Chen, Y. T.; Brinen, L. S.; Kerr, I. D.; Hansell, E.; Doyle, P. S.; McKerrow, J. H.; Roush, W. R. *PLoS Negl Trop. Dis.* **2010**, 4, e825.

(73) Leslie, M. *Science* **2011**, *333*, 933-935.

(74) McKerrow, J.; Doyle, P.; Engel, J.; Podust, L.; Robertson, S.; Ferreira, R.; Saxton, T.; Arkin, M.; Kerr, I.; Brinen, L.; Craik, C. *Memórias do Instituto Oswaldo Cruz* **200**9, *10*4, 263-269.

(75) Barr, S. C.; Warner, K. L.; Kornreic, B. G.; Piscitelli, J.; Wolfe, A.; Benet, L.; McKerrow, J. H. *Antimicrob. Agents Chemother.* **2005**, *4*9, 5160-5161.

(76) Doyle, P. S.; Zhou, Y. M.; Engel, J. C.; McKerrow, J. H. *Antimicrob. Agents Chemother.* **2007**, *5*1, 3932-3939.

(77) Benet, L. Z.; Wu, C.; Hebert, M. F.; Wacher, V. J. *J. Controlled Release* **1996**, *3*9, 139-143.

(78) Watkins, P. B.; Wrighton, S. A.; Schuetz, E. G.; Molowa, D. T.; Guzelian, P. S. *J. Clin. Invest.* **1987**, *8*0, 1029-1036.

(79) Kolars, J. C.; Watkins, P. B.; Merion, R. M.; Awni, W. M. *The Lancet* **1991**, *338*, 1488-1490.

(80) Nahm, S.; Weinreb, S. M. *Tetrahedron Lett.* **1981**, *2*2, 3815-3818.

(81) Wadsworth, W. S.; Emmons, W. D. *J. Am. Chem. Soc.* **1961**, *8*3, 1733-1738.

(82) Mizuno, H.; Domon, K.; Masuya, K.; Tanino, K.; Kuwajima, I. *J. Org. Chem.* **1999**, *6*4, 2648-2656.

(83) Parham, W. E.; Motter, R. F. *J. Am. Chem. Soc.* **1959**, *8*1, 2146-2148.

(84) Trost, B. M.; Lavoie, A. C. *J. Am. Chem. Soc.* **1983**, *105*, 5075-5090.

(85) Wenkert, E.; Ferreira, T. W.; Michelotti, E. L. *J. Chem. Soc. Chem. Commun.* **1979**, 637-638.

(86) Sabarre, A.; Love, J. *Org. Lett.* **2008**, *1*0, 3941-3944.

(87) Bates, C. G.; Saejueng, P.; Doherty, M. Q.; Venkataraman, D. *Org. Lett.* **2004**, 6, 5005-5008.

(88) Zheng, Y.; Du, X.; Bao, W. *Tetrahedron Lett.* **2006**, *4*7, 1217-1220.

(89) Ranu, B. C.; Chattopadhyay, K.; Banerjee, S. *J. Org. Chem.* **2006**, *7*1, 423-425.

(90) Truce, W. E.; Simms, J. A.; Boudakian, M. M. *J. Am. Chem. Soc.* **1956**, *7*8, 695-696.

(91) Carey, F. A.; Court, A. S. *J. Org. Chem.* **1972**, *3*7, 939-943.

(92) Peterson, D. J. *J. Org. Chem.* **1968**, *3*3, 780-784.

(93) Shoai, S.; Love, J. A. Regioselective Rhodium-Catalyzed Alkyne Hydrothiolation with Alkane Thiols: Substrate Scope and Mechanistics Investigations, University of British Columbia, Vancouver, 2010.

(94) Oswald, A. A.; Griesbaum, K.; Hudson, B. E.; Bregman, J. M. *J. Am. Chem. Soc.* **1964**, *86*, 2877-2884.

(95) Bader, H.; Cross, L. C.; Heilbron, I.; Jones, E. R. H. *J. Chem. Soc.* **1949**, 619-623.

(96) McDonald, J. W.; Corbin, J. L.; Newton, W. E. *Inorg. Chem.* **1976**, *15*, 2056-2061.

(97) Kuniyasu, H.; Ogawa, A.; Sato, K.; Ryu, I.; Kambe, N.; Sonoda, N. *J. Am. Chem. Soc.* **1992**, *114*, 5902-5903.

(98) Ogawa, A.; Ikeda, T.; Kimura, K.; Hirao, T. *J. Am. Chem. Soc.* **1999**, *121*, 5108-5114.

(99) Yang, J.; Sabarre, A.; Fraser, L. R.; Patrick, B. O.; Love, J. A. *J. Org. Chem.* **2009**, *74*, 182-187.

(100) Fraser, L. R.; Bird, J.; Wu, Q.; Cao, C.; Patrick, B. O.; Love, J. A. *Organometallics* **2007**, *26*, 5602-5611.

(101) Shoai, S.; Bichler, P.; Kang, B.; Buckley, H.; Love, J. A. *Organometallics* **2007**, *26*, 5778-5781.

(102) Corey, E. J.; Fuchs, P. L. *Tetrahedron Lett.* **1972**, *13*, 3769-3772.

(103) Gilbert, J. C.; Weerasooriya, U. *J. Org. Chem.* **1982**, *47*, 1837-1845.

(104) Muller, S.; Liepold, B.; Roth, G. J.; Bestmann, H. J. *Synlett* **2000**, *1996*, 521,522.

(105) Liu, G.; Cogan, D. A.; Ellman, J. A. *J. Am. Chem. Soc.* **1997**, *119*, 9913-9914.

(106) Cogan, D. A.; Liu, G.; Ellman, J. *Tetrahedron* **1999**, *55*, 8883-8904.

(107) Ellman, J. A.; Owens, T. D.; Tang, T. P. *Acc. Chem. Res.* **2002**, *35*, 984-995.

(108) Wakayama, M.; Ellman, J. A. *J. Org. Chem.* **2009**, *74*, 2646-2650.

(109) Mecozzi, T.; Petrini, M. *J. Org. Chem.* **1999**, *64*, 8970-8972.

(110) Dale, J. A.; Dull, D. L.; Mosher, H. S. *J. Org. Chem.* **1969**, *34*, 2543-2549.

(111) Dale, J. A.; Mosher, H. S. *J. Am. Chem. Soc.* **1973**, *95*, 512-519.

(112) Aggarwal, V. K.; Barbero, N.; McGarrigle, E. M.; Mickle, G.; Navas, R.; Suajrez, J. R.; Unthank, M. G.; Yar, M. *Tetrahedron Lett.* **2009**, *50*, 3482-3484.

(113) Martinez, P. H.; Hultzsch, K. C.; Hampel, F. *Chem. Commun.* **2006**, , 2221-2223.

(114) Dourtoglou, V.; Gross, B.; Lambropoulou, V.; Zioudrou, C. *Synthesis* **2002**, *1984*, 572,574.

(115) Reddick, J. J.; Cheng, J.; Roush, W. R. *Org. Lett.* **2003**, *5*, 1967-1970.

(116) Dvorak, C. A.; Schmitz, W. D.; Poon, D. J.; Pryde, D. C.; Lawson, J. P.; Amos, R. A.; Meyers, A. I. *Angewandte Chemie International Edition* **2000**, *39*, 1664-1666.

(117) Ettari, R.; Nizi, E.; Di Francesco, M. E.; Dude, M.; Pradel, G.; Vicik, R.; Schirmeister, T.; Micale, N.; Grasso, S.; Zappala, M. *J. Med. Chem.* **2008**, *51*, 988-996.

Appendices

Appendix I: ^{1}H NMR and ^{13}C NMR Spectroscopic Data

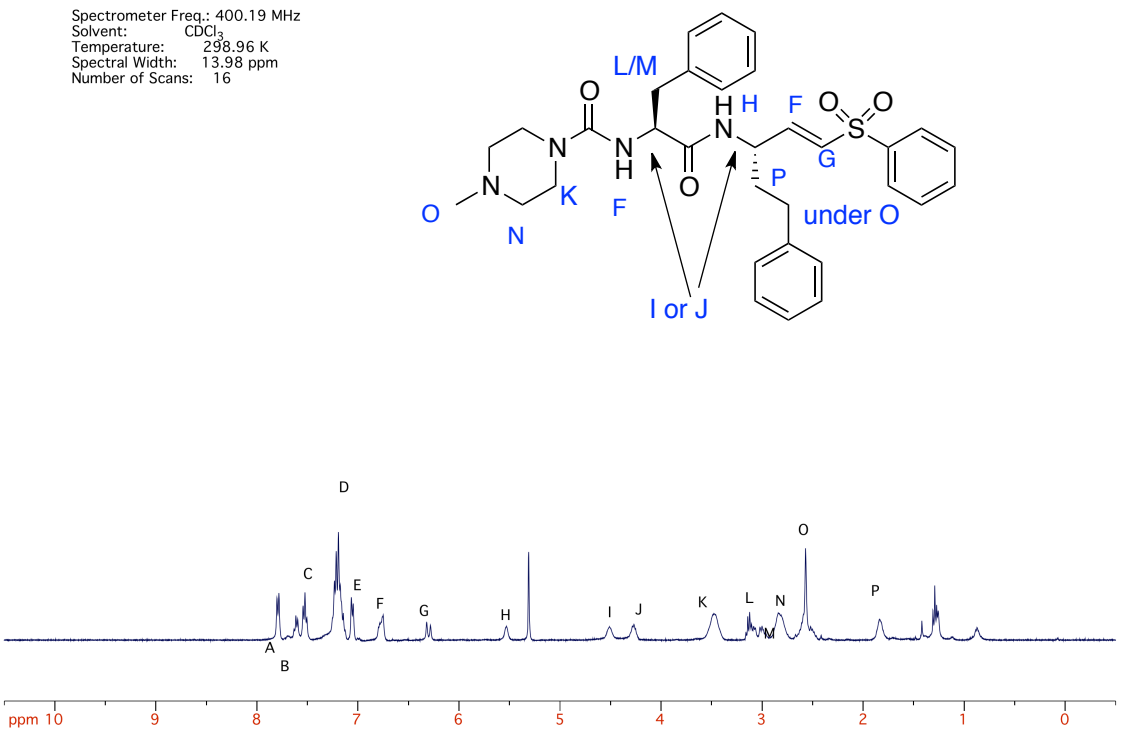

^{1}H NMR spectrum of compound **13**

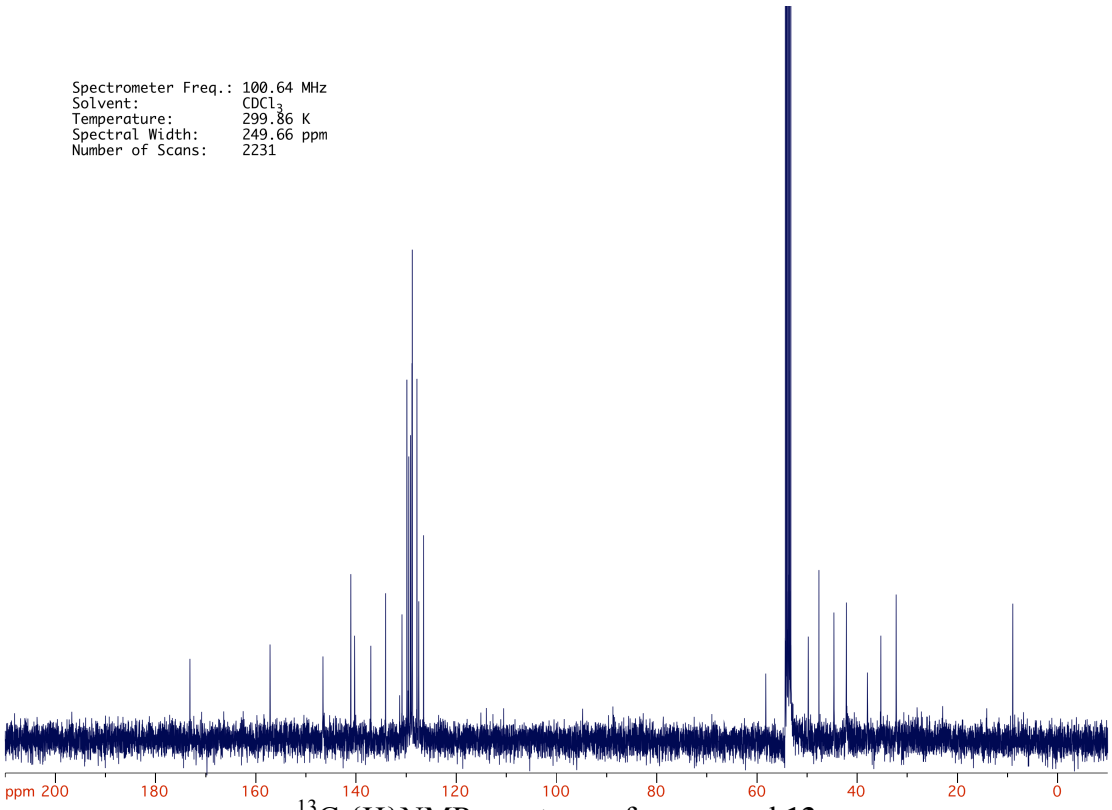

^{13}C {H}NMR spectrum of compound **13**

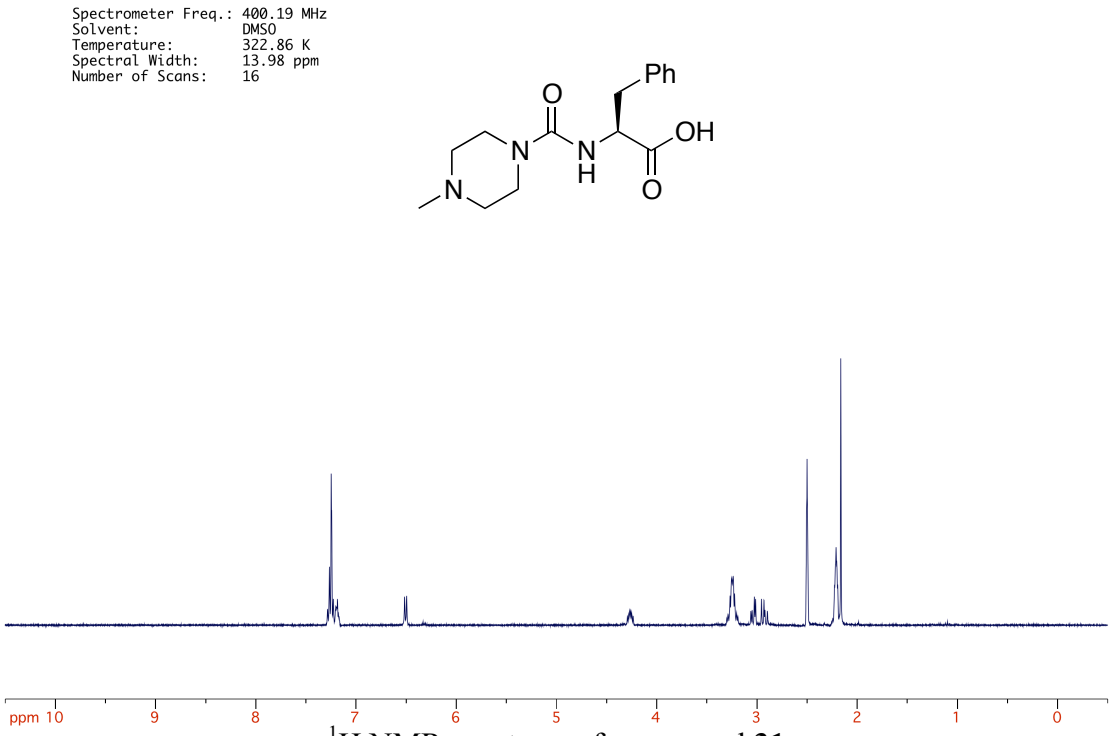

^{1}H NMR spectrum of compound **31**

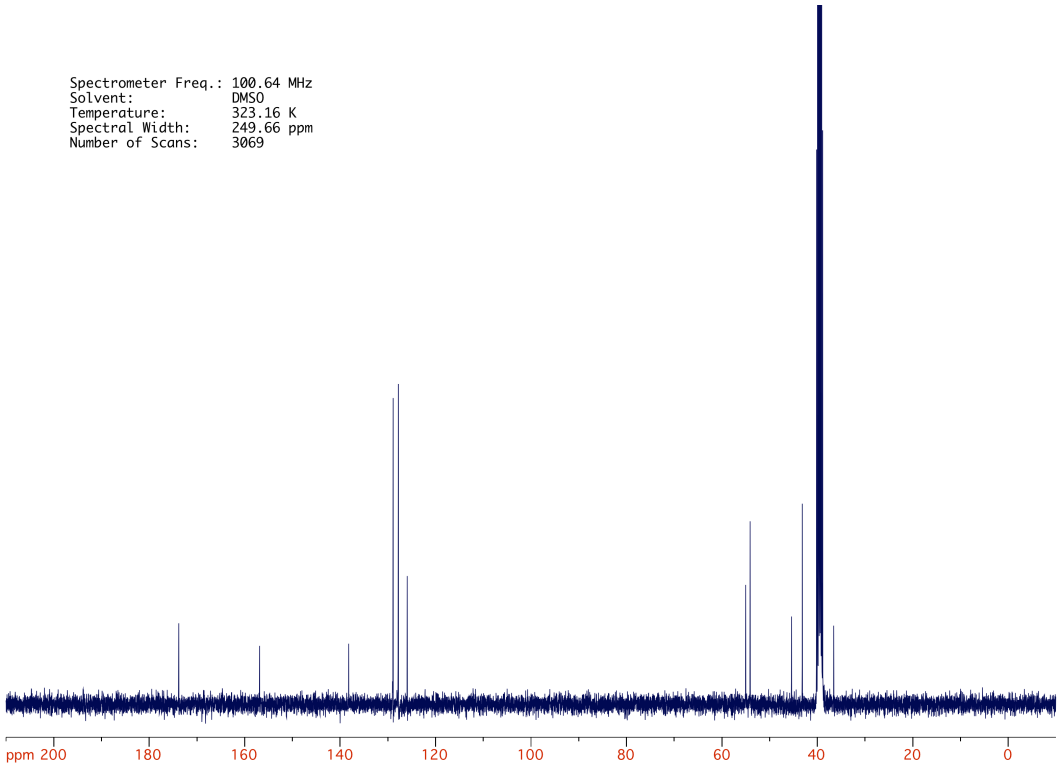

^{13}C {H}NMR spectrum of compound **31**

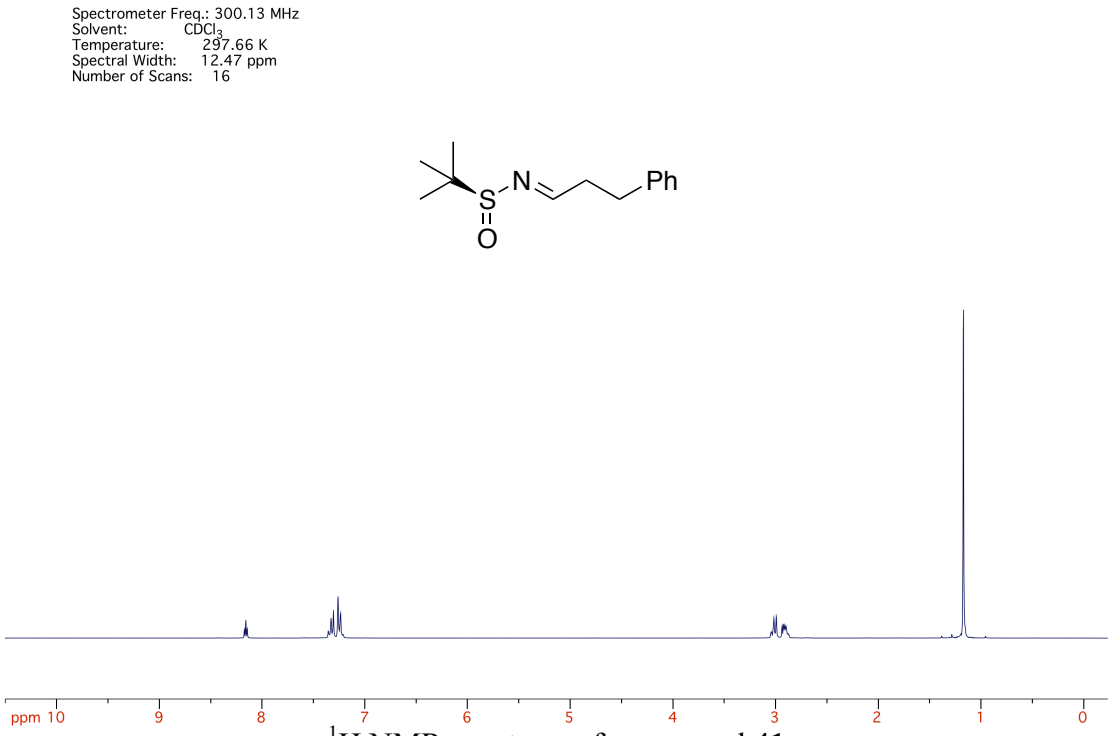

^{1}H NMR spectrum of compound **41**

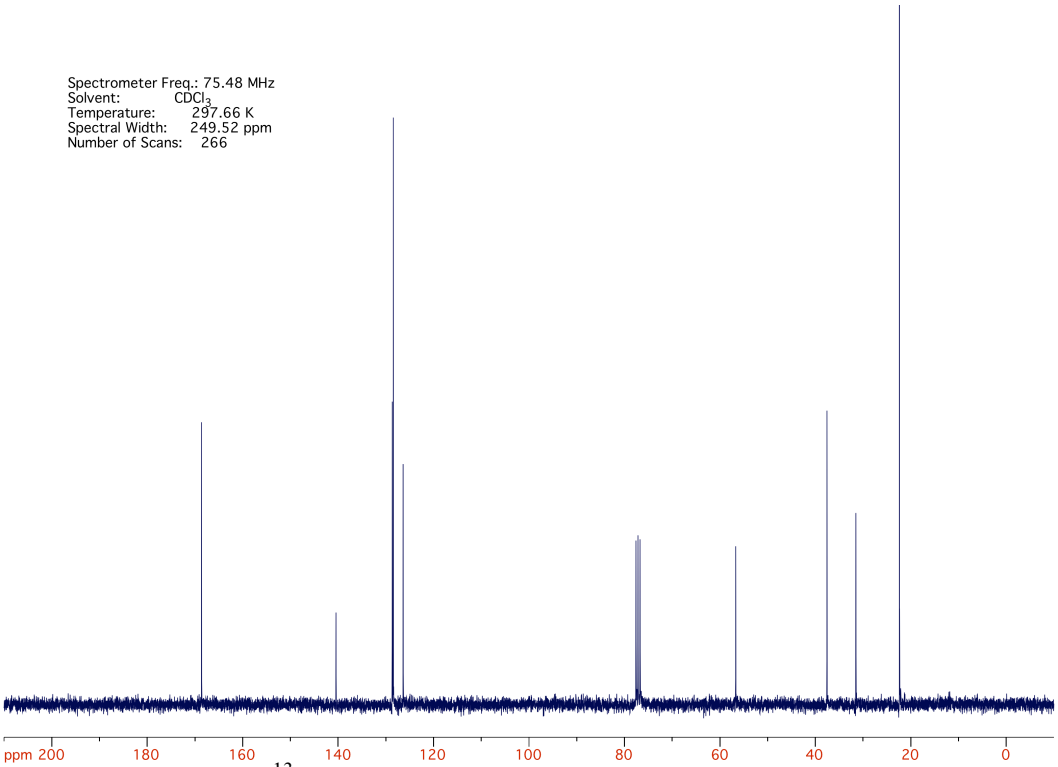

^{13}C {H}NMR spectrum of compound **41**

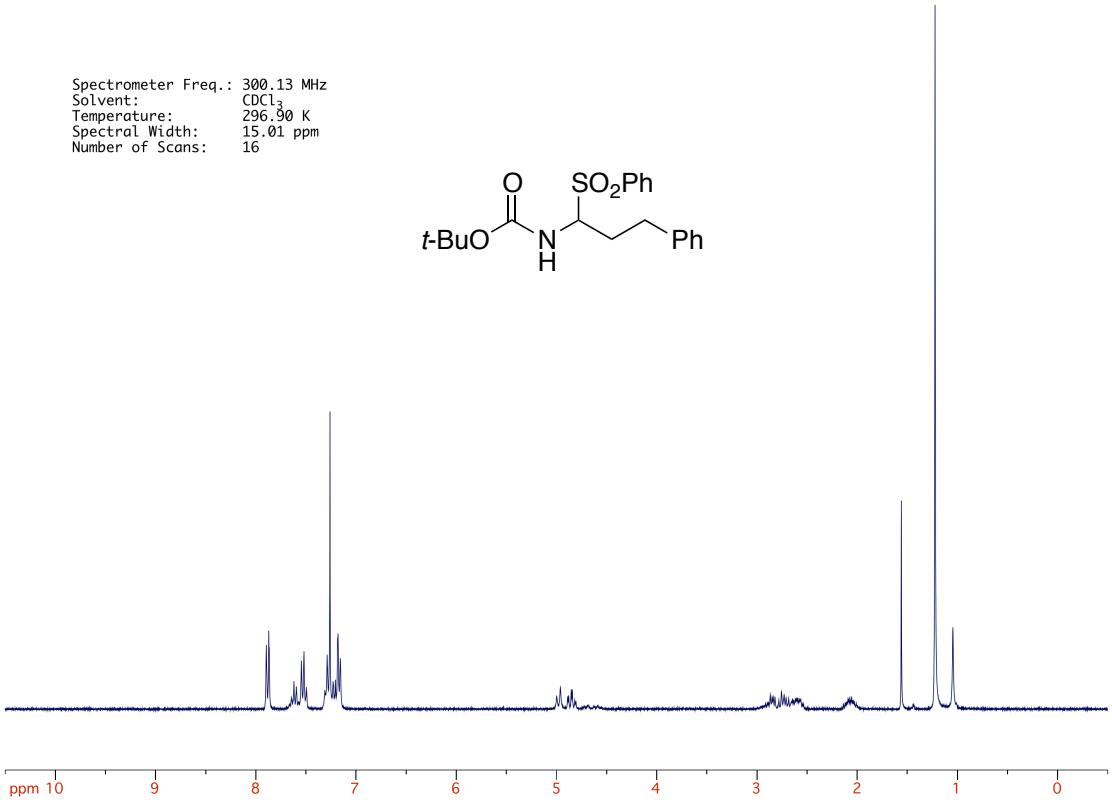

^{1}H NMR spectrum of compound **44**

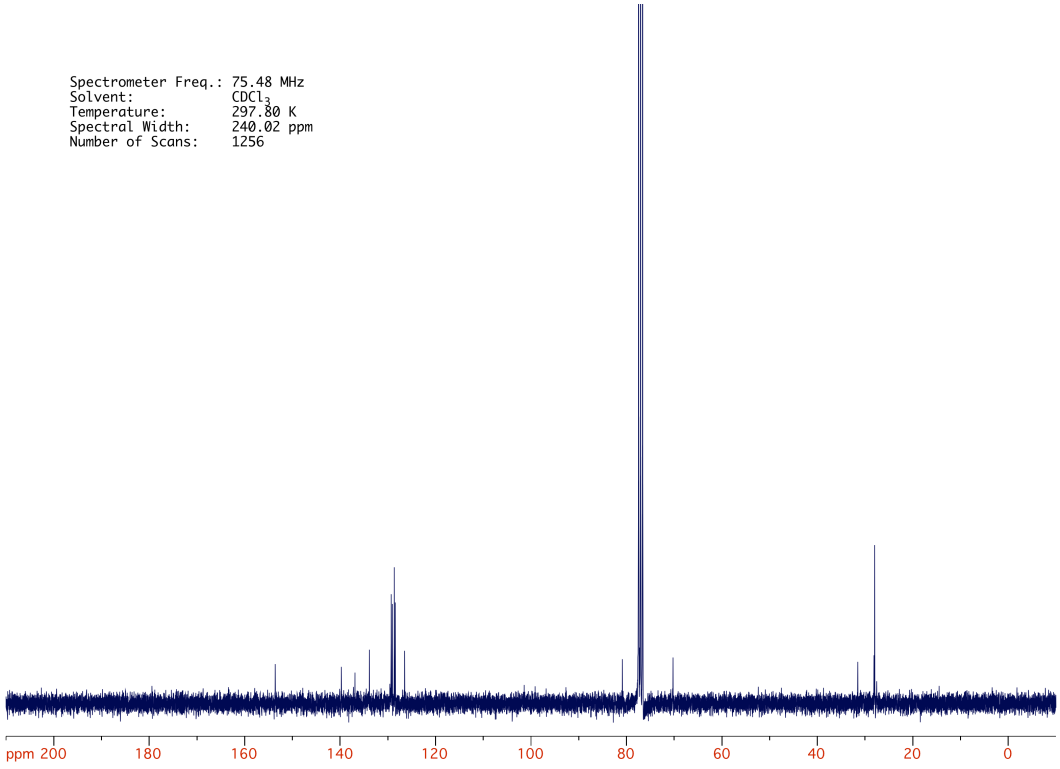

^{13}C {H}NMR spectrum of compound **44**

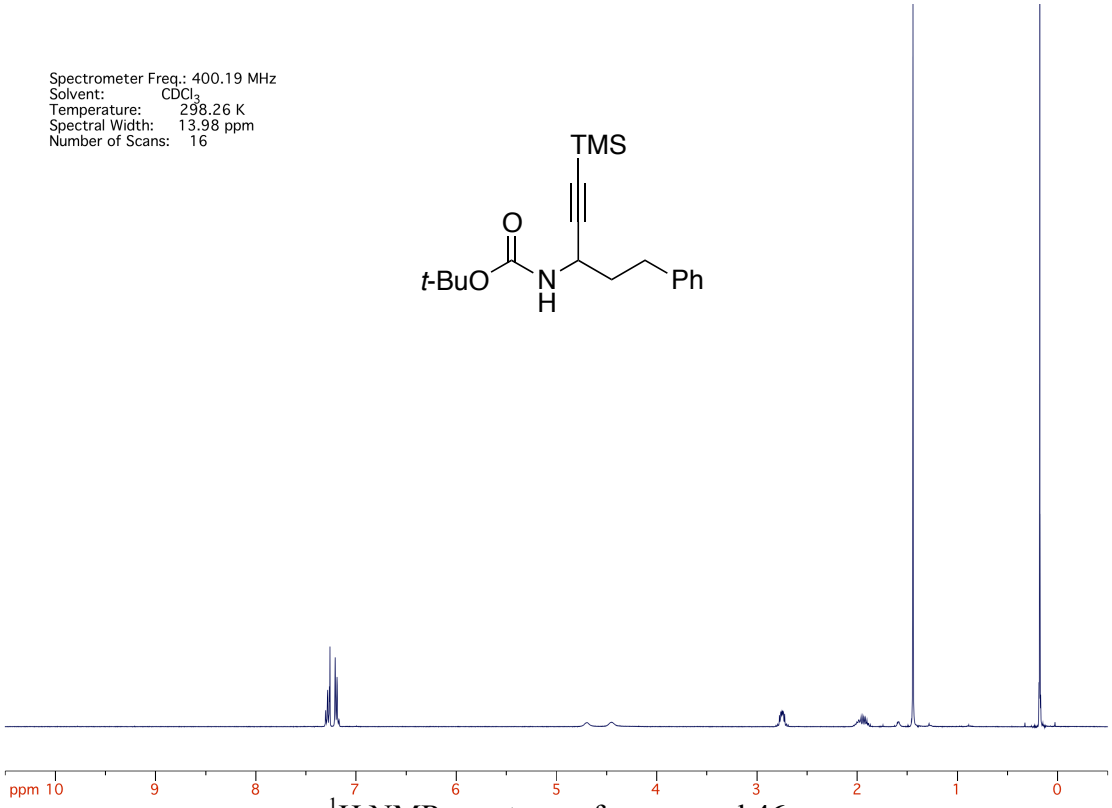

^{1}H NMR spectrum of compound **46**

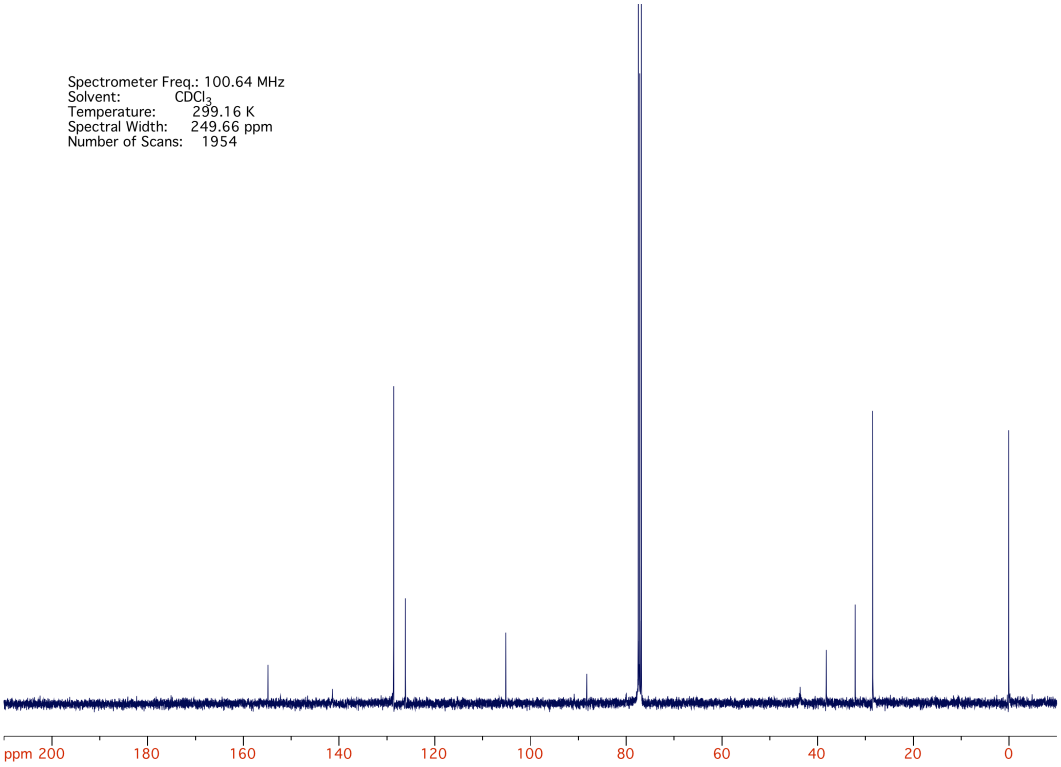

^{13}C {H}NMR spectrum of compound **46**

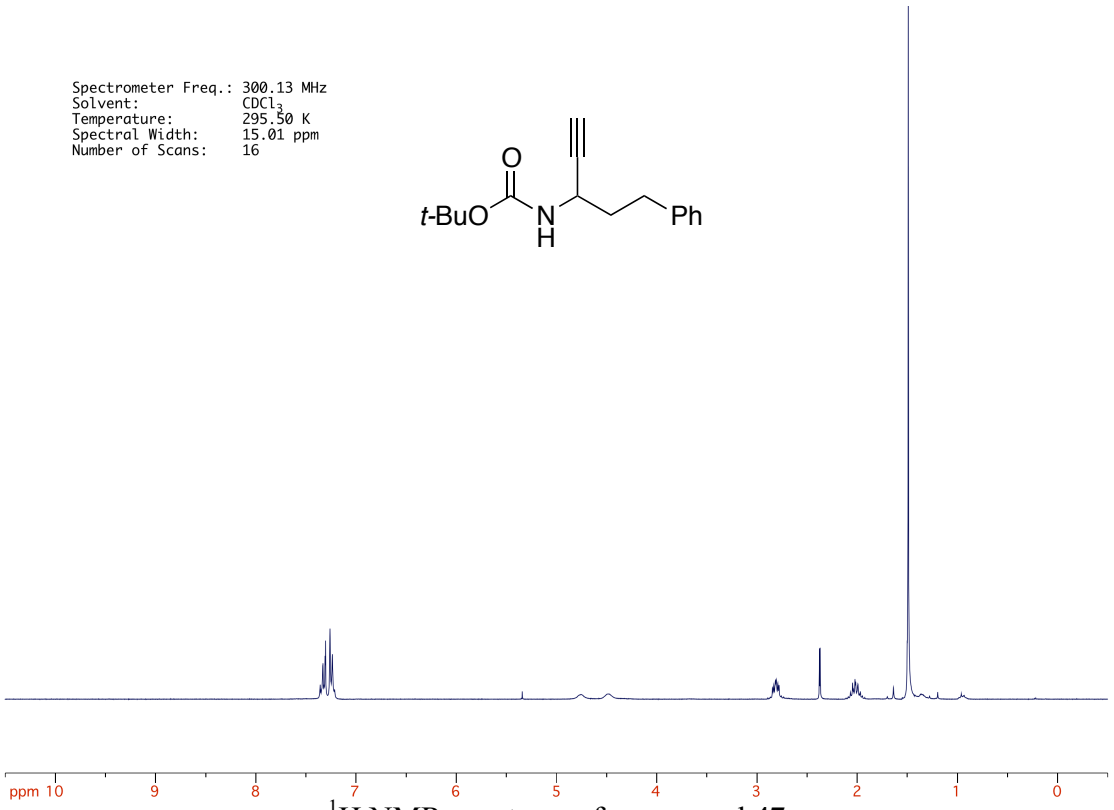

^{1}H NMR spectrum of compound **47**

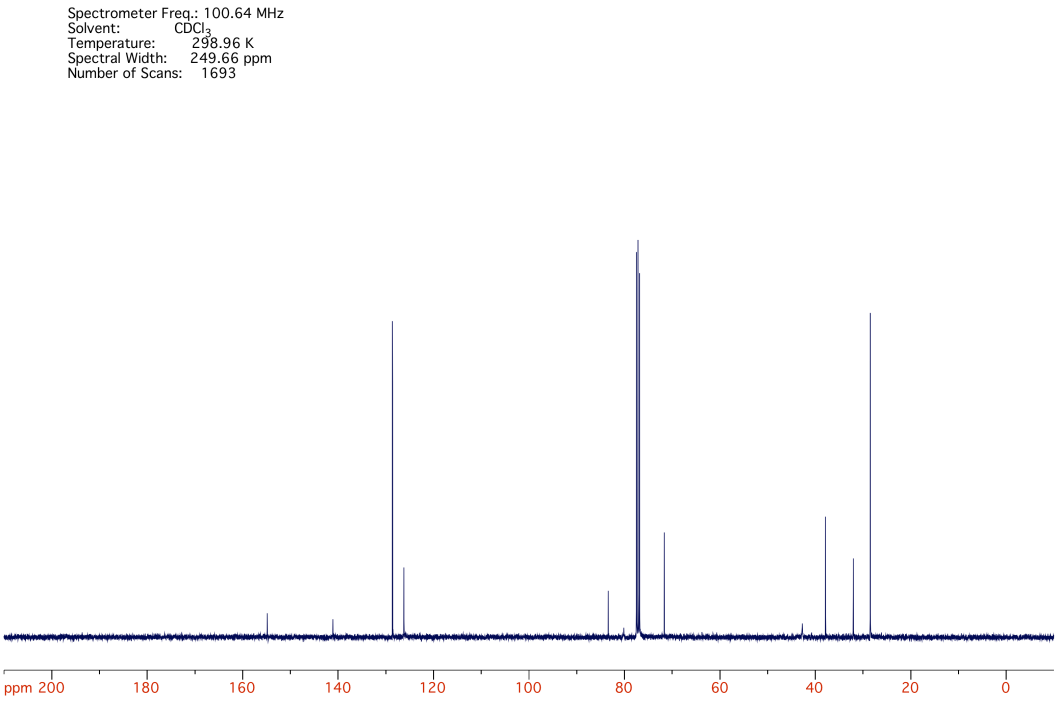

^{13}C {H}NMR spectrum of compound **47**

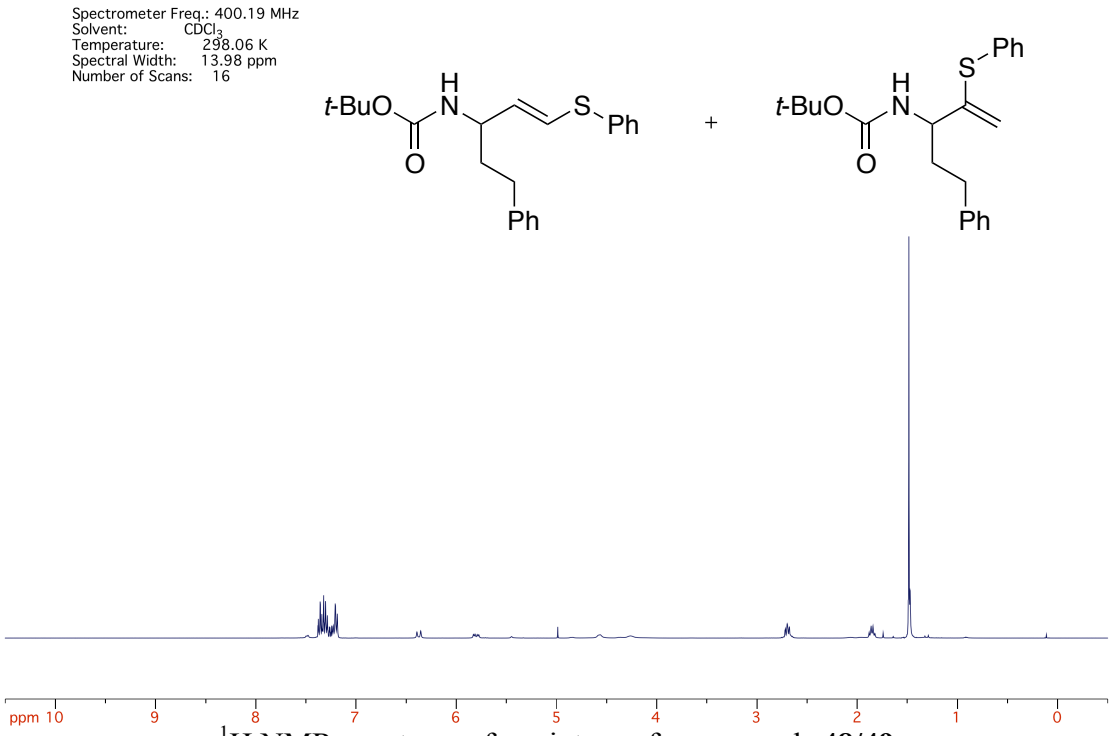

^{1}H NMR spectrum of a mixture of compounds **48/49**

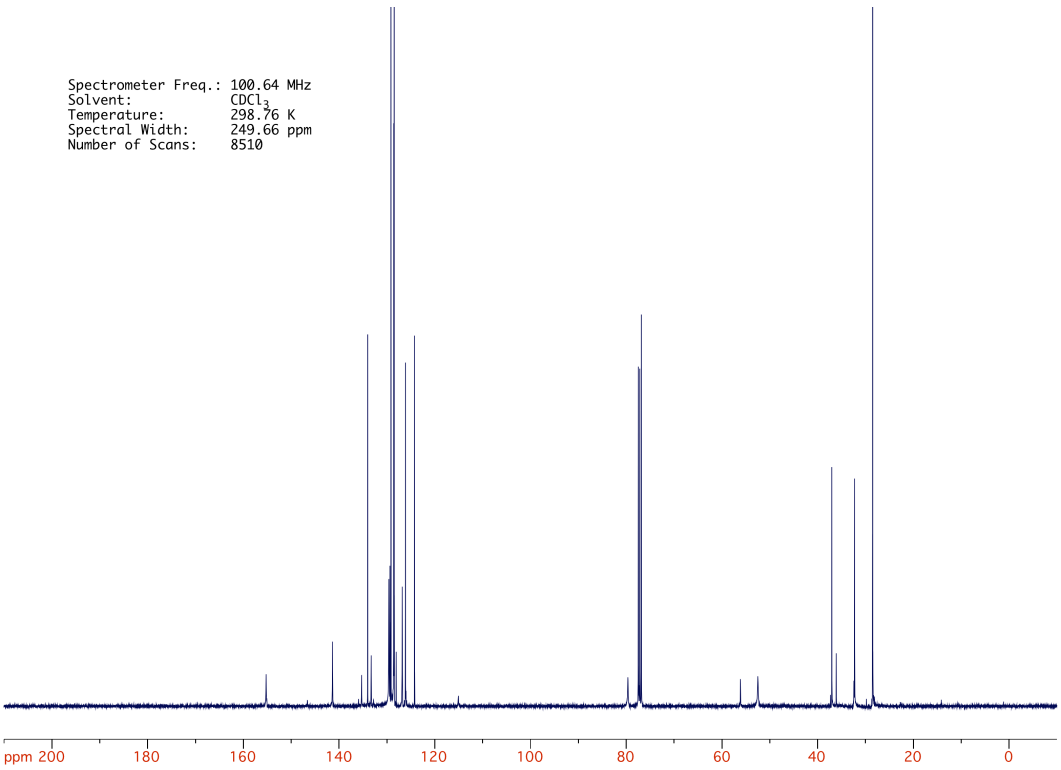

^{13}C {H}NMR spectrum of a mixture of compounds **48/49**

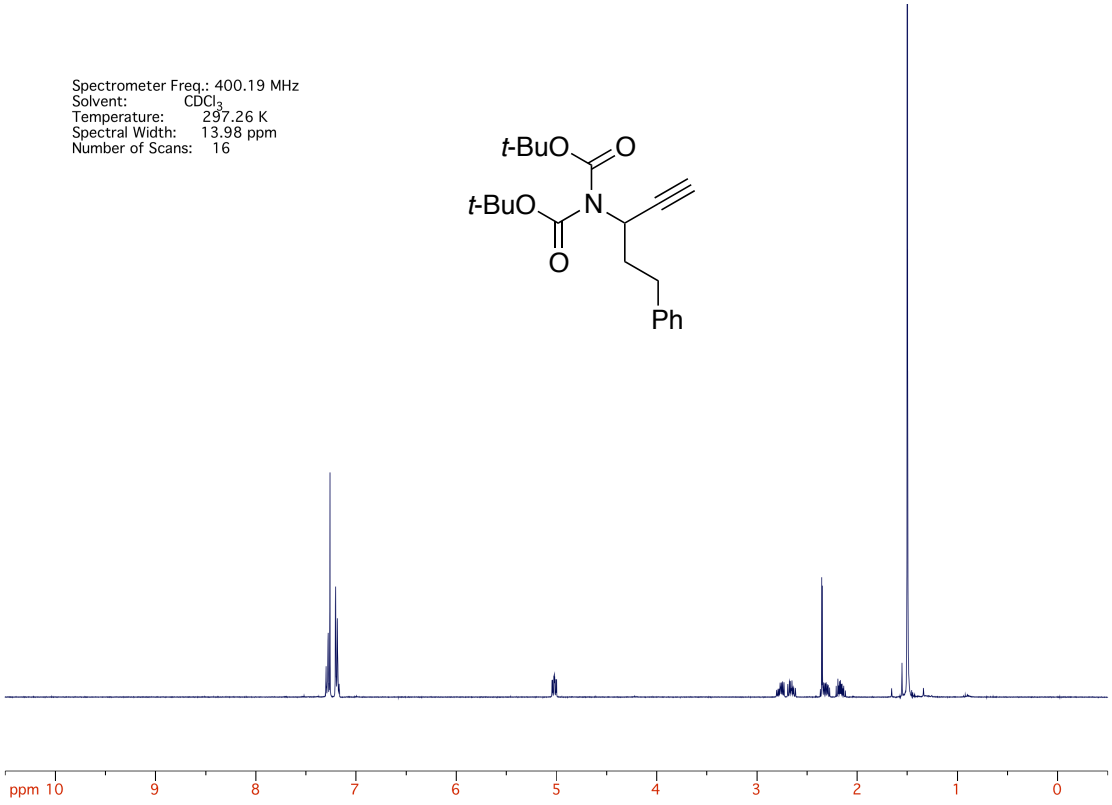

^{1}H NMR spectrum of compound **50**

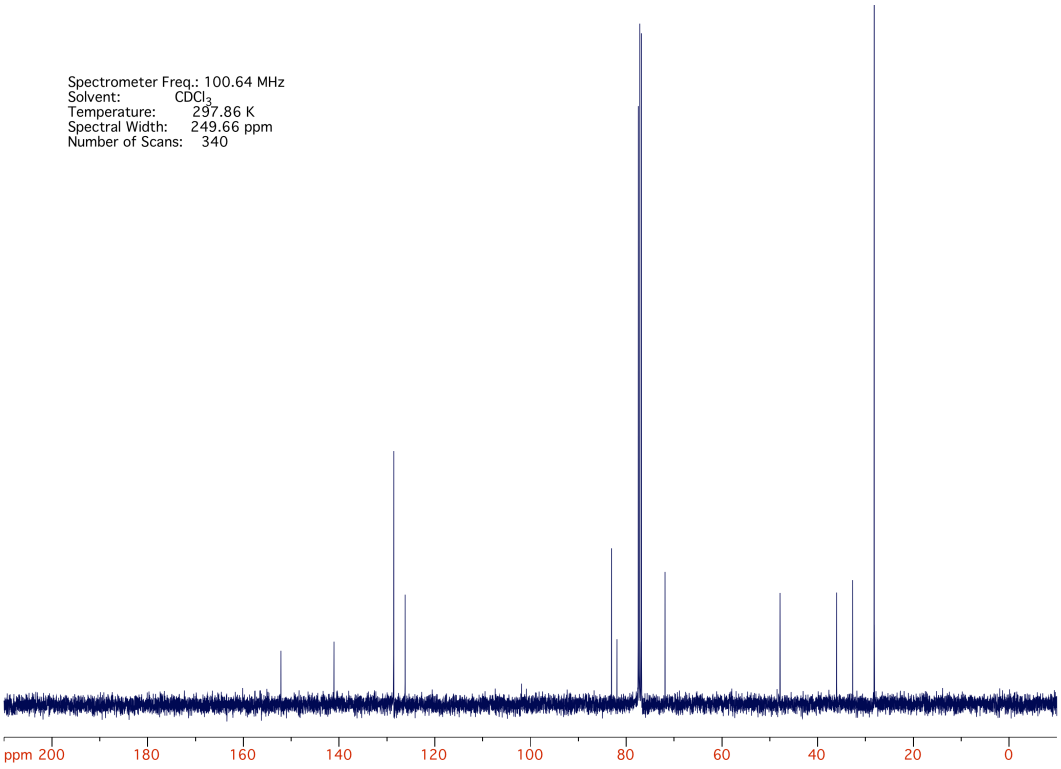

^{13}C {H}NMR spectrum of compound **50**

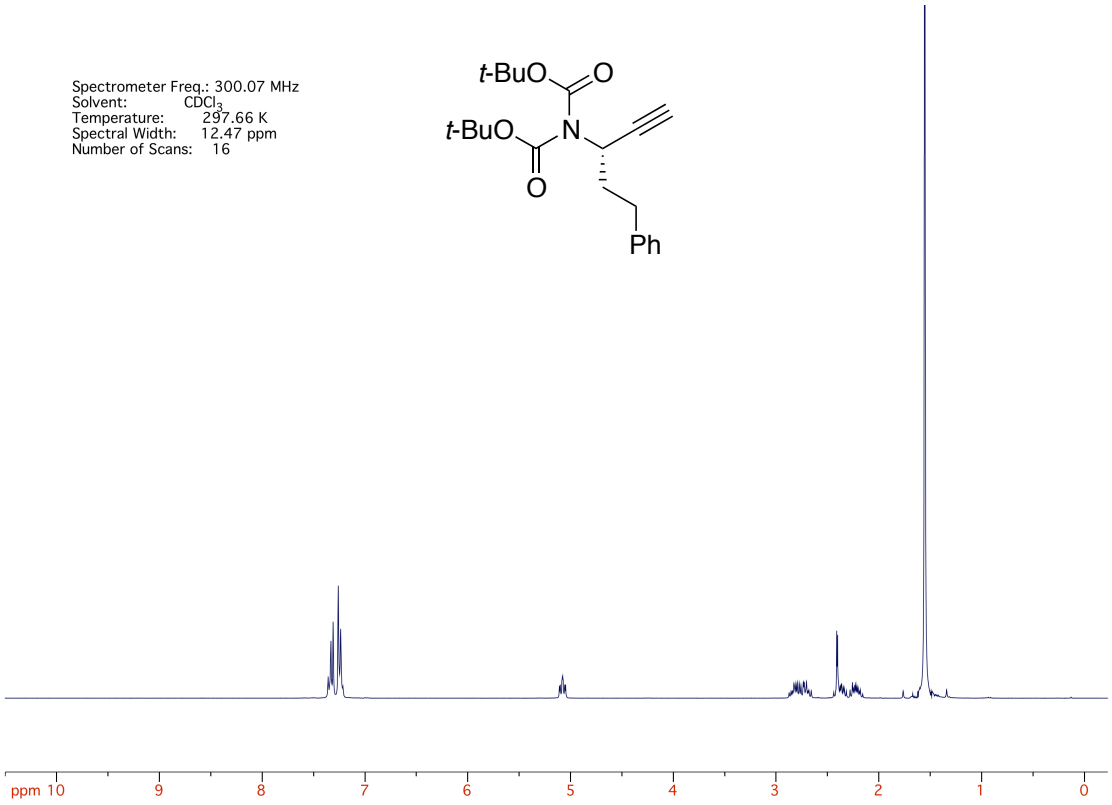

^{1}H NMR spectrum of compound **53**

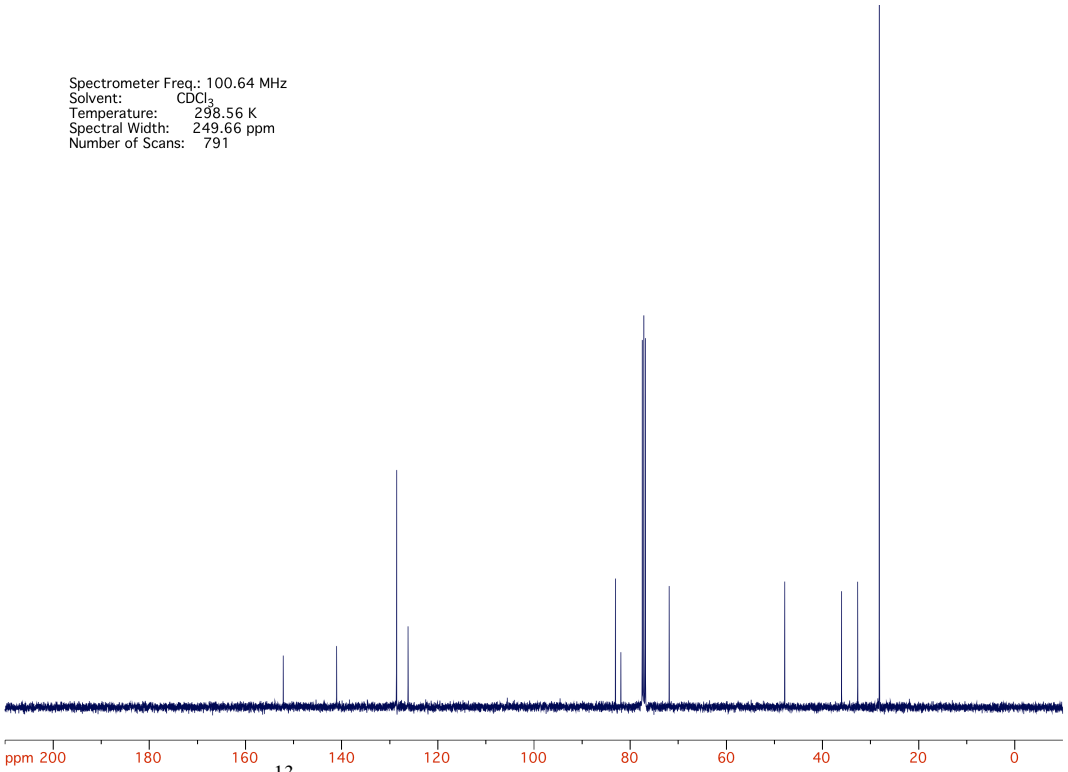

^{13}C {H}NMR spectrum of compound **53**

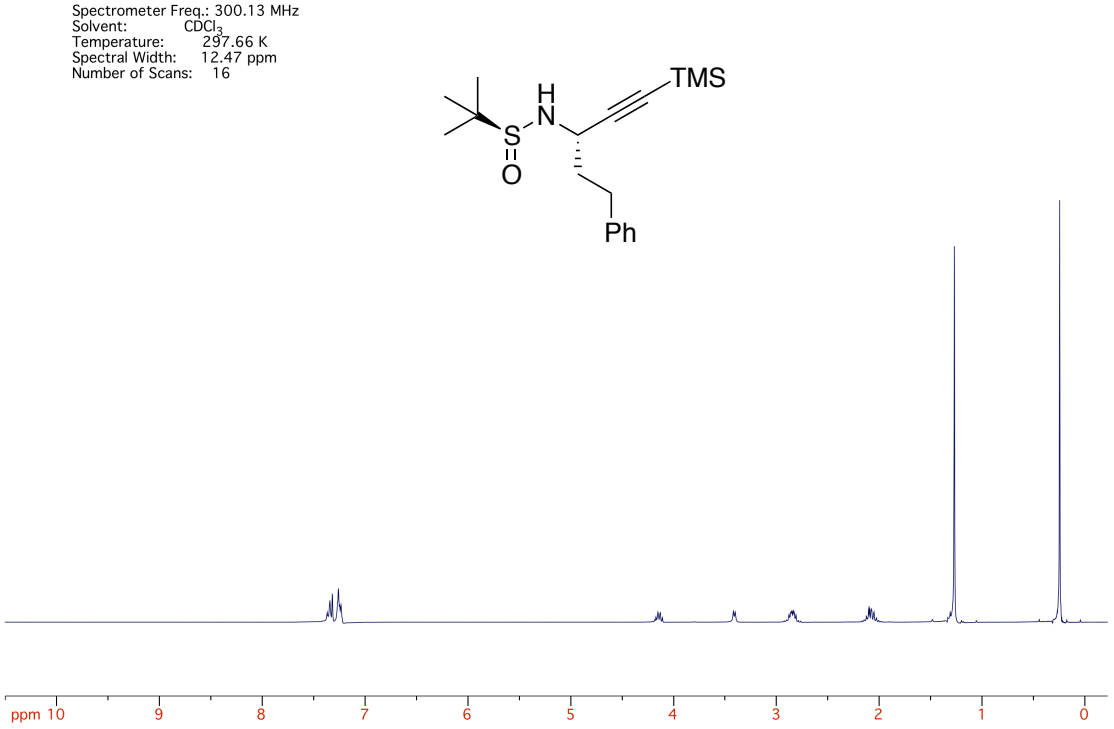

^{1}H NMR spectrum of compound **54**

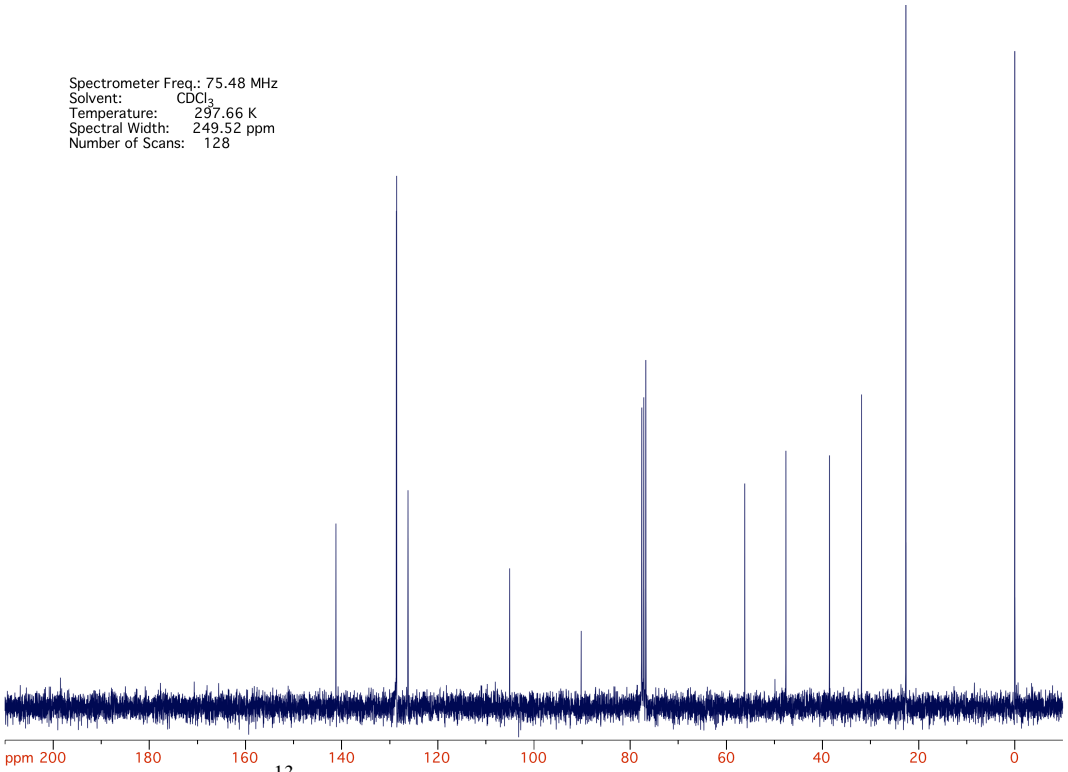

^{13}C {H}NMR spectrum of compound **54**

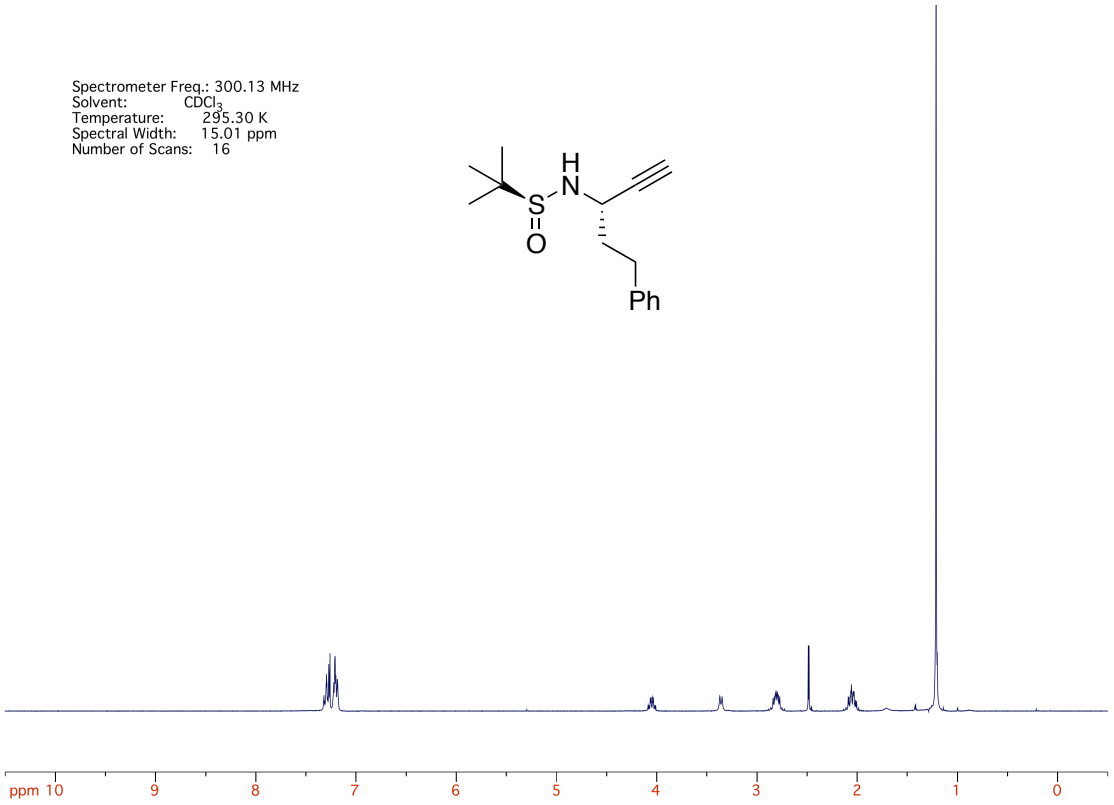

^{1}H NMR spectrum of compound **55**

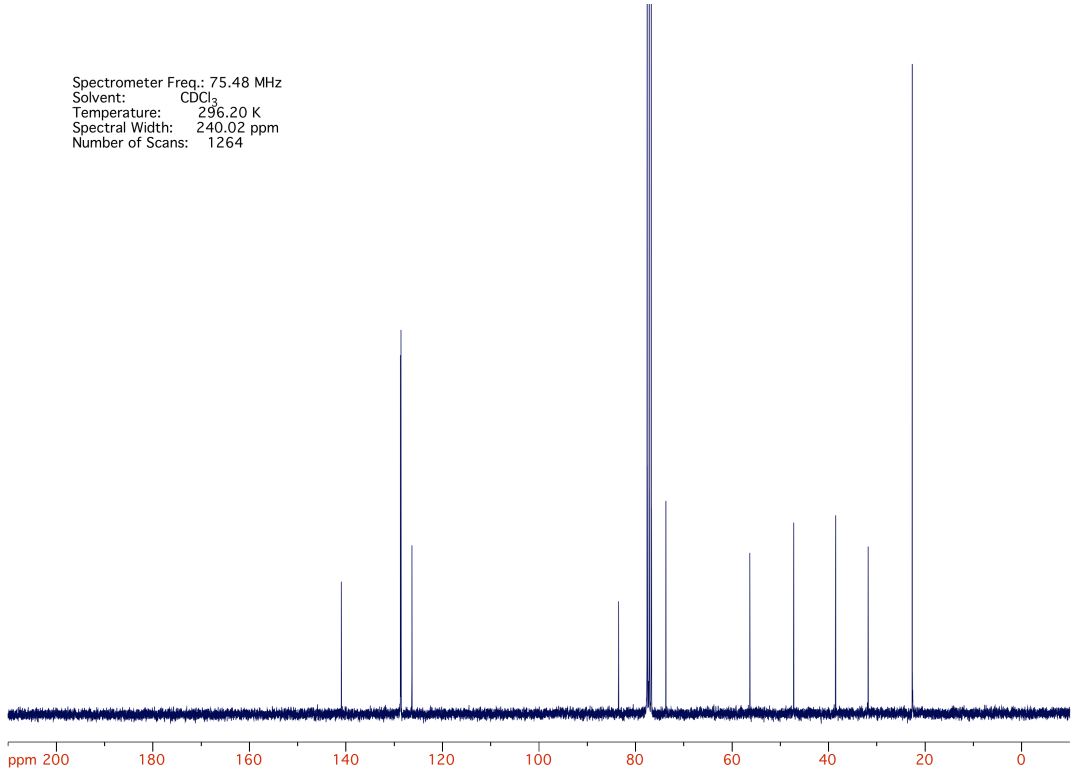

^{13}C {H}NMR spectrum of compound **55**

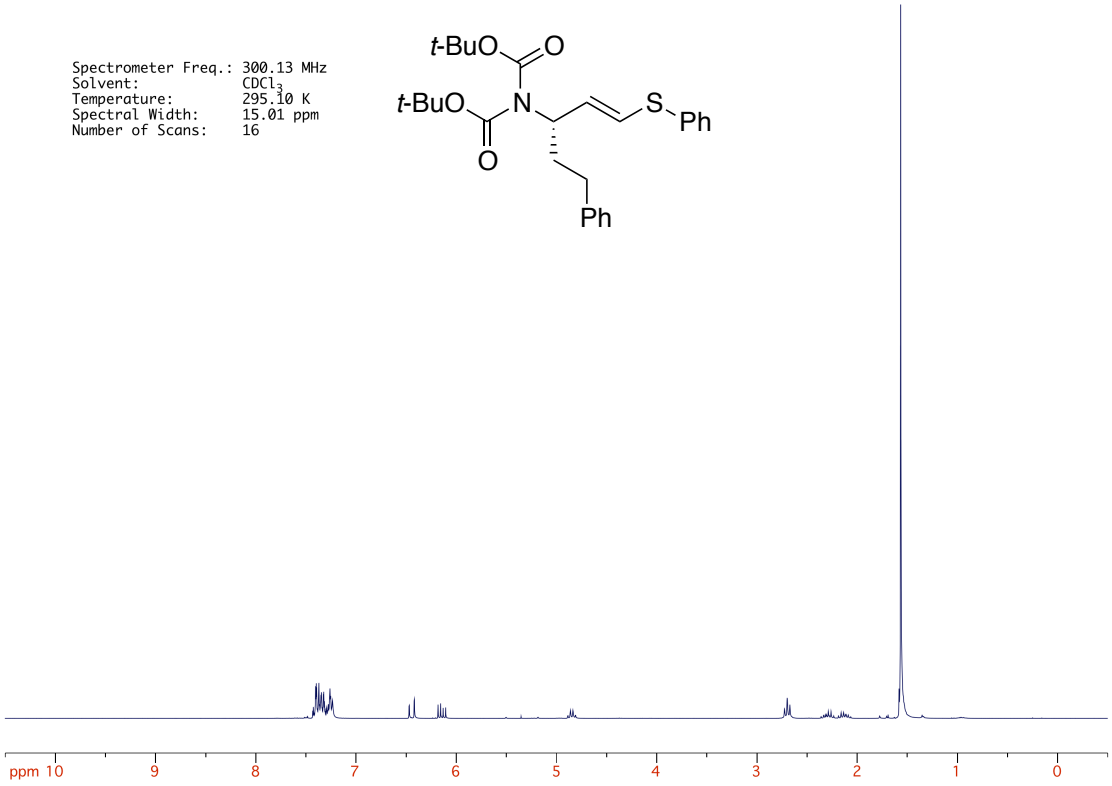

^{1}H NMR spectrum of compound **59**

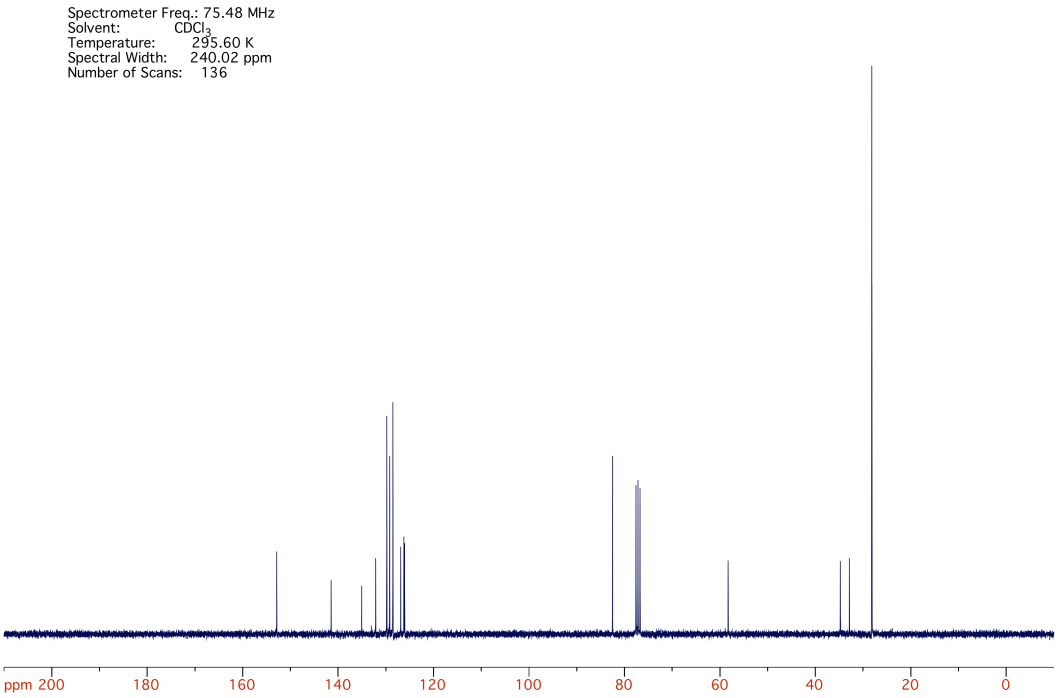

^{13}C {H}NMR spectrum of compound **59**

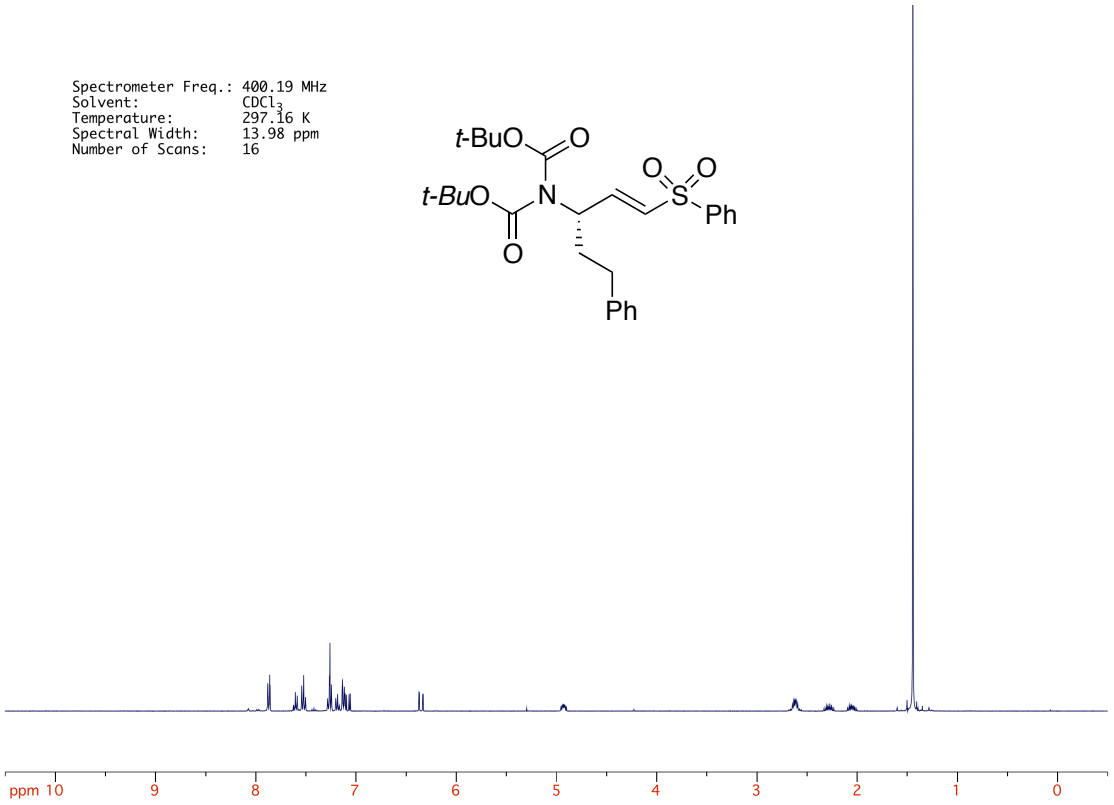

^{1}H NMR spectrum of compound **60**

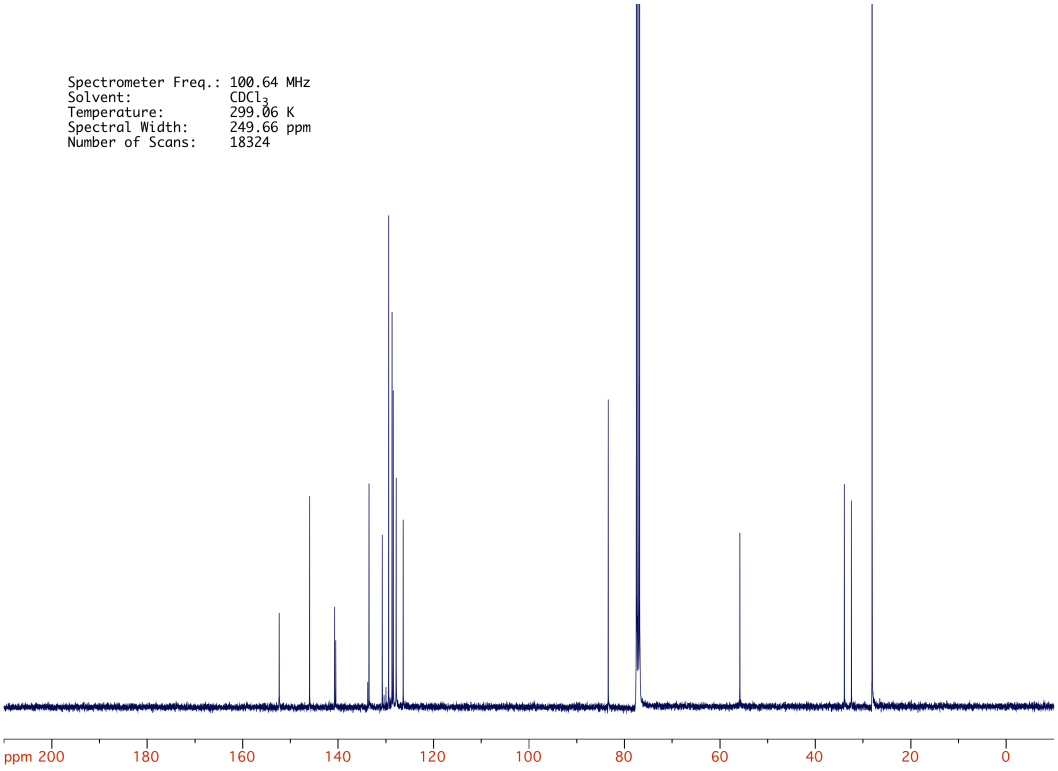

^{13}C {H}NMR spectrum of compound **60**

Spectrometer Freq.: 282.39 MHz
Solvent: $CDCl_3$
Temperature: 297.66 K
Spectral Width: 160.60 ppm
Number of Scans: 8

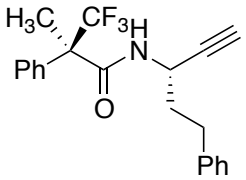

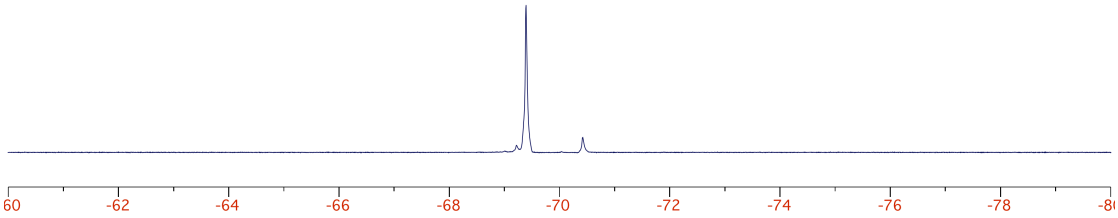

^{19}F NMR spectrum of compound **65**

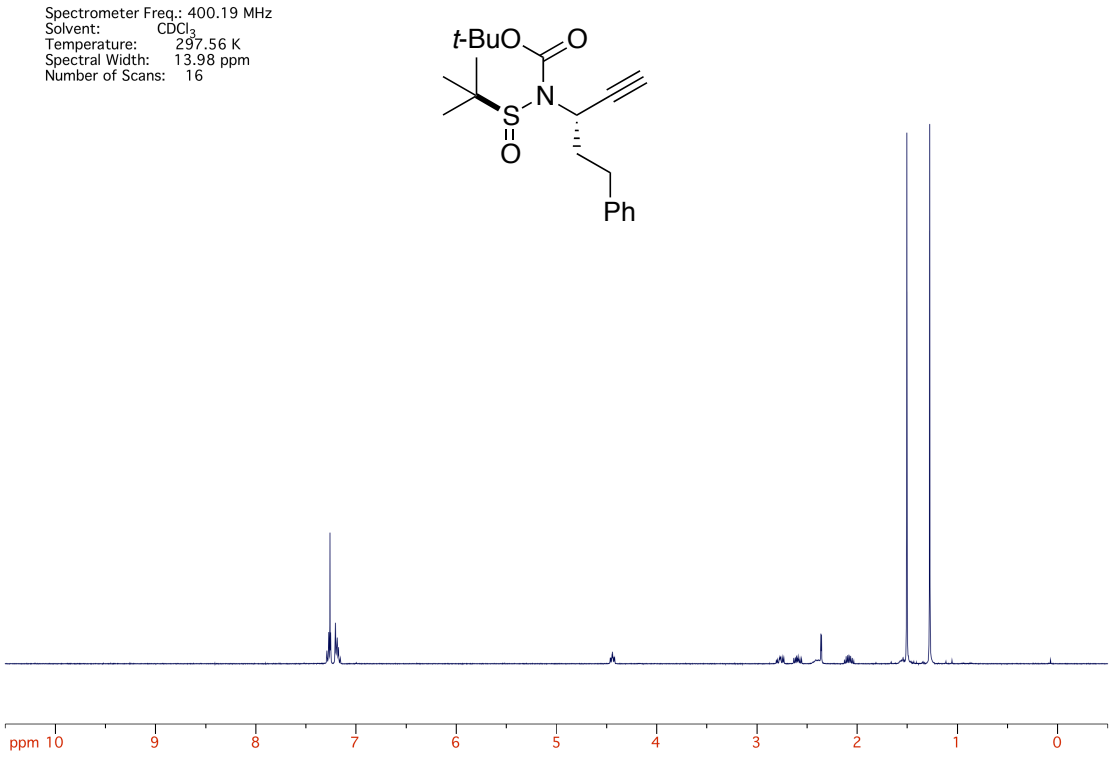

^{1}H NMR spectrum of compound **66**

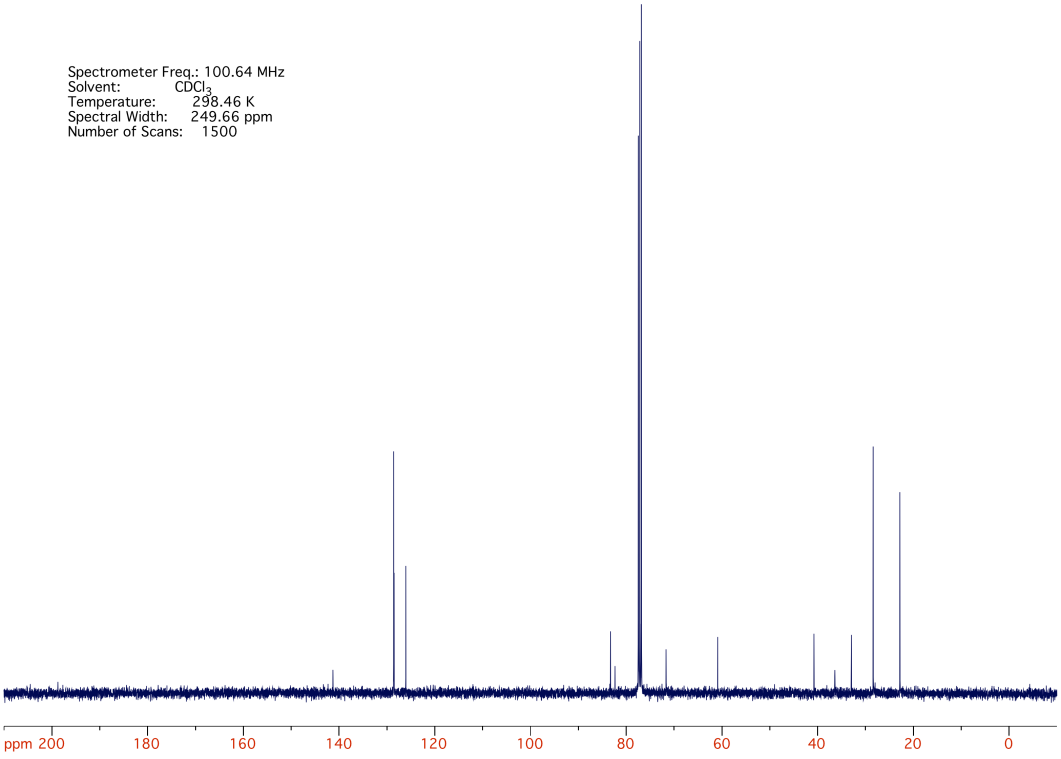

^{13}C {H}NMR spectrum of compound **66**

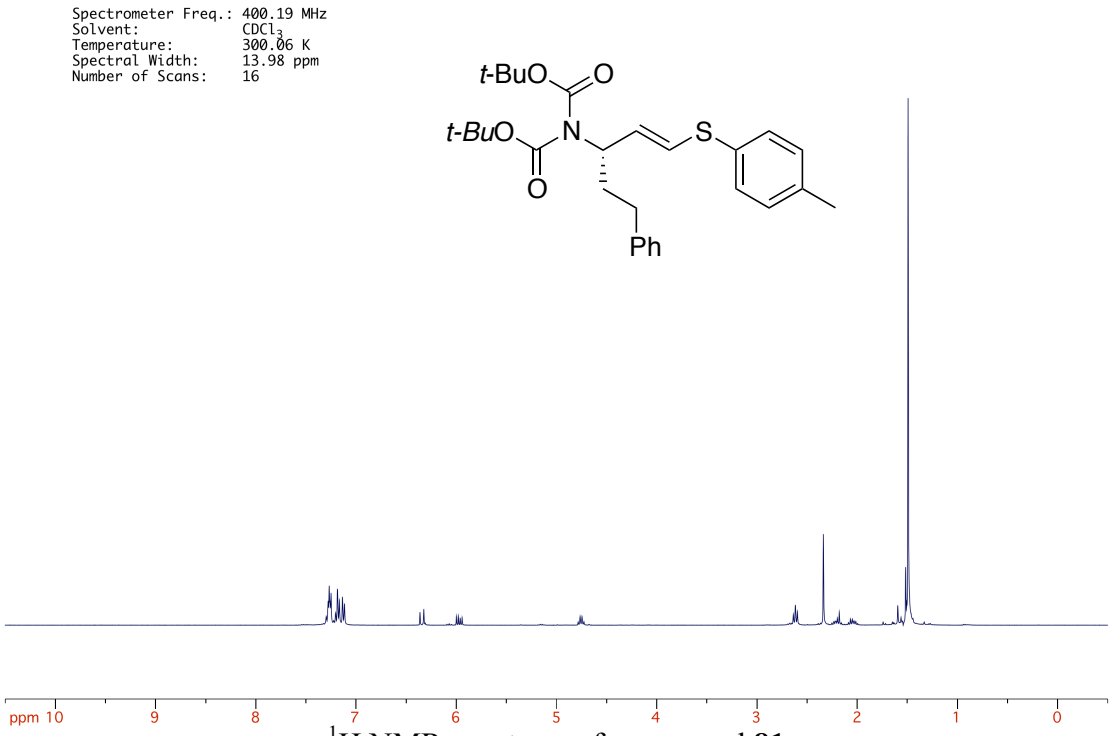

^{1}H NMR spectrum of compound **81**

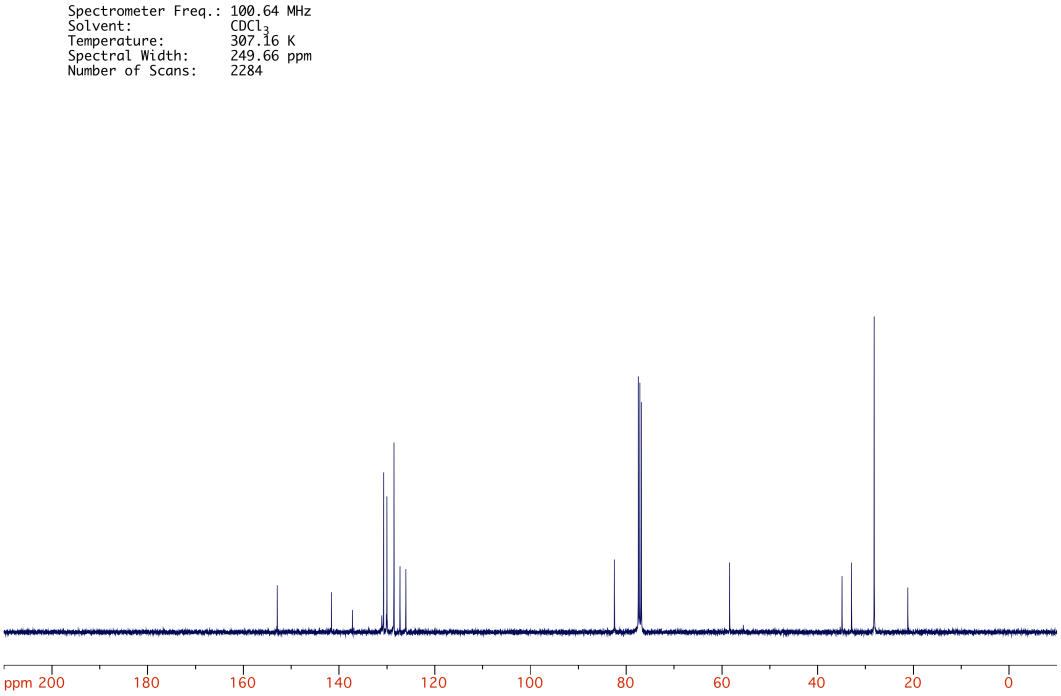

^{13}C {H}NMR spectrum of compound **81**

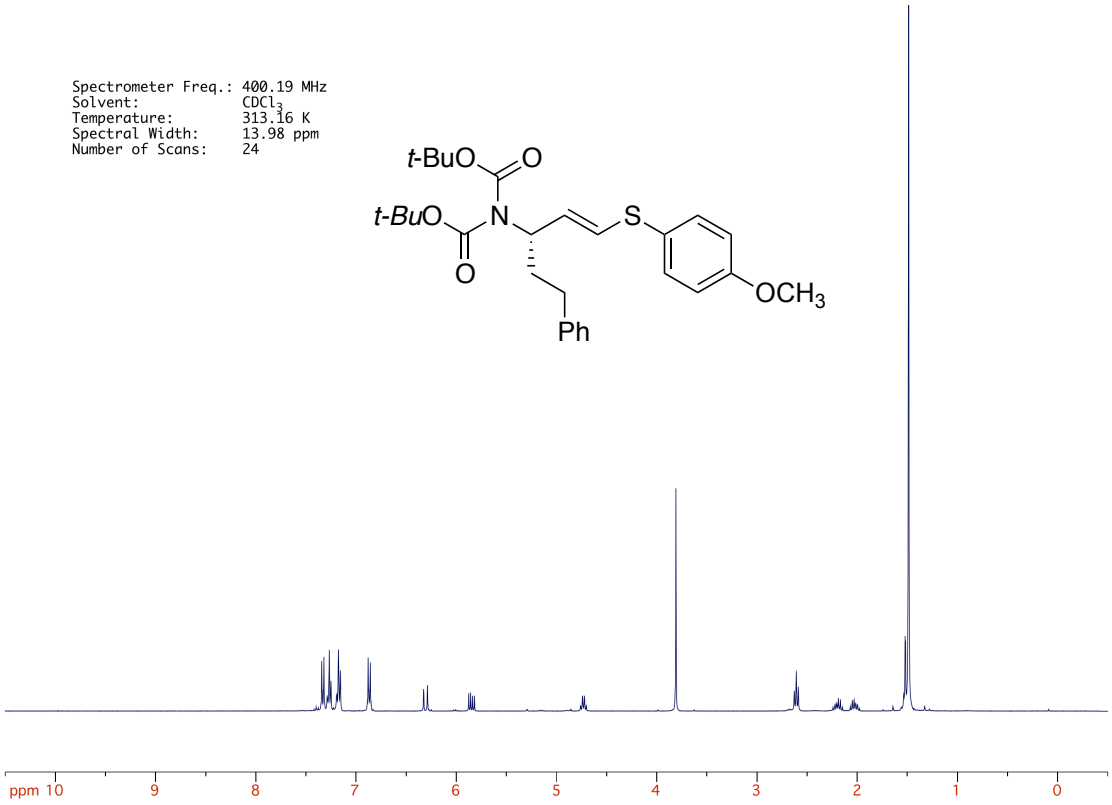

^{1}H NMR spectrum of compound **82**

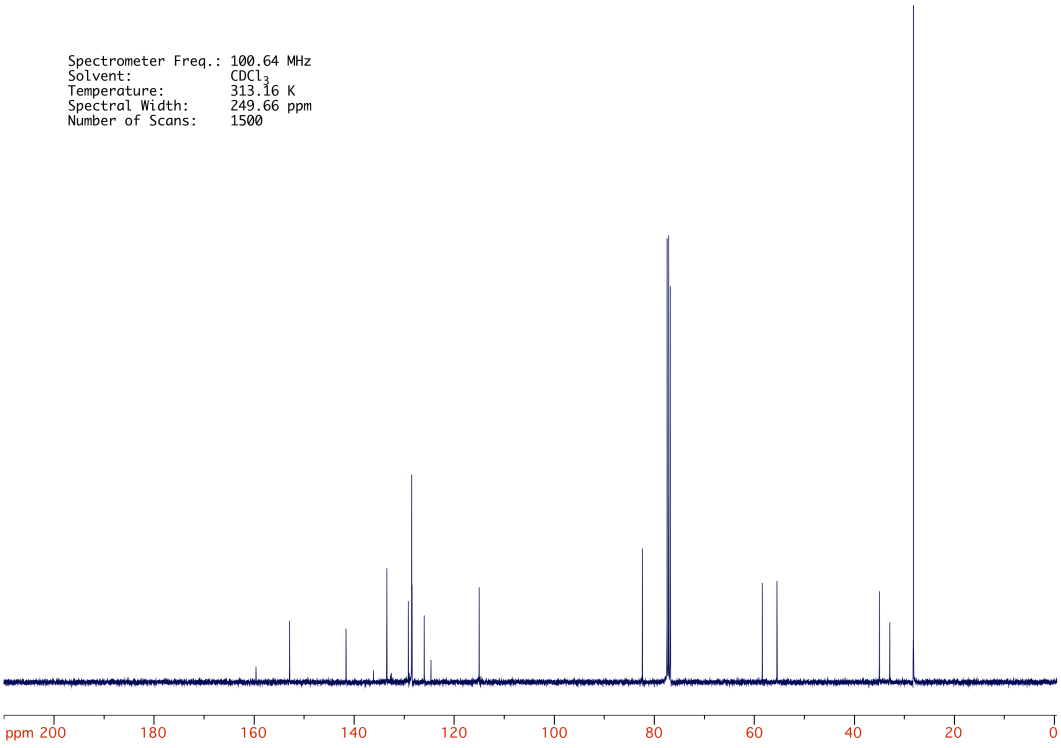

^{13}C NMR spectrum of compound **82**

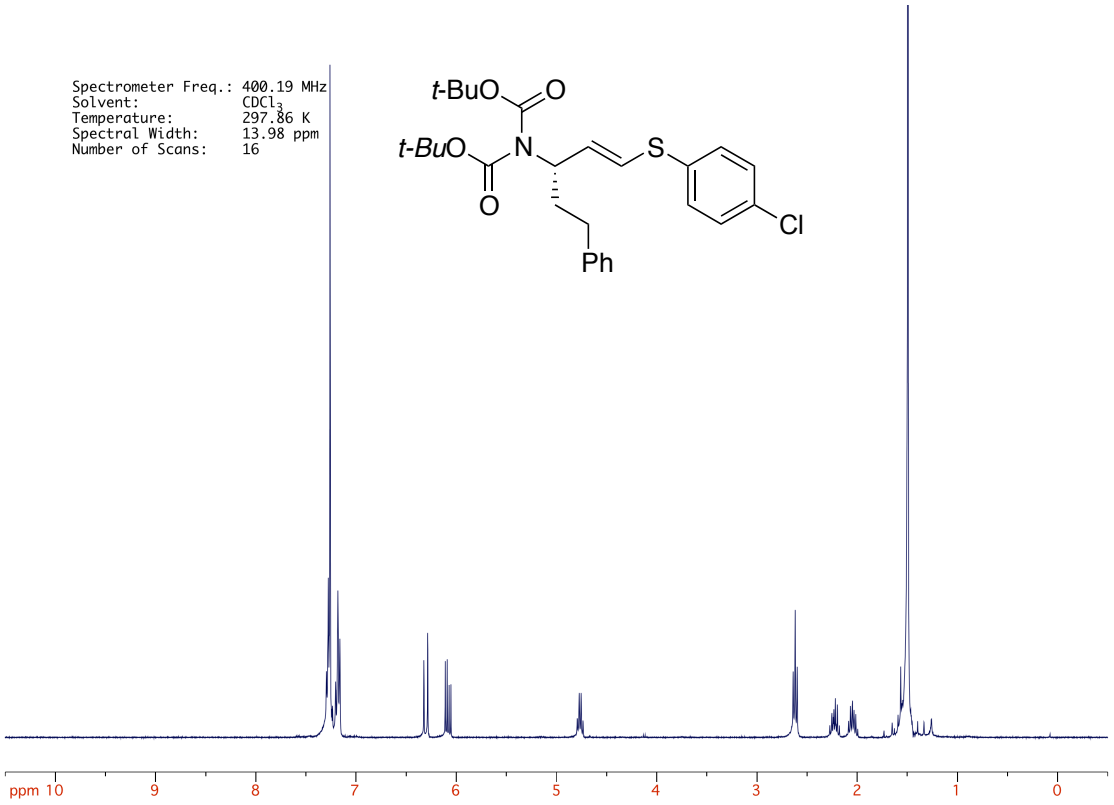

^{1}H NMR spectrum of compound **83**

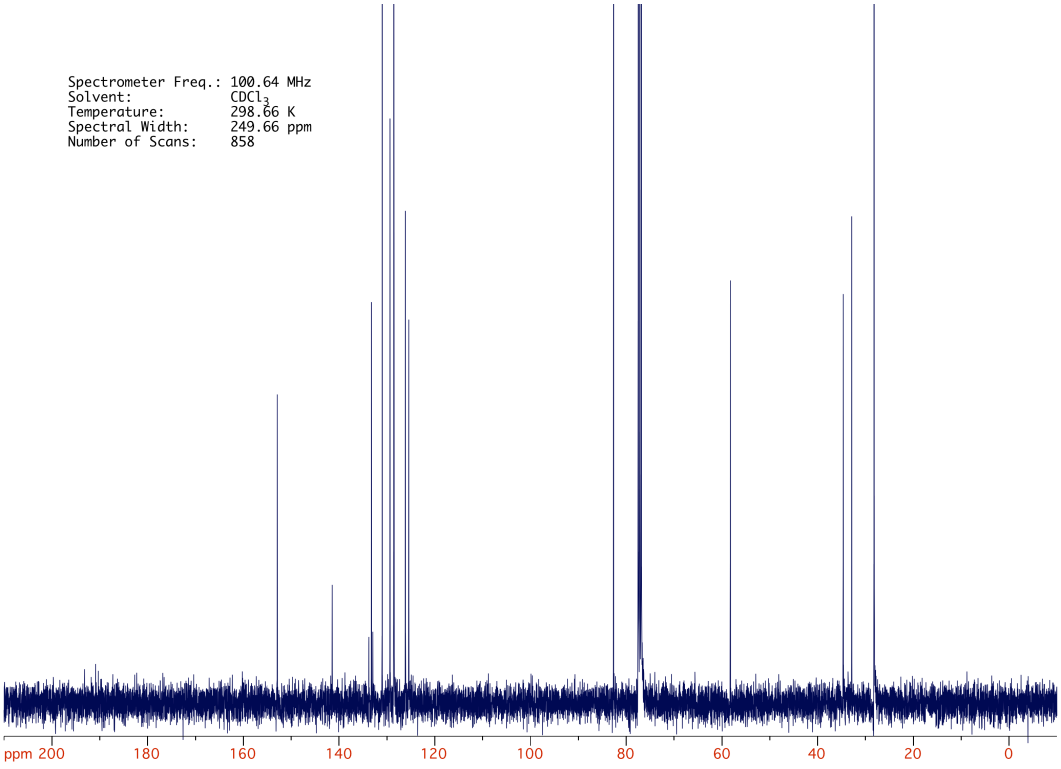

^{13}C {H}NMR spectrum of compound **83**

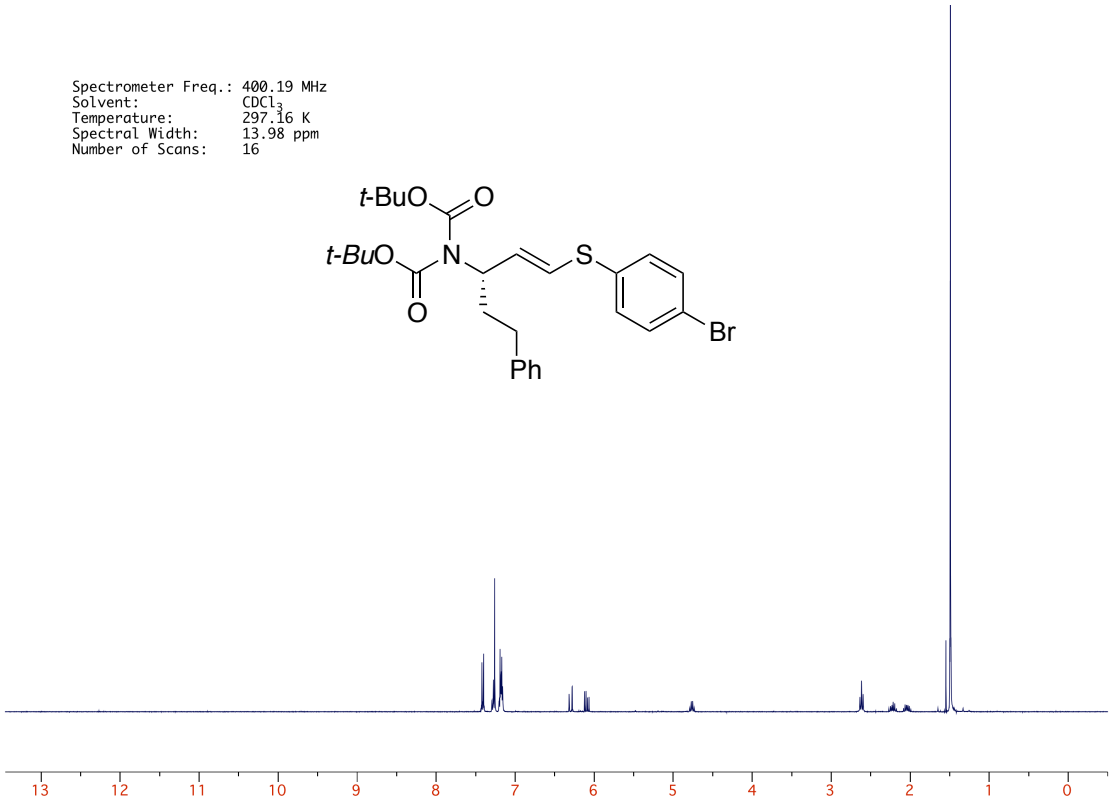

^{1}H NMR spectrum of compound **84**

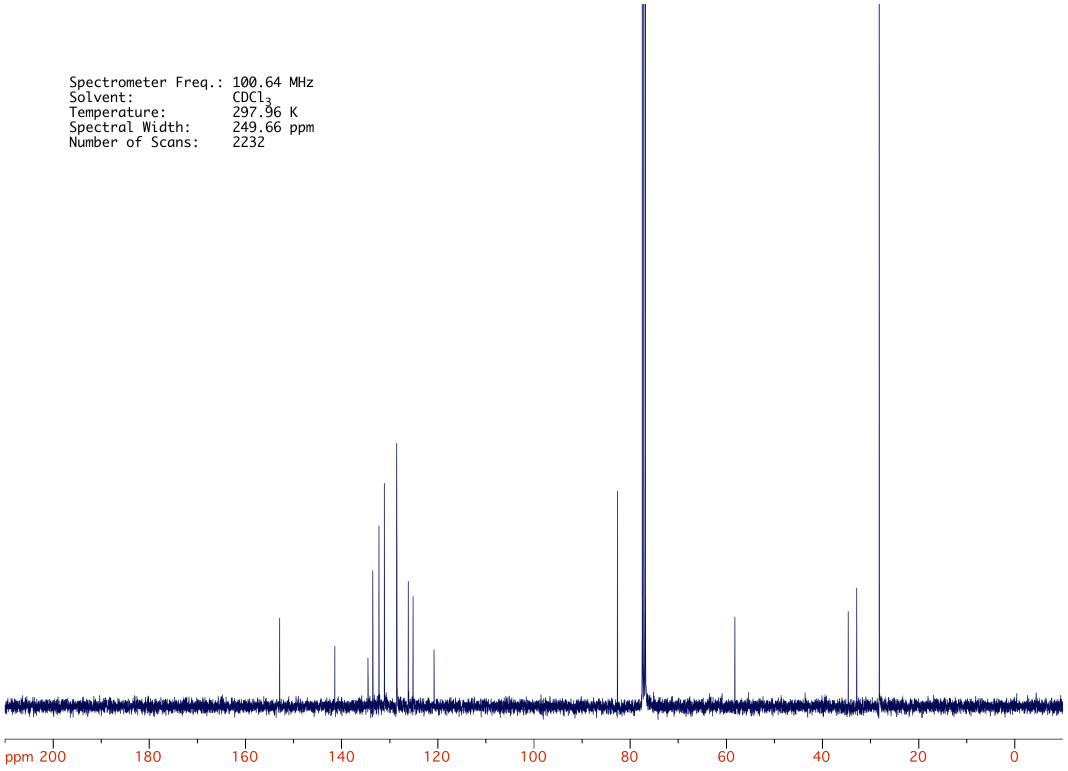

^{13}C {H}NMR spectrum of compound **84**

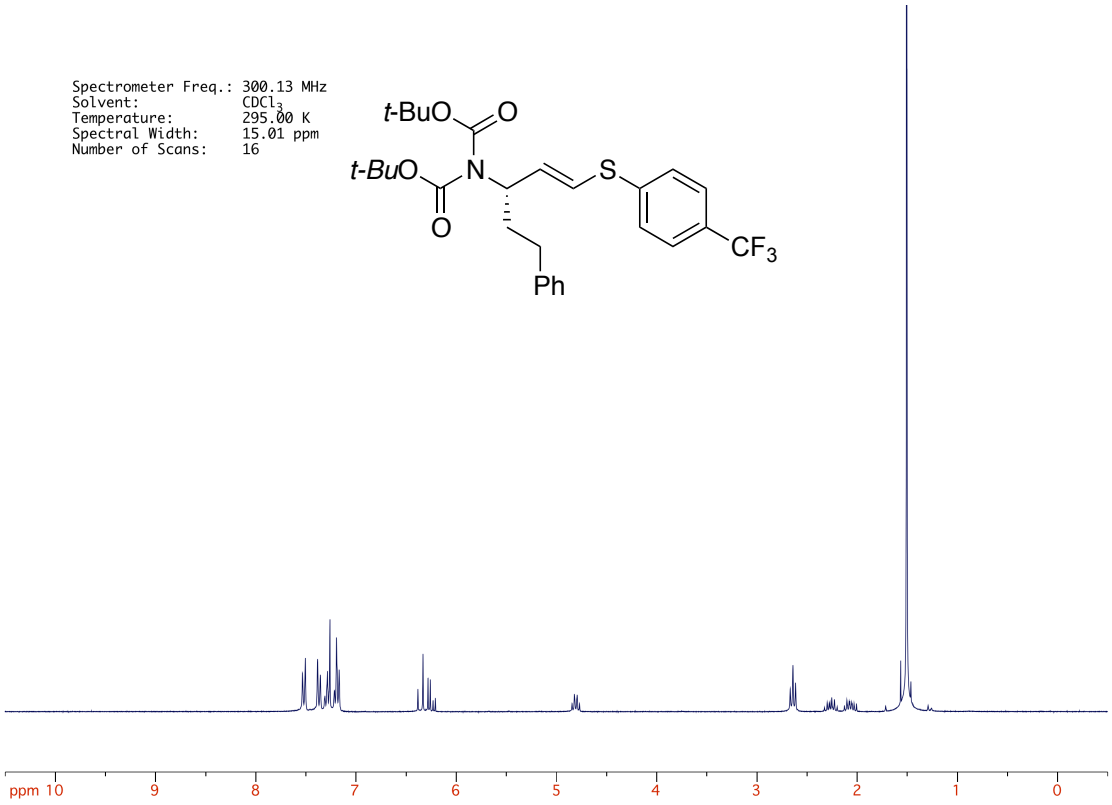

^{1}H NMR spectrum of compound **85**

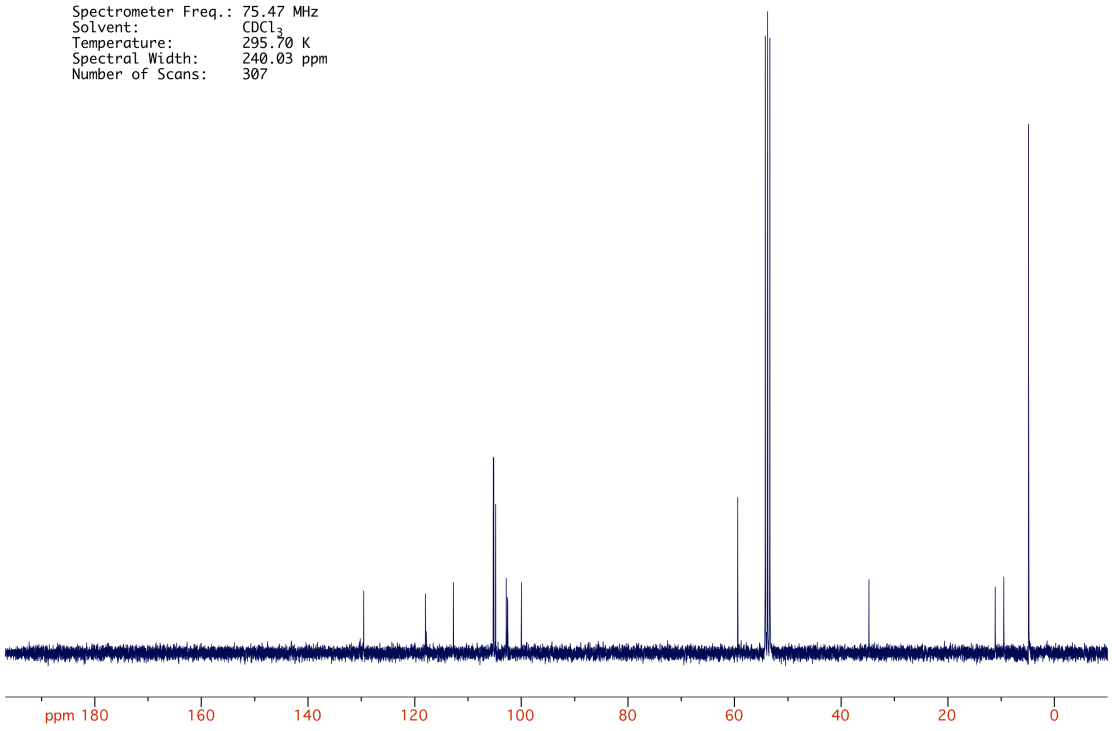

^{13}C {H}NMR spectrum of compound **85**

Spectrometer Freq.: 282.38 MHz
Solvent: $CDCl_3$
Temperature: 296.10 K
Spectral Width: 349.47 ppm
Number of Scans: 16

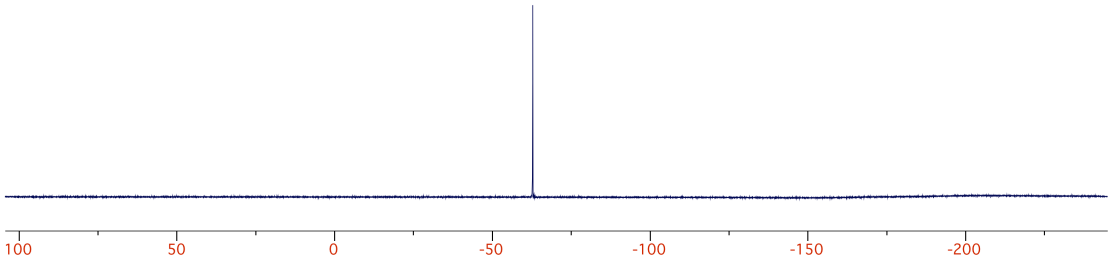

^{19}F NMR spectrum of compound **85**

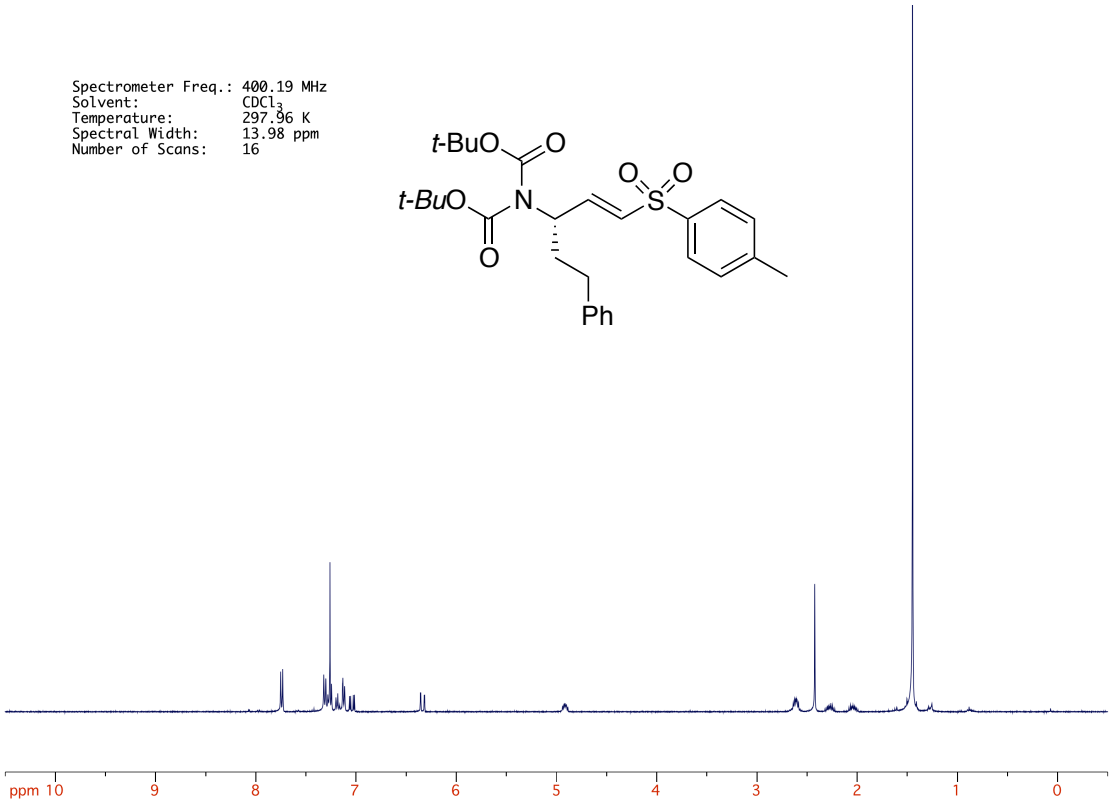

^{1}H NMR spectrum of compound **86**

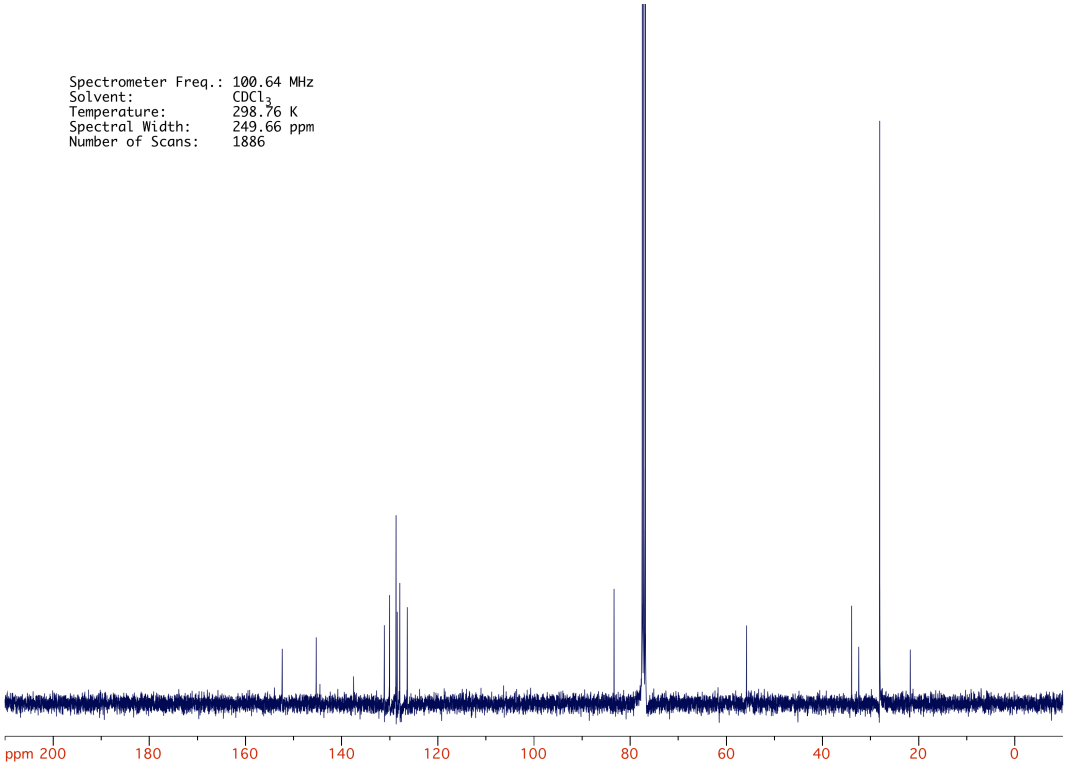

^{13}C {H}NMR spectrum of compound **86**

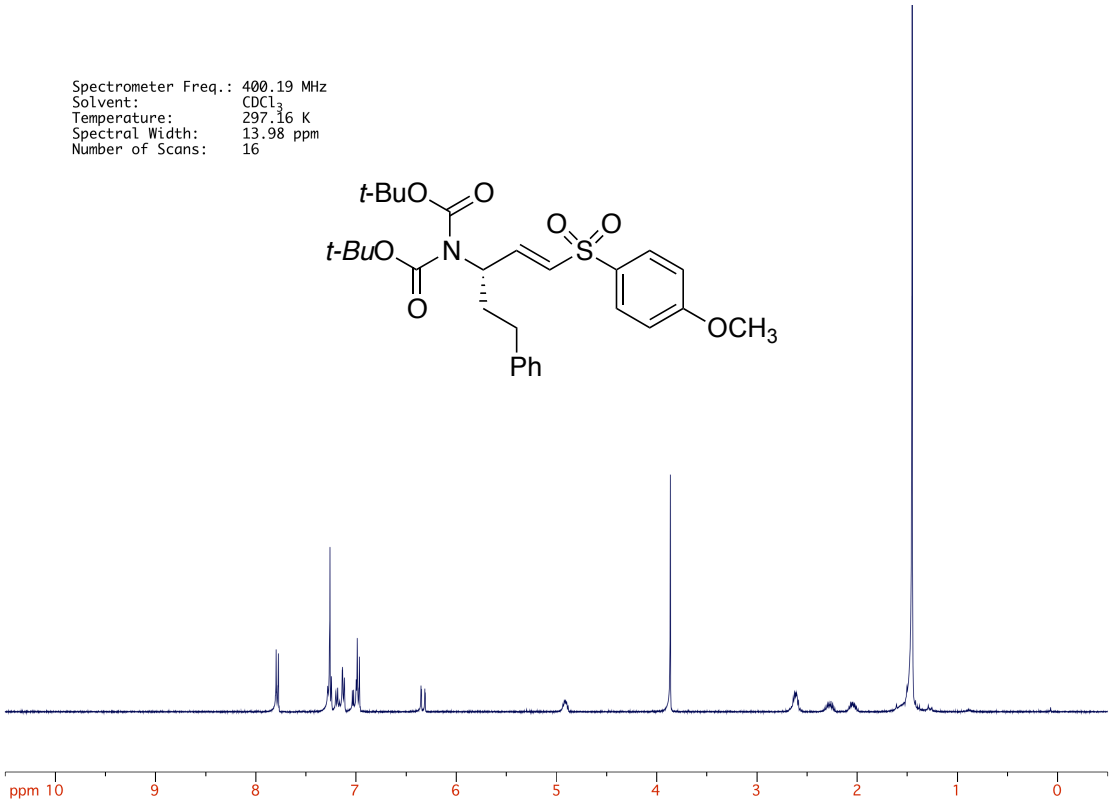

^{1}H NMR spectrum of compound **87**

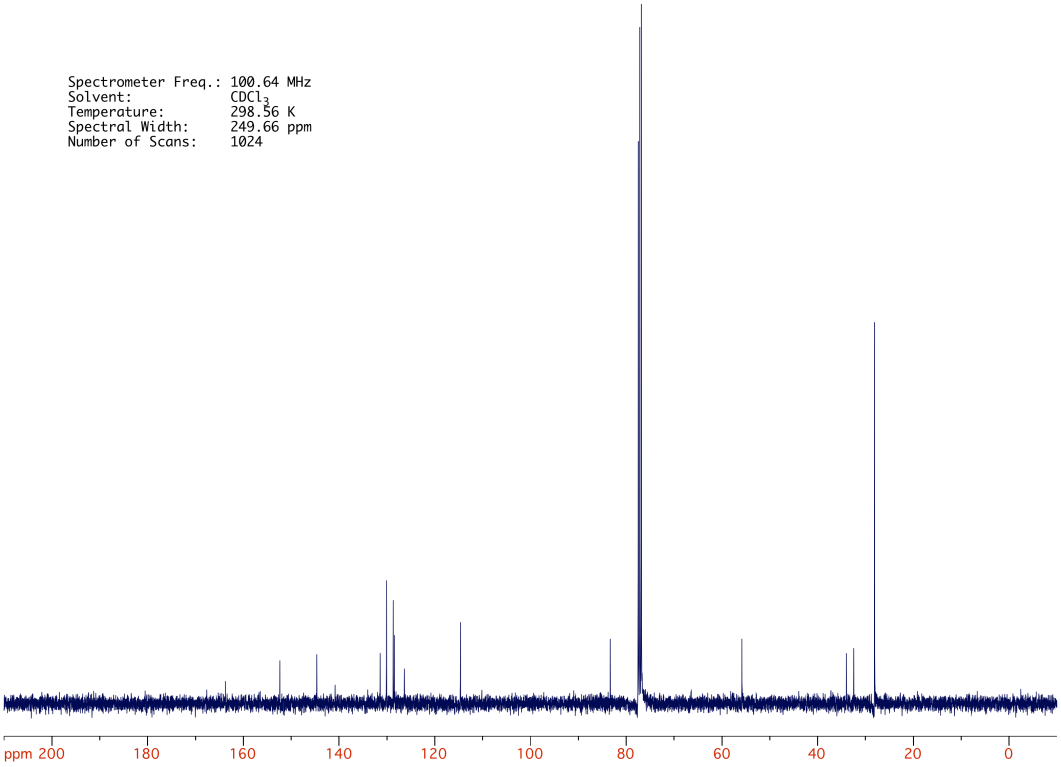

^{13}C {H}NMR spectrum of compound **87**

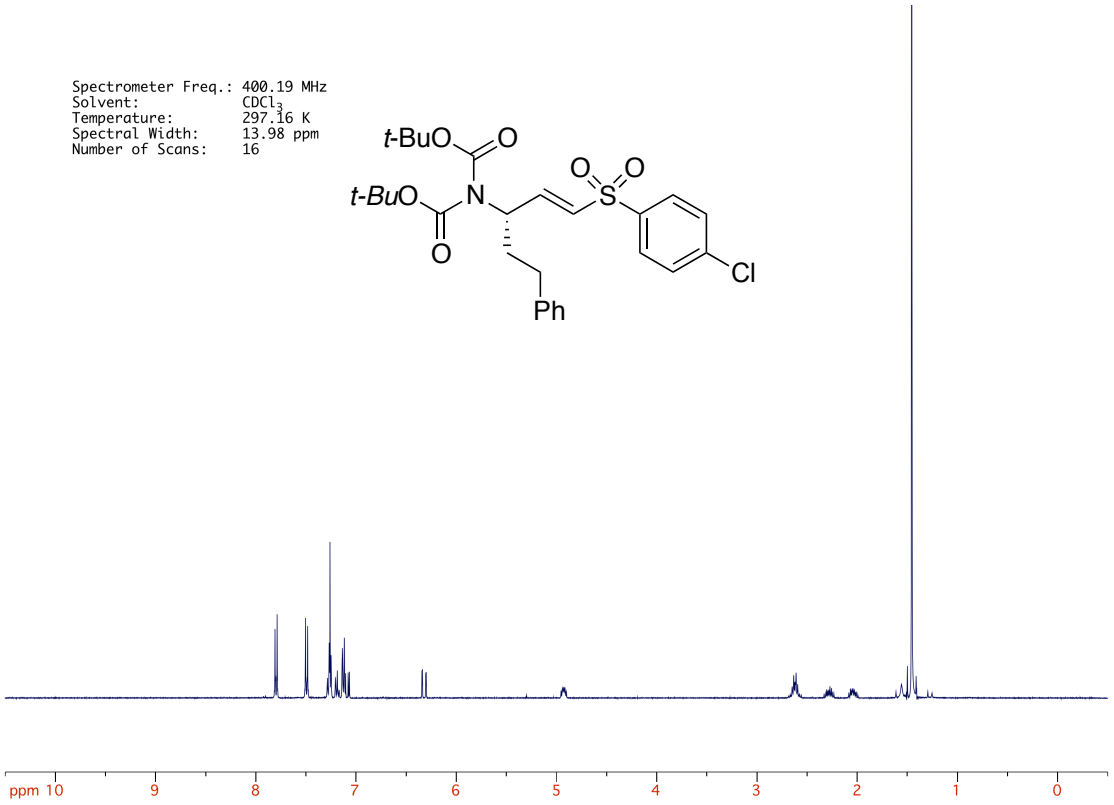

^{1}H NMR spectrum of compound **88**

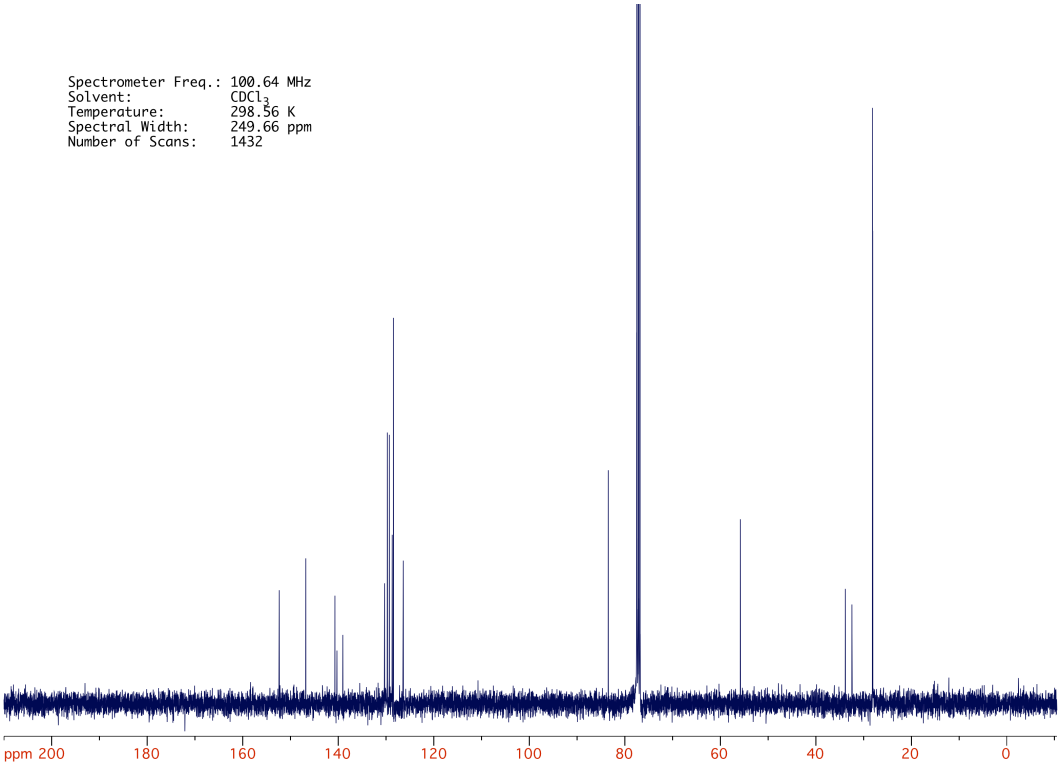

^{13}C {H}NMR spectrum of compound **88**

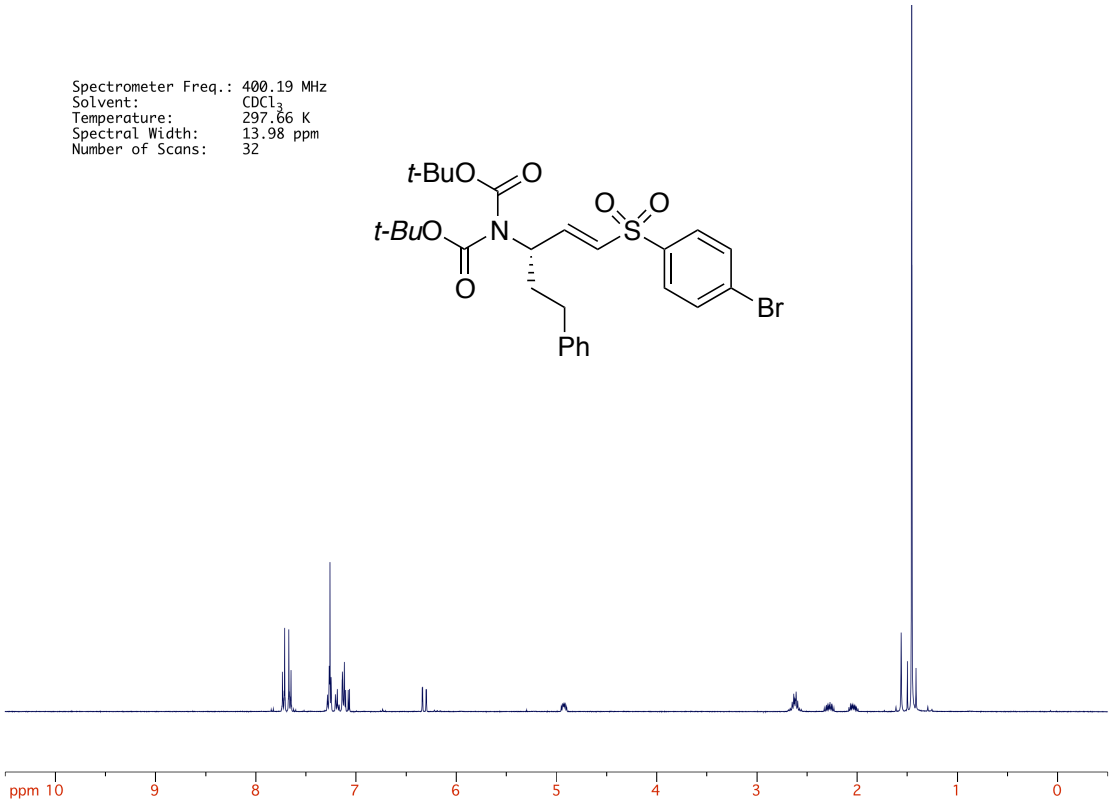

^{1}H NMR spectrum of compound **89**

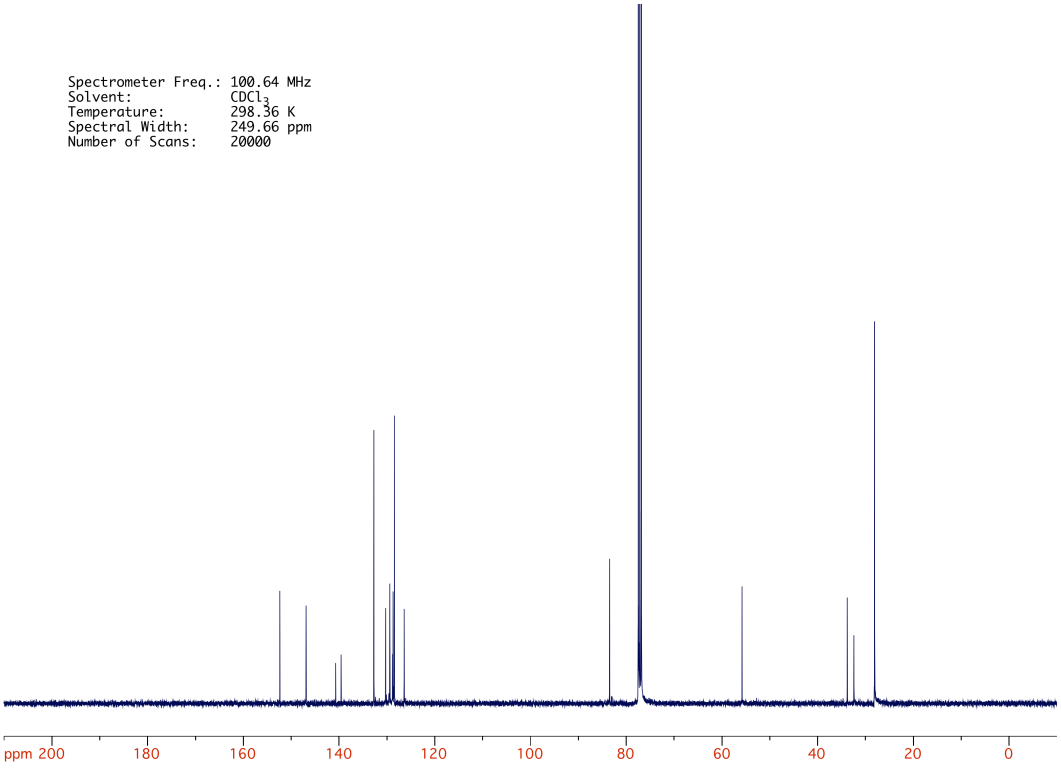

^{13}C {H}NMR spectrum of compound **89**

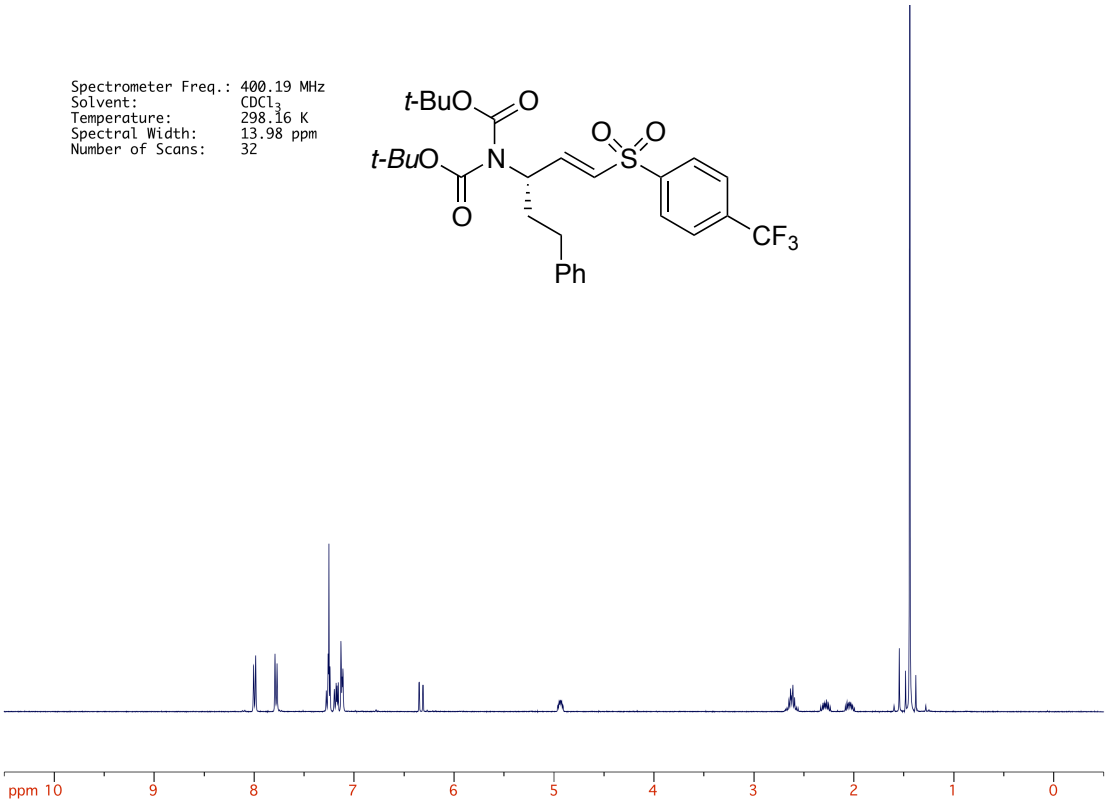

^{1}H NMR spectrum of compound **90**

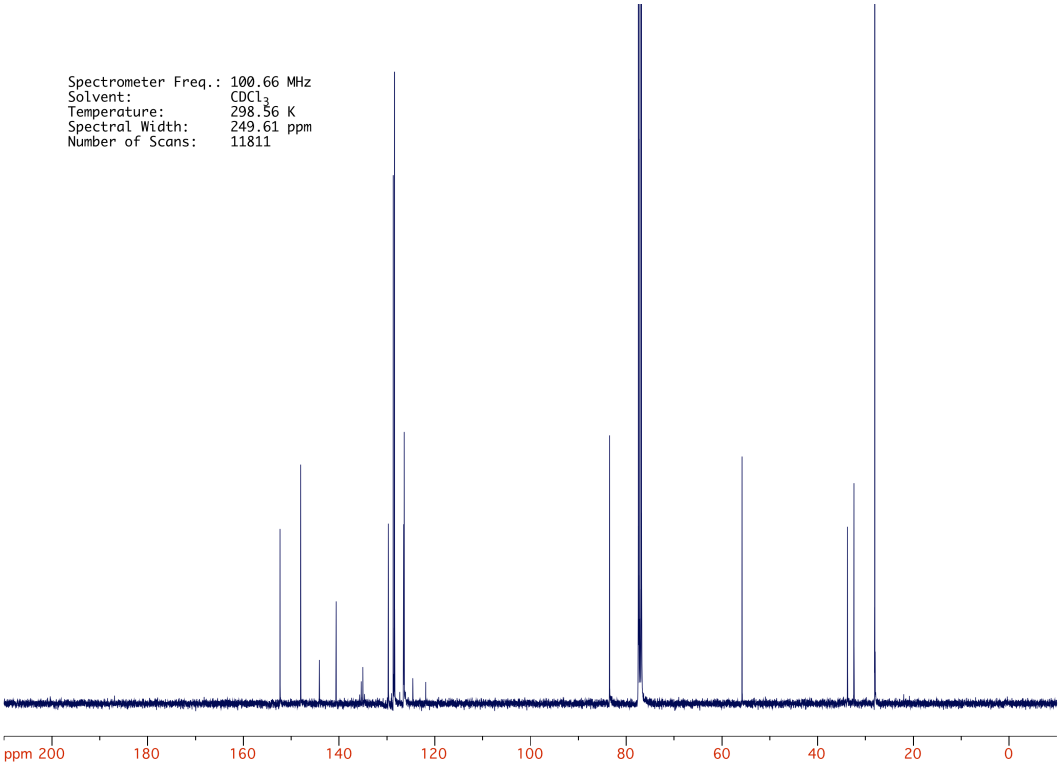

^{13}C {H}NMR spectrum of compound **90**

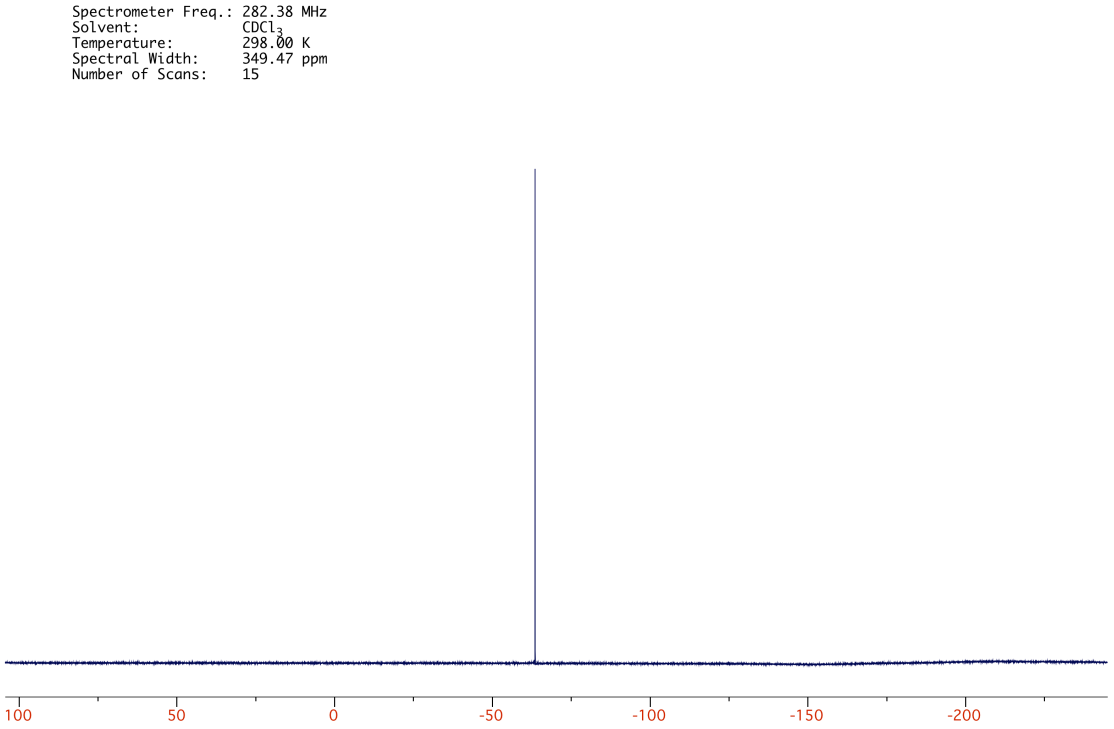

^{19}F NMR spectrum of compound **90**

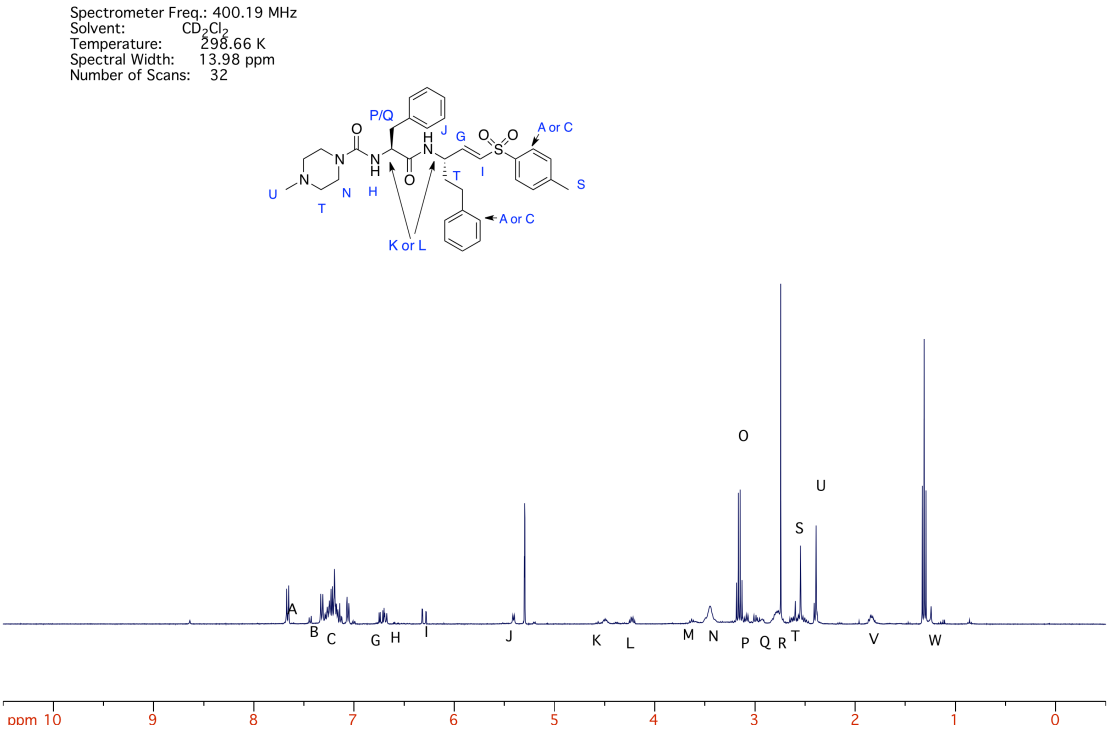

^{1}H NMR spectrum of compound **91**

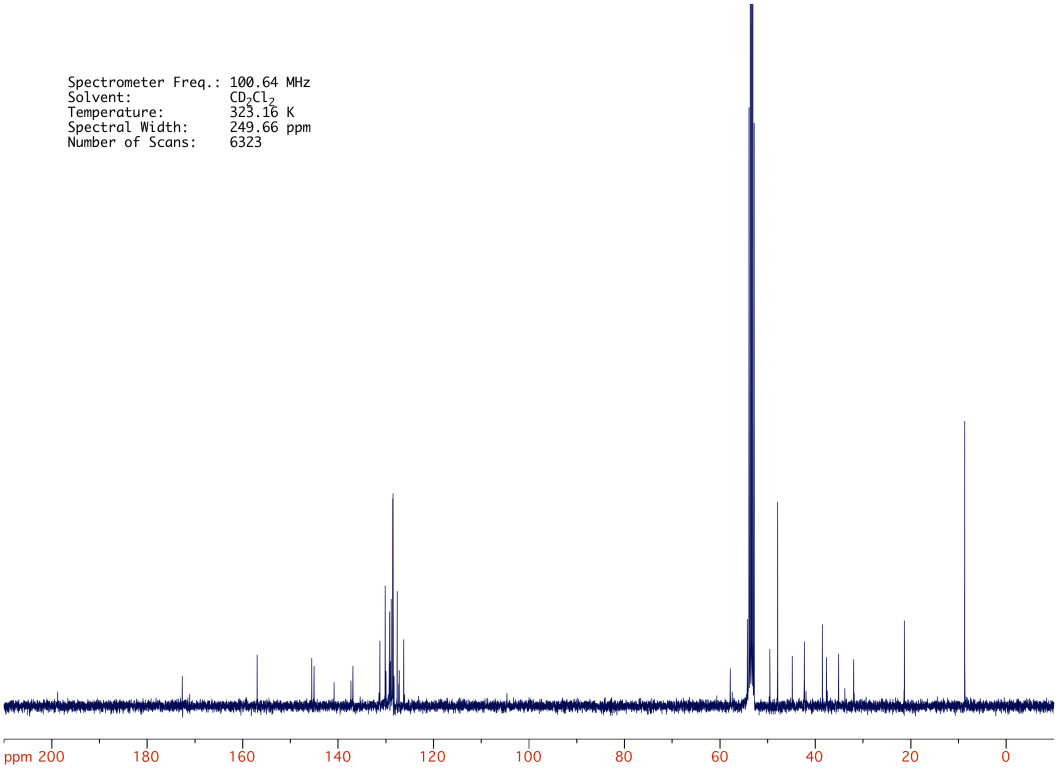

^{13}C NMR spectrum of compound **91**

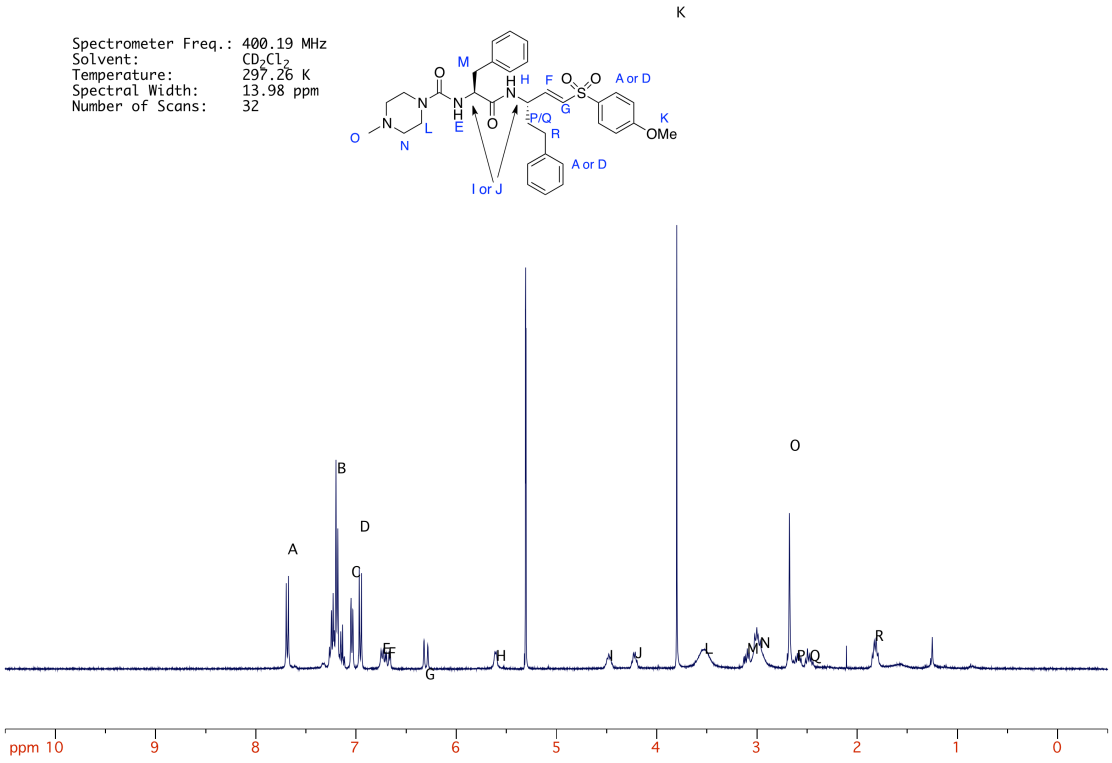

^{1}H NMR spectrum of compound **92**

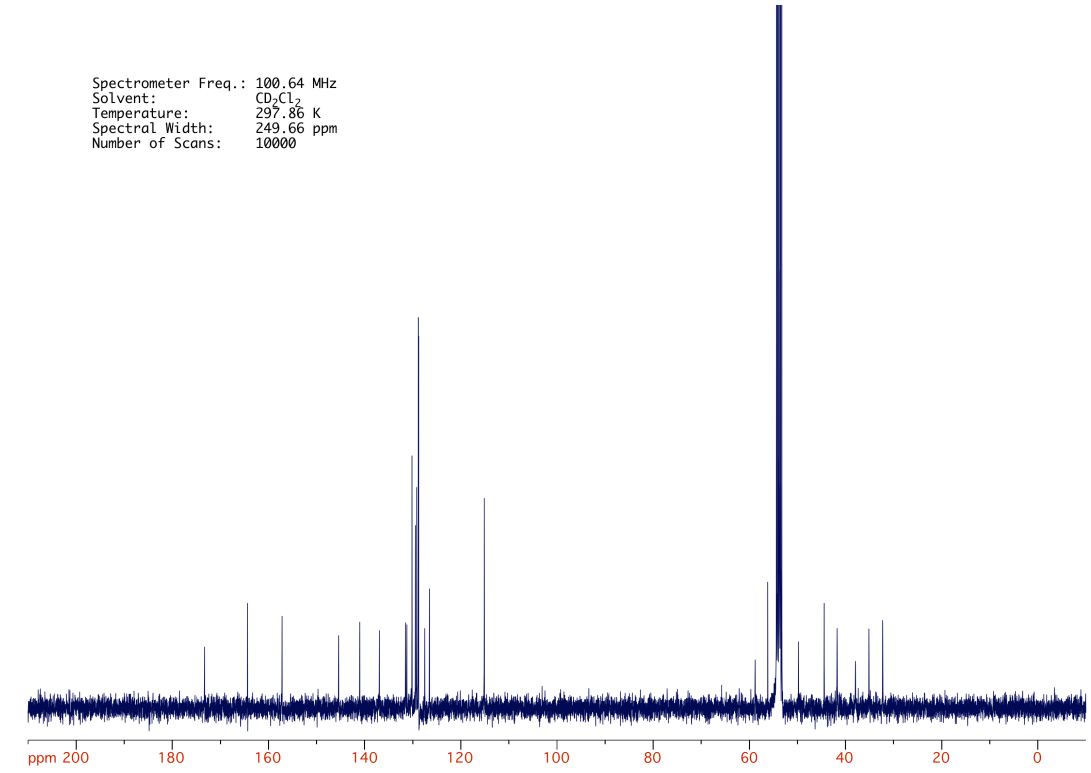

^{13}C NMR spectrum of compound **92**

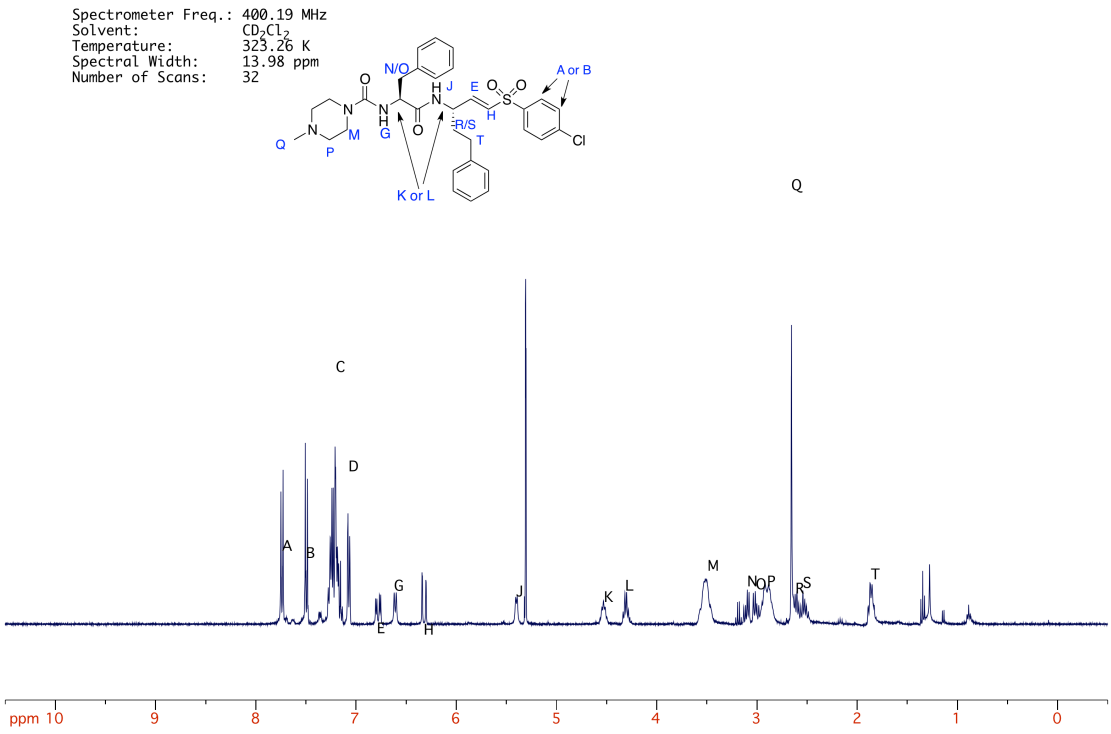

^{1}H NMR spectrum of compound **93**

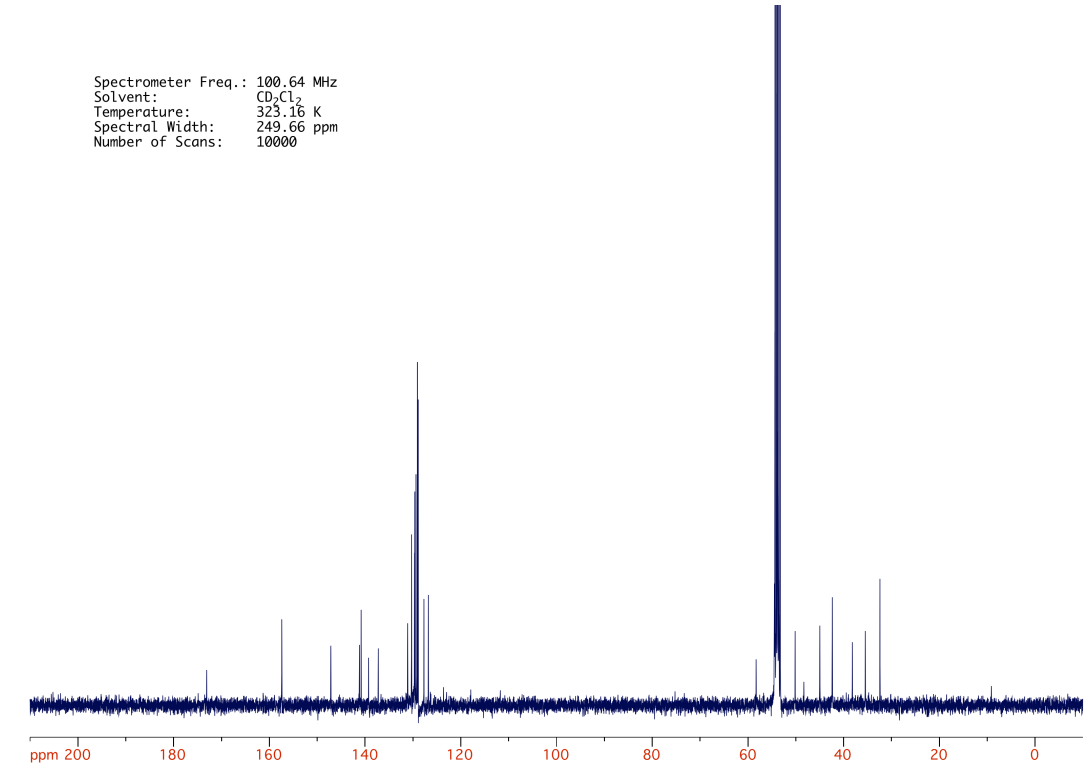

^{13}C {H}NMR spectrum of compound **93**

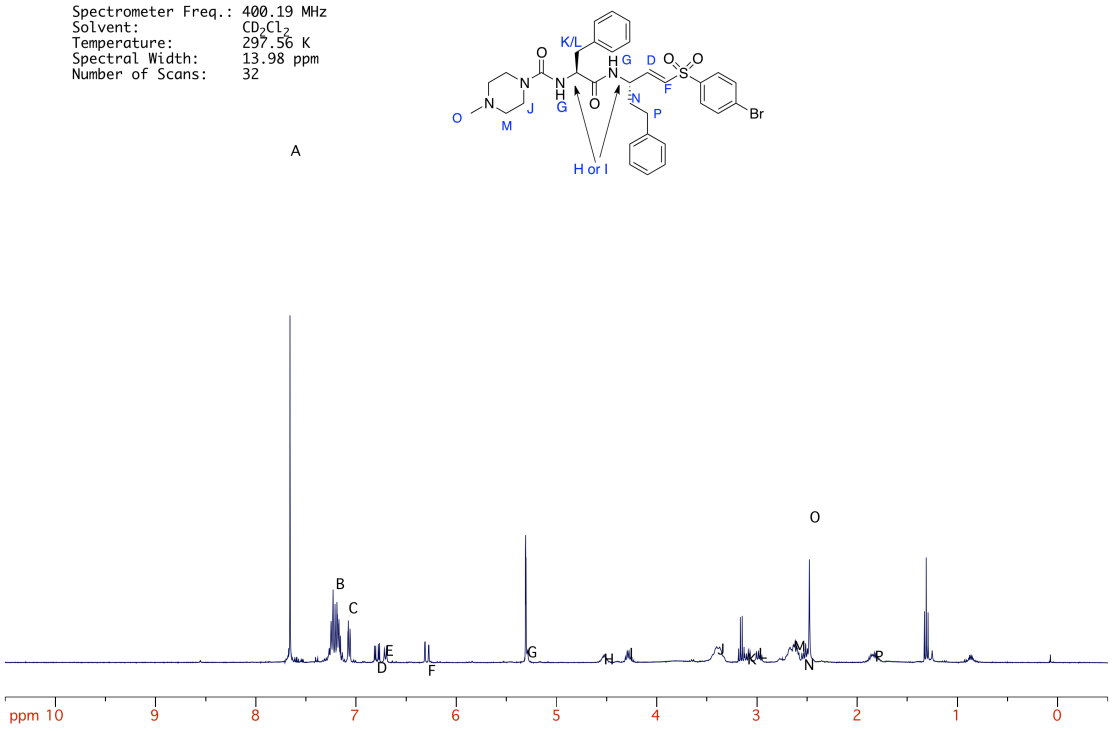

^{1}H NMR spectrum of compound **94**

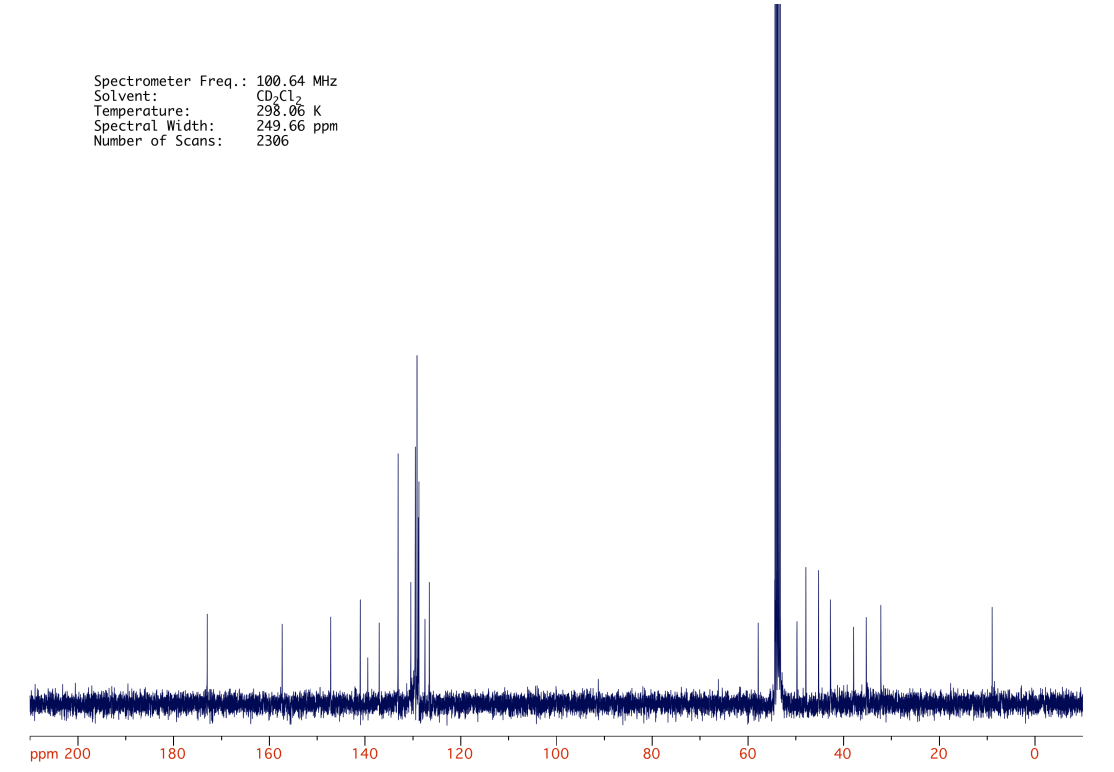

^{13}C {H}NMR spectrum of compound **94**

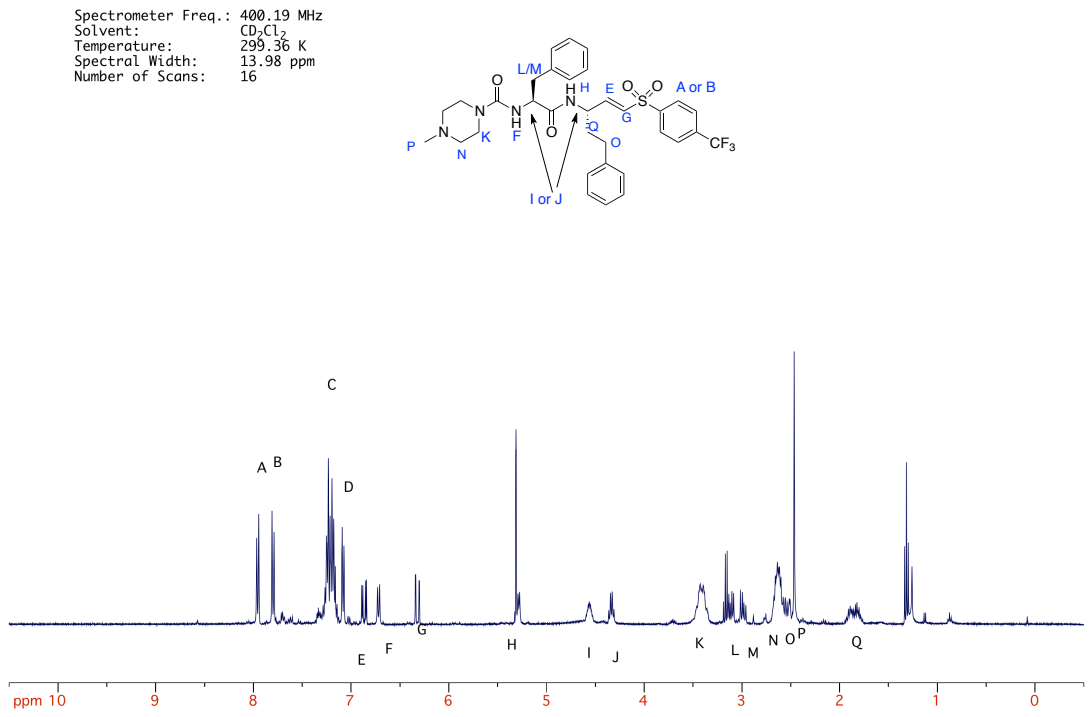

^{1}H NMR spectrum of compound **95**

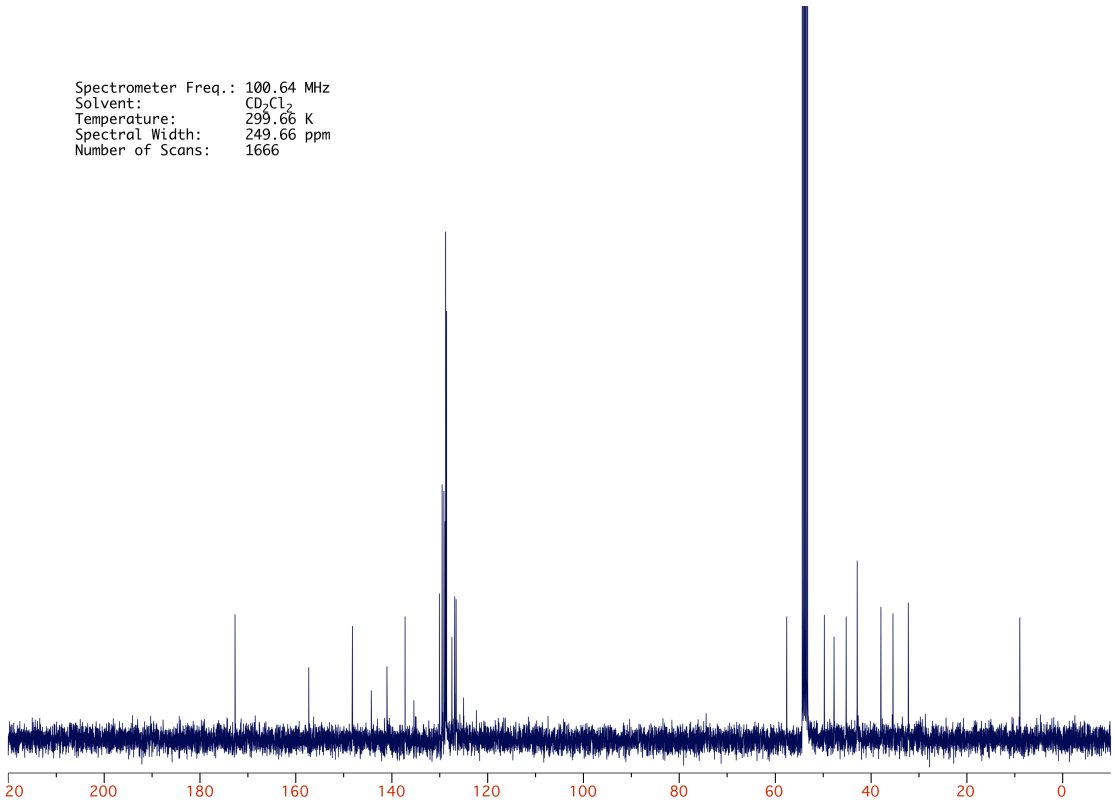

^{13}C {H}NMR spectrum of compound **95**

Spectrometer Freq.: 282.38 MHz
Solvent: CD_2Cl_2
Temperature: 295.70 K
Spectral Width: 349.47 ppm
Number of Scans: 8

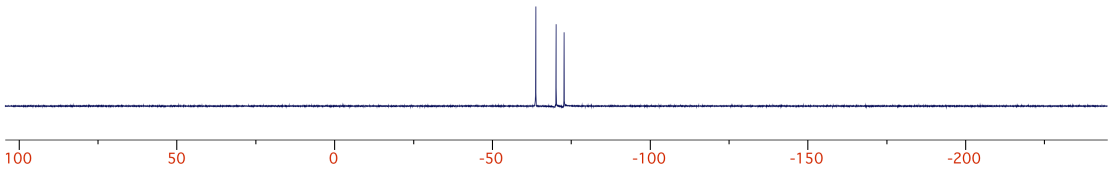

^{19}F NMR spectrum of compound **95**

Appendix II: Supercritical Fluid Chromatography Data

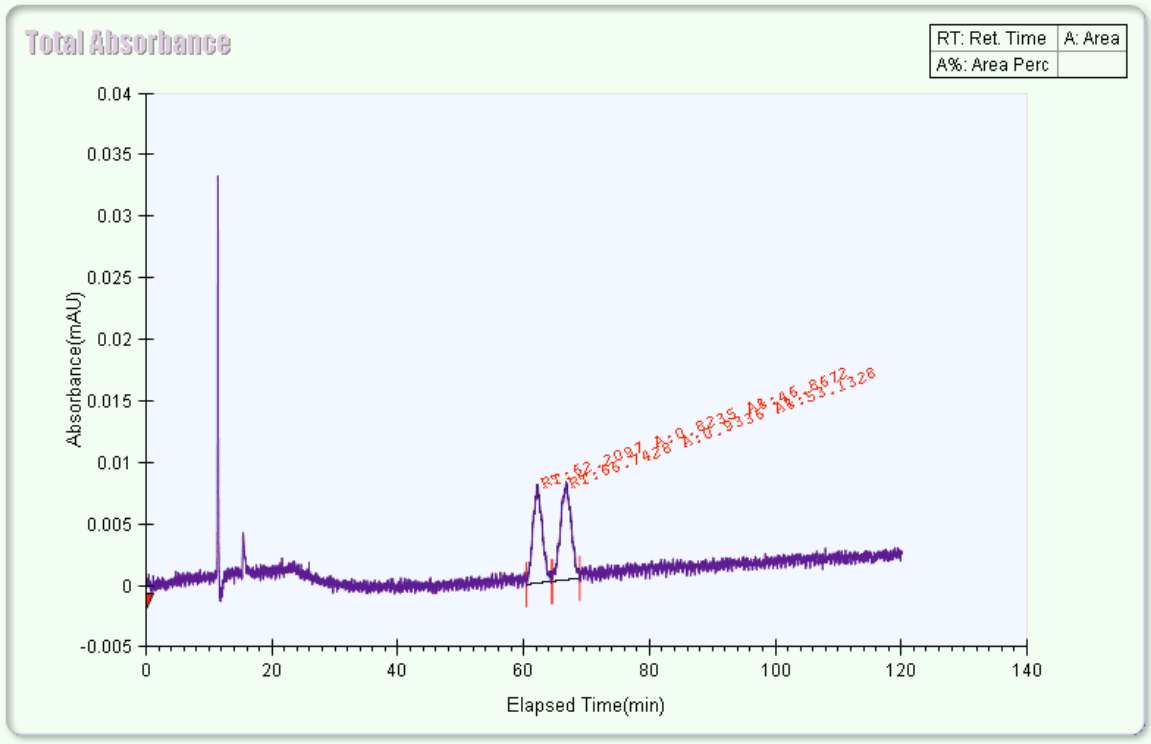

Chromatogram of compound **61**

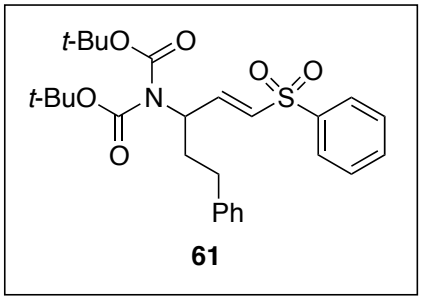

61

Run Parameters:
System: Thar Supercritical Fluid Chromatography
Column: OD-H Chiralpak
Co-solvent: Isopropyl alcohol
Temperature: 30.4 ^{o}C
CO_2 flow rate: 0.776 mL/min
Co-solvent flow rate: 0.024 mL/min
Co-solvent percentage: 3%
Total flow rate:0.8 mL/min
Back Pressure:121 bar
Front Pressure:122 bar
PDA wavelength rage: 190 – 399 nm

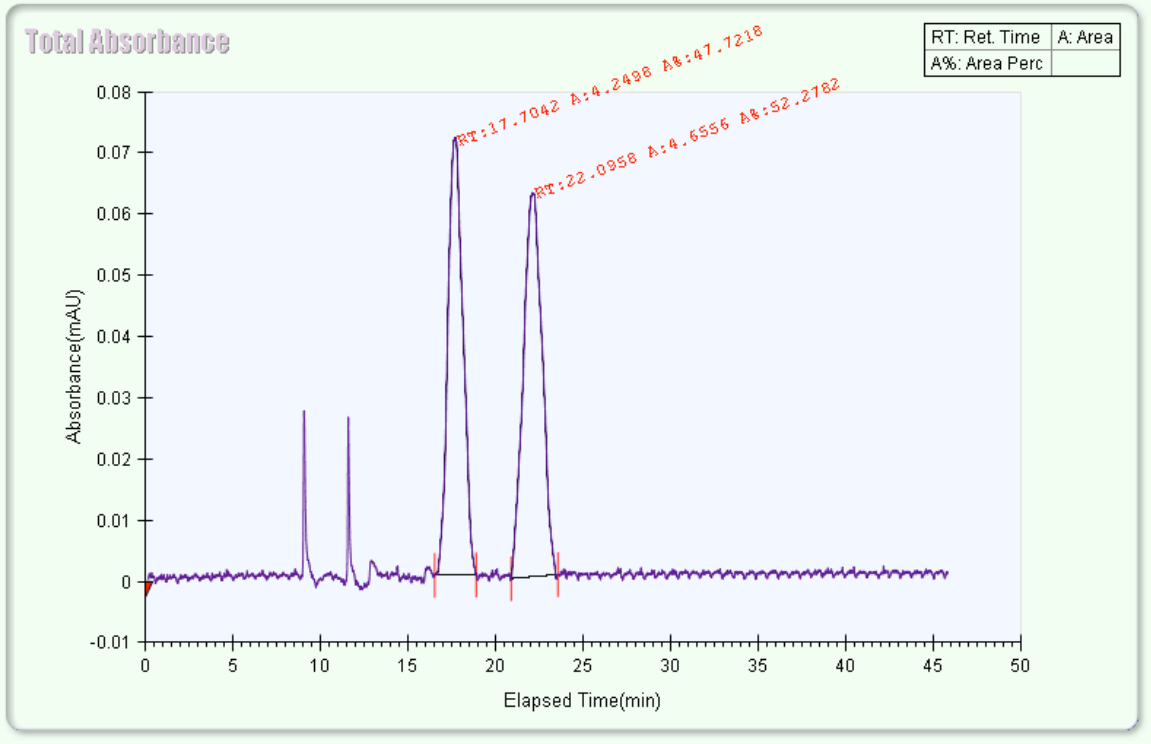

Chromatogram of compound **50**

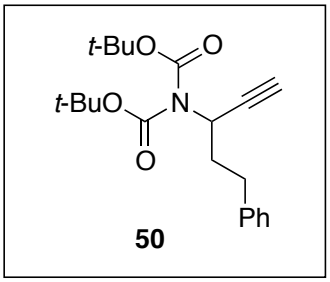

50

Run Parameters:
System: Thar Supercritical Fluid Chromatography
Column: OD-H Chiralpak
Co-solvent: Isopropyl alcohol
Temperature: 29.5 ^{o}C
CO_2 flow rate: 0.792 mL/min
Co-solvent flow rate: 0.008 mL/min
Co-solvent percentage: 1%
Total flow rate:0.8 mL/min
Back Pressure:123 bar
Front Pressure:127 bar
PDA wavelength rage: 190 – 399 nm